Carbon-based Nanomaterials for Adsorptive Desulfurization of Selected Sulfur Compounds from Liquid Fuels

BY

Faisal Alrasheed

A Thesis Presented to the

DEANSHIP OF GRADUATE STUDIES

KING FAHD UNIVERSITY OF PETROLEUM & MINERALS

DHAHRAN, SAUDI ARABIA

In Partial Fulfillment of the
Requirements for the Degree of

MASTER OF SCIENCE

In

Chemistry

January, 2017

KING FAHD UNIVERSITY OF PETROLEUM & MINERALS

DHAHRAN- 31261, SAUDI ARABIA

DEANSHIP OF GRADUATE STUDIES

This thesis, written by **Faisal A. Alrasheed** under the direction of his thesis advisor and approved by his thesis committee, has been presented and accepted by the Dean of Graduate Studies, in partial fulfillment of the requirements for the degree of MASTER **OF SCIENCE IN CHEMISTRY**.

Dr. Tawfik A. Saleh
(Advisor)

Dr. Abdulaziz AL-Saadi
Department Chairman

Dr. Khalid Alhooshani
(Member)

Dr. Salam A. Zummo
Dean of Graduate Studies

Dr. Emad N Shafie
(Member)

12/3/17
Date

Carbon-based Nanomaterials for Adsorptive Desulfurization of Selected Sulfur Compounds from Liquid Fuels

By

Faisal Alrasheed

A Thesis Presented to the

DEANSHIP of GRADUATE STUDIES

KING FAHD UNIVERSITY OF PETROLEUM & MINERALS

Dhahran, Saudi Arabia

In Partial Fulfillment of the

Requirements for the Degree of

MASTER OF SCIENCE

In

CHEMISTRY

Jan, 2017

DEDICATION

To my father may Allah has mercy on his soul,

To my mother may Allah bless her and linger her with us,

To my wife and daughter may Allah protect you, bless you and guide you to the right path

To all my family :brothers, sisters, nephews and nieces, May Allah protect you and may this work inspire you.

ACKNOWLEDGMENTS

All praise and thanks are due to Almighty Allah. He bestowed upon me wisdom, knowledge and time to complete this work.

I would like to start by thanking the department of chemistry in KFUPM for their support to accomplish this work. Furthermore, I am highly appreciative for my thesis advisor Dr. Tawfik Saleh for his many challenges during the courses of the thesis work. I thank will take this opportunity to acknowledge, with sincere gratitude and indebtedness, the encouragement, valuable time and guidance given to me by my mentor Dr. Emad AlShafie. I am also highly grateful to my thesis advisor members: Dr. Tawfik Saleh and the thesis committee: Dr. Hooshani and Dr. Shafie for their valuable guidance, comments, suggestions and motivation throughout the research period. Thanks to all faculty members staffs and students of the chemistry department. Sincere thanks to Saudi Aramco and KFUPM for the support extended towards my research and for granting me the opportunity to pursue graduate studies. I wish to thank R&DC management for their support during my studies. My heartfelt thanks are due to my parents, beloved family for their prayers, guidance, love, care and moral support throughout my academic life. My heartfelt thanks to my brothers and sisters for their prayers and guidance. I would like to thank Dr. Shen, Dr. Zaidi, Mr. Abadi, and Mr. Dekheel for characterizing the materials by XRD. I would like to thank Dr. Badairy for the SEM characterization. Finally, many thanks are due to my senior colleagues at Saudi Aramco and KFUPM for their help and prayers.

TABLE OF CONTENT

LIST OF TABLES

LIST OF FIGURES

LIST OF ABBREVIATIONS

T	Thiophene
BT	Benzothiophene
DBT	Dibenzothiophene
BDS	Biodesulfurization
ODS	Oxidative Desulfurization
AC	Activated Carbon
S-M	Sulfur Metal
HOMO	Highest Occupied Molecular Orbital
LUMO	Lowest Unoccupied Molecular Orbital
API	American Petroleum Institute
SOx	Sulfur Oxides
NOx	Nitrogen Oxides
EPA	Environmental Protection Agency
ppm	parts per million
HDS	Hydrodesulfurization
ULSD	Ultra-Low Sulfur Diesel
XRD	X-Ray Diffraction
BET	Brunauer–Emmett–Teller
ESEM	Environmental Scanning Electron Microscopy
NAP	Naphthalene
1-mNAP	1-Methyl Naphthalene
4,6-DMDBT	4,6- Dimethyldibenzothiophene
HPLC	High-Performance Liquid Chromatography
GC	Gas Chromatography
SCD	Sulfur Chemiluminescence Detector
FID	Flame Ionization Detector
LHSV	Liquid Hourly Space Velocity
Ea	Activation Energy
ODS	Oxidative Desulfurization
MOF	Metal Organic Framework
IR	Infrared
FPD	Flame Photometric Detector
GAC	Granular Activated Charcoal
ILs	Ionic liquids
PAC	Powdered Activated Charcoal
NAP	Naphthalene
4,6-DMDBT	4,6-Dimethyldiebenzothiophene
IE	Ion exchange
P	Precipitation
EDS or EDX	Energy-dispersive X-ray spectroscopy
Ads	Adsorbent

ABSTRACT

Full Name : Faisal A. Alrasheed

Thesis Title : Carbon-based Nanomaterials for Adsorptive Desulfurization of Selected Sulfur Compounds from Liquid Fuels

Major Field : Chemistry

Date of Degree : January, 2017

Sulfur compounds and its organic homologues are unwanted in the liquid fuels for several reasons. Sulfur compounds cause severe environmental pollution, hinder a variant of the refining process, poison catalysts and corrosive. Furthermore, a major requirement for fuel cell application is to reduce the sulfur in the feedstock to below 1 ppmw of Sulfur. The objective of this work is to develop, test and characterize carbonic based nanomaterials for adsorptive desulfurization of selected sulfur compounds of diesel. Hence, several activated carbon-based nanomaterials were prepared by doping different metals (Fe, W, La and Ni) at different ratios using different adsorbents' methods. The fixed bed adsorption continues system was used to test model fuel at atmospheric pressure and room temperature. GC-SCD and GC-FID analysis were used to monitor the desulfurization process. The activated carbon based adsorbent was characterized by XRD, ESEM, and BET.

The adsorptive capacity for sulfur compounds was examined and compared using the breakthrough capacity at 1 ppmw of total sulfur using the breakthrough curves. The breakthrough capacity results showed that synthesized activated carbon is superior to zeolites. The low metals doping has higher breakthrough capacity than the high metal. In

terms of the effect of catalyst preparation methods, FeO/AC (ion-exchange) > AC support > FeO/AC (precipitation) with a breakthrough capacity of 1.67 mg S/g, 1.25 mg S/g, and 0.70 mg S/g, respectively. The effect of model fuel composition is studied and the results indicate that the total sulfur and the aromatic content of the model fuel affects the breakthrough capacity of the feed where higher sulfur feeds increase the adsorption capacity and higher aromatic feeds decrease the adsorption capacity. Single metal and bimetallic impregnation were studied and the desulfurization performance with respect to metal impregnation follows the order: FeO-LaO/AC < AC < FeO-WO_3/AC(LL) < FeO-NiO/AC(ULL) < 2%LaO/AC < FeO-WO_3/AC(ULL) < 2%Fe/AC < 2%WO_3/AC < 2%NiO/AC < 1%NiO/1%WO_3/AC. The bimetallic oxide adsorbent of 1%NiO/1%WO_3/AC showed the highest adsorption capacity.

The results of testing carbon-based nanomaterials for the adsorptive desulfurization of selected sulfur compounds from liquid fuels indicated their potential in being applied as a complementary step to Hydrodesulfurization and demonstrates high efficiency in the refractory sulfur compounds removal.

ملخص الرسالة

الاسم الكامل: فيصل عبد الله الرشيد

عنوان الرسالة: تطوير مواد بحجم النانو على اساس من الكربون النشط لإزاله الكبريت من وقود الديزل.

التخصص: الكيمياء

تاريخ الدرجة العلمية:يناير 2017.

المركبات الكبريتية ومشتقاتها العضوية غير مرغوب فيها في الوقود السائل لعدة اسباب: مركبات الكبريت تسبب تلوث بيئي حاد، تثبط عمليات التصفية، وتسمم المحفزات، واخيرا تسبب التآكل للعديد من المعدات. بالإضافة إلى ذلك، فأحد متطلبات تطبيقات خلية الوقود هو ان تكون نسبة الكبريت في الوقود المستخدم أقل من 1 جزء في المليون.

الهدف من هذا البحث هو تطوير واختبار وتحليل مواد بحجم النانو على اساس من الكربون النشط لإزالة بعض مركبات الكبريت من وقود الديزل عن طريق الامتصاص.

تم إضافة عدة معادن (حديد، تنجستن، لانثانيوم، ونيكل) الى الكربون النشط بنسب مختلفة باستخدام طرق تحضير مختلفة. بعد ذلك تم اختبار أداء المواد باستخدام نظام امتصاص بقاعدة ثابتة ووقود نموذجي تحت الضغط الجوي ودرجة حرارة الغرفة. تمت مراقبة عملية إزالة الكبريت باستخدام كروماتوغرافيا الغاز وكاشف الكبريت بخاصية التوهج والتأيين باللهب. تم فحص المواد الماصة باستخدام جهاز الحيود السيني والمجهر الالكتروني وجهاز البي اي تي. تم فحص قدرة الامتصاص للمواد الماصة ومقارنتها باستخدام المنحنيات المنفرجة واظهرت النتائج ان الكربون النشط اقوى امتصاصا من بعض المواد الاخرى. وكذلك اظهرت الدراسات أن إضافة معادن بكمية قليلة على الكربون النشط أفضل من اضافتهم بكمية أعلى. أضف إلى ذلك، فأن تحضير المواد الماصة باستخدام طريقة التبادل الأيوني أفضل من طريقة الترسيب. بالنسبة إلى تأثير مكونات الوقود النموذجي، فالدراسة أثبتت أن المركبات العطرية تؤثر سلبا على كفاءة مواد الامتصاص وأنه كلما زادت نسبة الكبريت في الوقود كلما زادت كفاءة المحفز. بالنسبة إلى المعادن المضافة فالنتائج تشير إلى ان ترتيب المواد الماصة من ناحة كفاءة إزالة الكبريت يتبع الترتيب التالي:

$FeO\text{-}LaO/AC < AC < FeO\text{-}WO_3/AC(LL) < FeO\text{-}NiO/AC(ULL) < 2\%LaO/AC < FeO\text{-}WO_3/AC(ULL) < 2\%Fe/AC < 2\%WO_3/AC < 2\%NiO/AC < 1\%NiO/1\%WO_3/AC.$

تمت دراسة إضافة معدنين مؤكسدين الى الكربون النشط والنتائج تشير إلى أن $1\%NiO/1\%WO_3/AC$ لديه كفاءة اعلى في إزالة الكبريت بقدرة 2.30 mg S/g ads. نتائج هذه الدراسة تبين أن المواد الكربونية النشطة بحجم النانو لها القدرة على إزالة الكبريت عن طريق الامتصاص بكفاءة عالية وعلى قدرتها على تكميل عملية إزالة الكبريت باستخدام الهيدروجين والمحفزات.

CHAPTER 1 INTRODUCTION

1.1 Background of Desulfurization

The crude oils worldwide have a ranging percentage of sulfur compounds. Figure 1 shows the sulfur content and the API gravity of several crude oils. Sulfur compounds and its organic homologues are unwanted in the liquid fuels for several reasons: they cause severe environmental pollution and corrosion, hinder a variety of refining process, and poison catalysts (Shirashi et al 1998; Song 2002). Furthermore, as shown in Table 1, the United States Department of Transportation mandates that the diesel and gasoline to have a sulfur level less than 15 and 30 ppm, respectively (Mohammad et al 2006). In Europe, the clean fuel legislation allowed sulfur limit is dropped town from 50 ppm to 10 ppm (Mohammad et al 2006). This strong regulation that imposes the trend in the oil and refining industry to reduce the sulfur content worldwide to via researching several processes.

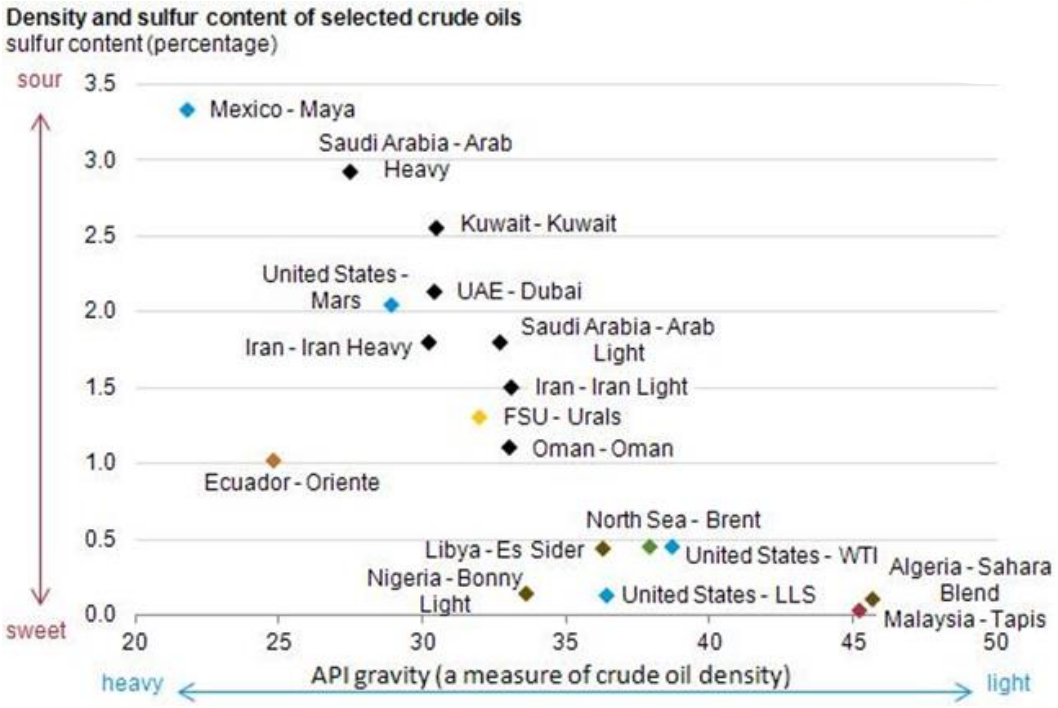

Figure 1. Crude oil API gravity and sulfur content (U.S. Energy information Administration, based on Energy Intelligence Group-International Crude Oil Market Handbook.

Sulfur compounds in liquid fuels reduce their quality marginally. In addition, they reduce the fuel economy due to the SO_x emissions. Moreover, the sulfur compounds increase the exhaust particulate matter emissions resulting in sulfates emissions, which are harmful to the environment (Song 2003). In addition to that, they poison the catalyst in the automobile catalytic converters hindering the efficiency in adsorbing NOx and particulate matter. When sulfur compounds undergo combustion, sulfates and SOx are produced. Sulfur oxides can undergo several reactions in the environment. SOx can be converted into sulfuric acid that causes acid rains. The effects of acid rains to the environment and

civilizations are substantial. Acid rains can threaten the ecosystems, which harm the wildlife and shorten the lifetime of the building, paints, and statues.

Table 1. EPA limits for maximum sulfur levels allowed in commercial liquid fuels in the USA. (Song 2003).

Fuel type	S content (ppm)	Enforcing year
Gasoline	3-80	2006
On road Diesel	<15	2006
Non-road Diesel	<15	2010
Marine and Locomotive Diesel	<15	2012

1.2 The importance of sulfur removal from liquid fuels

Before desulfurization, the sulfur levels in liquid fuels are higher than the EPA standards. These high sulfur concentrations are harmful to the environment, engines and catalysts. The sulfur levels in the liquid fuels are too high for the fuel cell applications which require a maximum of 1 ppm of sulfur in order to avoid catalyst and electrode poisoning (Song 2002; Novochinskii et al 2004). Figure 2 shows the effects of organosulfur compounds on the fuels and environment. Therefore, reducing the sulfur content has emerged as a need in several industries to avoid its shortcomings and improve the quality of liquid fuels which make them suitable for fuel cell applications or for exporting. The sulfur removal improves the ignition qualities of the liquid fuels significantly, reduce the environmental hazards, and reduce the SOx emissions produced from liquid fuels combustion. All of these major

factors in addition to the increased economic value were the motivations for refiners worldwide to produce cleaner fuels.

The EPA standards limits are expected to improve the environment by reducing the harmful emissions from highway diesel vehicles. The EPA standards, illustrated in Table 1, reduced the harmful emission from highway vehicles and non-road engines and equipment by more than 90 % . (9 pp, 3 MB, September 26, 2011).

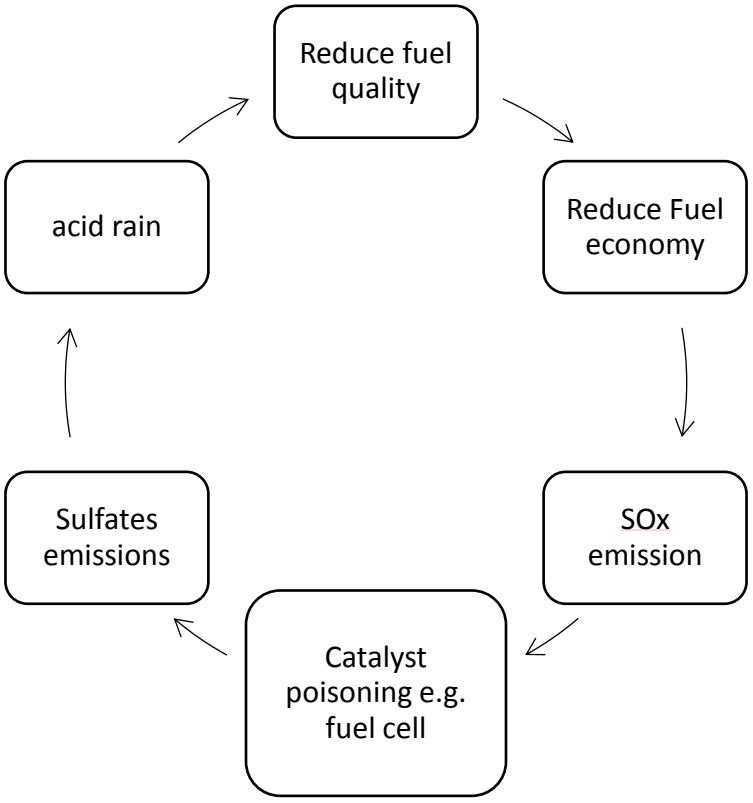

Figure 2.Effect of organosulfur compounds on fuels and environment (Soog 2004).

1.3 Statement of Problem

The reduction in the sulfur content of liquid fuels is vital to meet the EPA requirements and achieves high-quality fuels that have less effect on health and environment. In addition, the fuel cell application requires that the diesel used has a sulfur content of a maximum of 1 ppm. Furthermore, the crudes are getting sourer with higher sulfur content which creates a demand for cleaner fuels with less sulfur content, especially for fuel cell applications.

Although the HDS process is widely used technology for desulfurization of liquid fuels, it has several shortcomings. The HDS is ineffective in removing thiophenic compounds (TC) including benzothiophene (BT), dibenzothiophene (DBT), and 4,6-dimethyldibenzothiophene (4,6-DMDBT) due to their low reactivity and complicated removal mechanism as illustrated in Figure 4. Hence, achieving the EPA standards of sulfur content in liquid fuels using HDS processes is very challenging. Therefore, the need emerges for other desulfurization methods to achieve sulfur content of less than 15 ppm in liquid fuels or less than 1 ppm for fuel cell.

1.4 Significance of the Study

The importance of producing liquid fuels with ultra-low sulfur content (ULSD) (15 ppm) or with 1 ppm sulfur content has higher costs, especially when compared to producing low-sulfur content diesel oil (500 ppm). Nevertheless, a significant cost production of liquid fuels with sulfur content that is less than 15 ppm or even to 1 ppm can be accomplished by integrating the HDS units with a non-hydrogenation process, such adsorptive desulfurization. Furthermore, the Ultra-low sulfur fuels can be used for fuel cell application where the maximum allowable sulfur is 1 ppm. Adsorption desulfurization can be used effectively to remove refractory sulfur compounds as a complementary step to the HDS

while keeping the process cost effective. This study has the potential of creating new Nano adsorbent materials that can be used to produce Ultra-low sulfur liquid fuels meeting the EPA standards and/or the fuel cell application requirement.

Based on literature survey, nano-based adsorbents can be used for desulfurization of liquid fuels. This work will help developing in-house capability that improves the quality of research and innovation. This study is very critical for the oil industry where liquid fuels are crucial for various application worldwide. Improving the quality of liquid fuels by reducing the sulfur levels will improve our economy and environment. Furthermore, the refineries worldwide can use this process when fully developed especially when the demand has increased worldwide for liquid fuels with less sulfur content, for less SO_x emissions, fewer emissions particulates, less corrosive and less contribution of fine particulates emissions and no effect on the catalysts used for after treatment.

1.5 Thesis Objectives

There were three objectives for this thesis:

1. Developing nano-based activated carbon adsorbent materials that can improve the quality of liquid fuels via reducing the sulfur content using adsorptive desulfurization method.
2. Developing a method for testing the desulfurization performance of these materials using the fixed bed absorption process.
3. Characterizing the materials using XRD, BET, and SEM.

1.6 Thesis Tasks

In order to achieve the thesis objectives, the work has been broken down into the following tasks:

1- Choose the proper support for the adsorbents. In order to achieve this objective, activated carbon and H-Y-zeolite are tested and compared.
2- Synthesis in-house nano-based materials that have high selectivity and efficiency in removing the sulfur organic compounds from the liquid fuels.
3- Synthesis nanomaterials combined with metal oxide nanoparticles (Ni, W, Fe, La).
4- Conducting adsorptive desulphurization of model diesel fuel experiments using the synthesized materials using fixed bed absorber process.
5- Study the effect of model diesel composition on sulfur breakthrough capacity. This objective will be addressed by studying the effect of aromatic content and total sulfur of model diesel desulfurization breakthrough.
6- Study the effect of metal loading on desulfurization breakthrough by selecting different metals and different loading content.
7- Compare adsorption desulfurization performance at low and high sulfur levels of model fuels.
8- Test the adsorbent that performs the best desulfurization using model fuel with an actual HDS diesel.
9- Characterize the adsorbents material using XRD, SEM and (Texture property analyses)

CHAPTER 2 LITERATURE REVIEW:

2.1 Sulfur compounds in liquid fuels

There is a huge range of sulfur organic compounds that exist in liquid fuels with different kinds: thiols, sulfides, thiophene, benzothiophene and dibenzothiophenes and their alkylated derivatives as shown in Figure 3.

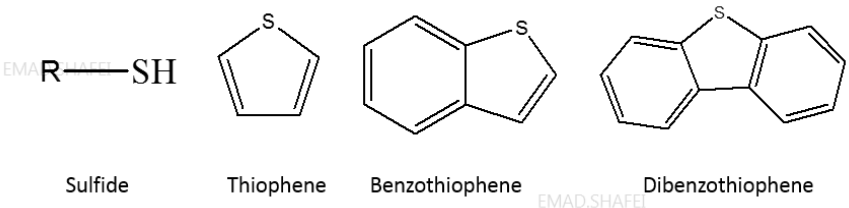

Figure 3. Examples of sulfur compounds in liquid fuels.

Liquid fuels contain a complex mixture of many hydrocarbons in addition to sulfur and nitrogen organic compounds. As the boiling point range of the petroleum fraction increases, as the complexity of the sulfur compounds increase as shown in Figure 4 (Ito et al 2006). For every aromatic ring present in the compound, the HDS reactivity is reduced by an order of magnitude. (Ito et al 2006). Figure 5 shows the sulfur compound in gasoline, jet fuel, and diesel. The diesel range has the most refractory sulfur organic compounds compared to the jet fuel and gasoline.

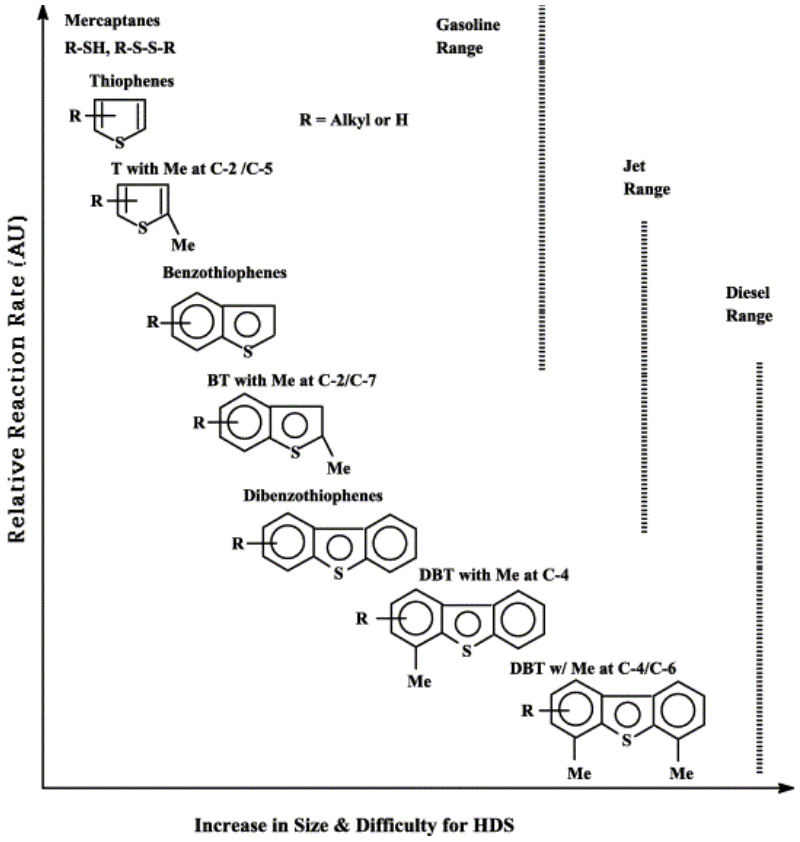

Figure 4. Reactivity of various sulfur compounds found in liquid transportation fuels (gasoline, jet fuel, and diesel) (Song 2003).

Song et al. (2003) conducted sulfur speciation of hydrotreated fuels by using GC-FPD (Figure 5) and as it is shown below, after HDS process, the sulfur compounds are shown for each liquid fuel fraction (gasoline, jet fuel, and diesel) which illustrates their reactivity and resistivity to desulfurization. In the gasoline fraction, the sulfur compounds are mostly thiols, sulfides, thiophene and some alkylated derivatives and benzothiophene. The five major sulfur compounds in gasoline are thiophene, 2-methylthiophene, 3-methylthiophene, 2,4-dimethylthiophene, and benzothiophenes. The jet fuel fraction has some benzothiophenes alkylated derivatives where the major sulfur compounds are a mixture of

isomers of dimethyl benzothiophene and trimethyl benzothiophenes. The diesel range has a boiling range of 160-380 °C and has a more complex mixture of sulfur compounds. The sulfur compounds that exist in the diesel range are benzothiophene and dibenzothiophene and their alkylated derivatives. As shown in their chromatograms, as the feed gets heavier, the hydrotreater efficiency is reduced. Furthermore, the complexity of the sulfur compounds and steric hindrance in some cases is increasing as well. Therefore, in order to desulfurize the liquid fuels, a thorough and deep understanding of the sulfur compounds in each fraction. The thorough knowledge of the composition of the diesel feed and the product after it undergoes desulfurization is very critical to provide information and understanding to improve the desulfurization process. For example, in order to achieve Ultra-Low sulfur diesel with a total sulfur of less than 10 ppm using Hydrodesulfurization, the reactor size has to be increased by a factor of 3-15 which increases the hydrogen consumption as well as temperature and pressure (Song 2002; Hernandez-Maldonado 2004) comparing to lowering the sulfur to 50 ppm.

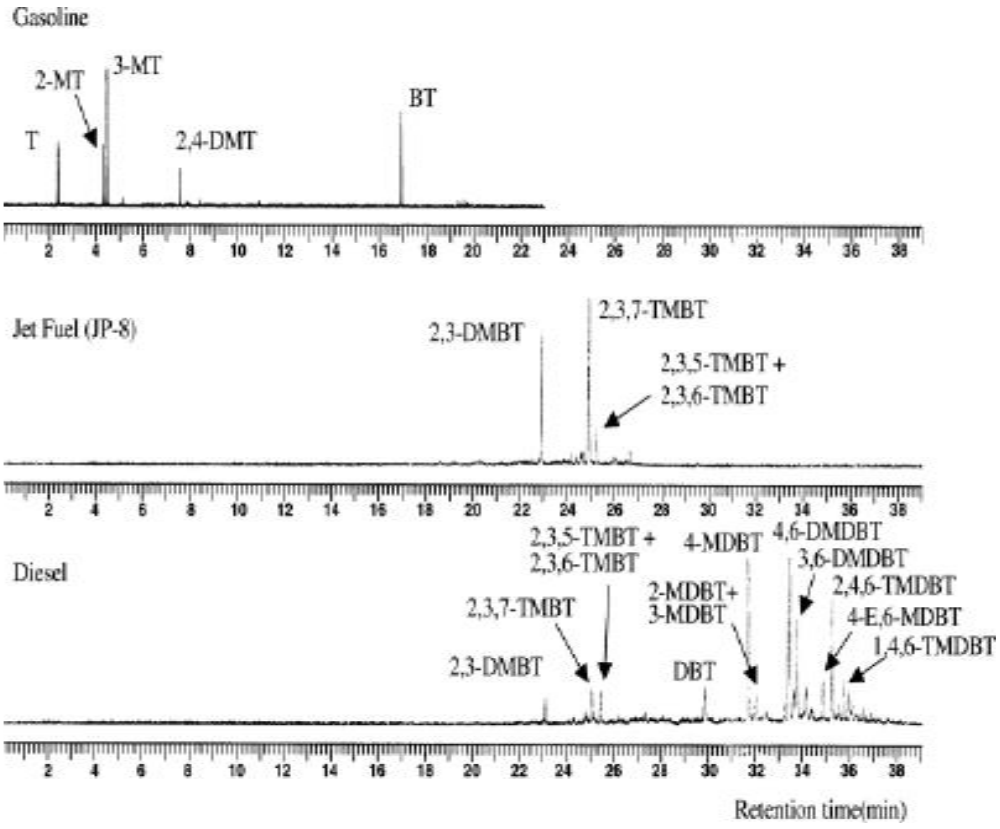

Figure 5. GC-FPD chromatograms for gasoline, jet fuel, diesel Refractory sulfur compounds and DBT and their content in hydrotreated fuels (Song 2003).

2.2. Difficulty of removing sulfur compounds

Sulfur compounds in liquid fuels can be categorized based on the organic sulfur type as shown in Figure 3. Each sulfur species type has different selectivity and reactivity during desulfurization processes (Kim et al 2006). The main sulfur organic in liquid fuels are sulfides, thiophenes, benzothiophenes, and dibenzothiophenes. It is important to note that upon the alkylation of the sulfur organic species, the reactivity and selectivity changes. The hydrodesulfurization is very effective in removing sulfides but limited in removing some refractory sulfur organic compounds especially DBTs having alkyl substituent on positions

4 or/and 6 due to steric hindrance and electron delocalization around the sulfur atom (Ito et al 2006). Subsequently, these molecules are preventing the sulfur atom from interacting with the catalyst surface (Dastgheib 2012; Song and Ma 2003). Figure 4 shows that the dibenzothiophenes have lower reactivity compared to benzothiophenes and thiophene. On the other hand, alkylated benzothiophenes have lesser reactivity and the higher boiling point sulfur organic compounds have lesser reactivity towards to hydrodesulfurization in general.

Furthermore, in order to increase the efficiency of HDS, the operating conditions have to be altered including temperature, pressure, catalyst type, reactor size, and contact time. Therefore, achieving the EPA tighter specifications require an increase in the volume of the catalyst bed or activity by more than a factor of three, for example (Shirashi et al 1998; Song 2002). Applying high temperature and hydrogen pressure reduces octane and cetane ratings which affect the quality of the liquid fuels (Parsi et al 1996). These HDS limitations motivated the investigations of alternative methods to produce ultra-low sulfur fuels.

2.3 Alternative desulfurization approaches

HDS remains the conventional and most widely used choice for refiners worldwide for desulfurization. Nevertheless, due to its limitations in achieving ultra-low sulfur diesel, there are several desulfurization methods to remove sulfur compounds from light petroleum that can be applied as a complementary step to HDS or standalone unit: adsorption, oxidation, extraction, and bio-desulfurization. As the EPA specifications drop down to below 15 ppmw, HDS of diesel fuel has become more increasingly difficult to

produce. At these tight specifications, the HDS conditions become very severe due to the refractory sulfur compounds in the fuel.

Hydrodesulfurization is the common method for most of the refineries worldwide and it is the sole tool employed to reduce the sulfur content of liquid fuels. However, the hydrodesulfurization process has many disadvantages. The hydrodesulfurization process operates at high temperature and pressure, consumes high and costly hydrogen gas, and requires expensive catalysts. The hydrodesulfurization process is very effective against sulfides and thiols molecules. One major drawback of the hydrodesulphurization is its low efficiency in removing refractory sulfur organic compounds. For examples, dibenzothiophene and 4,6 dibenzothiophene are difficult to be removed by hydrodesulphurization due to steric hindrance over the catalyst. It can be removed with a higher cost by altering the quality and the structure of the catalyst to be selective toward that compound which may not be suitable for other sulfur species (Song 2002; Mohebali 2008). Furthermore, the current sulfur levels in liquid fuels are too high to meet the EPA regulations and several applications such as the fuel cell.

The increasing demand of ultra-low sulfur fuels and the limitation of the Hydrodesulfurization impose the demand to develop more efficient, environmentally, and affordable processes to reduce the sulfur content of liquid fuels. The refineries worldwide are facing the challenge of producing liquid fuel with sulfur levels below 15 ppm or even to levels below 1 ppm for fuel cell applications. Using Hydrodesulfurization to achieve the ultra-low sulfur is very difficult since severe conditions are required due to the refractory sulfur compounds. The refractory sulfur compounds have low reactivity compared to thiols and sulfides. Furthermore, any change of the basic structure of the compounds reduces the

reactivity even further due to the steric hindrance. For example, when a methyl group is attached to the 4- or 6- position of Dibenzothiophene, the reactivity is reduced marginally. Furthermore, in order to refiners intend to achieve the EPA sulfur limits using convention hdyrodesulfurization, the volume of the catalyst bed or the catalyst activity must be increased by at least a factor of three. (Berrigan thesis). In addition, hydrodesulfurization degrades the quality of liquid fuels because the severe HDS process can saturate the aromatic rings and olefins which reduce the octane number for naphtha, and reduces the lubricant of diesel due to saturation of aromatics. Therefore, alternative desulfurization methods have been explored in the literature with the following objectives: removing of refractory sulfur organic compounds from liquid fuels without affecting their quality, reducing the hydrogen consumption and operational cost, and achieving the EPA sulfur tighter regulations and/or fuel cell applications.

Note that the HDS reactivity toward refractory sulfur organic compounds is reduced by an order of magnitude for every aromatic ring present in the compound. The order for HDS reactivity for organosulfur compounds are as such: thiophenes > benzothiophenes > dibenzothiophenes. Thus, the need emerges for another desulfurization methods that can be used to achieve the EPA specification for diesel and other liquid fuels. Therefore, the need for complementary steps or alternative methods that reduce the sulfur levels in liquid fuels and achieves the EPA limits and fuel cell applications is growing.

Further desulfurization applications were developed by researchers worldwide for desulfurization (Figure 6) including: Biodesulfurization [Mohebali and Adrew 2008; Soleimani et al 2007), desulfurization by precipitation (Shairullah et al 2009; Shirashi

2001) oxidative desulfurization (Dehkordi et al 2009; Ali 2009), photochemical desulfurization, membrane desulfurization, extractive desulfurization and adsorptive desulfurization (Tang et al 2008; Zhang et al 2005).

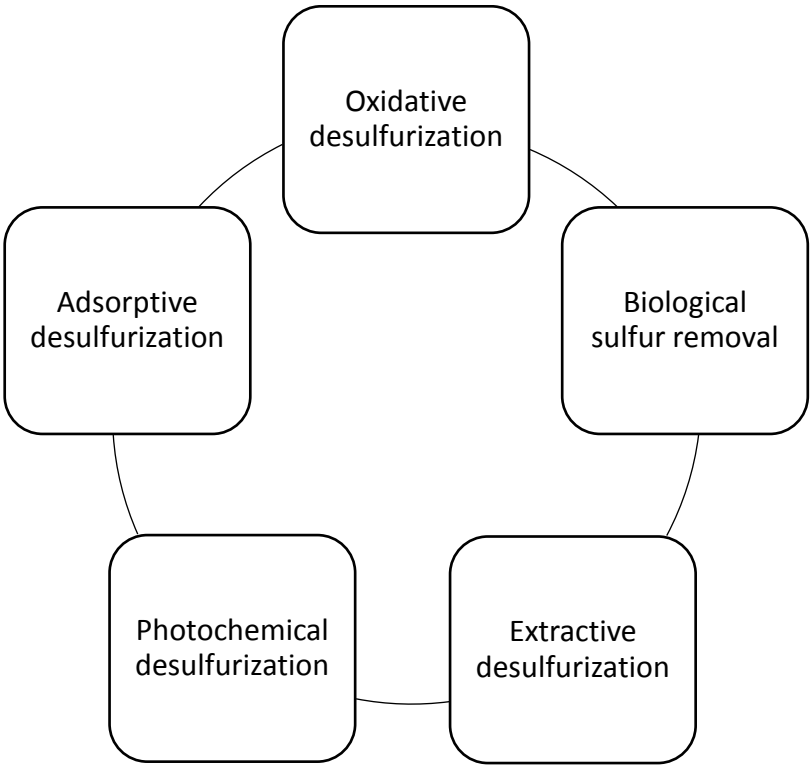

Figure 6. Liquid fuels Desulfurization methods.

2.3.1 Oxidative desulfurization:

Oxidative desulfurization (ODS) is a recently developed as an alternative approach for the production of ultra-low sulfur fuels. ODS involves two steps and the first step is the oxidation of the sulfur compounds into sulfoxides and sulfones using an oxidant. Figure 7 below shows the oxidation of thiophene into sulfoxide as an example of the first step. The second step, due to the polarity characteristic of sulfoxides and sulfones, they can be removed by adsorption, extraction, decomposition or distillation techniques.

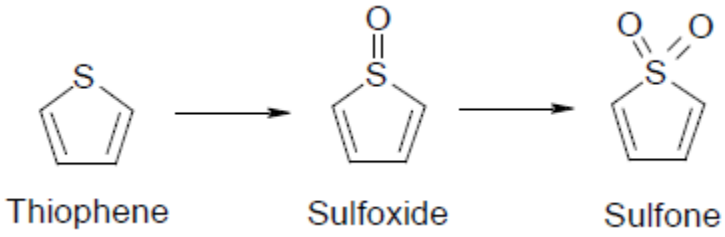

Figure 7. Thiophene oxidation to sulfoxide and then sulfones during ODS process (Levy 2002).

The sulfur organic compounds behave differently as they undergo the oxidation process. The compounds structure and the environment of the sulfur atom plays a major role in determining the reactivity at the oxidation process. For example, the 4, 6-DBT has higher oxidation process reactivity than the BT according to the electrophilic addition mechanism for the oxidation of sulfur. This is mainly due to the high electron density on the sulfur atom. The reactivity order of the sulfur organic compounds is varied based on the oxidant and catalyst (Collins et al, 1997). Furthermore, it is important to address that all categories of sulfur compounds are reactive towards ODS. The process has shown to be effective in removing all of the sulfur from diesel fuel streams including the polynuclear aromatic family of sulfur compounds including substituted DBT (Levy 2002; Shiraishi 2004; Yazu 2001).

ODS is a promising desulfurization tool where several studies were conducted on commercial and synthetic diesel oils showed the ability of ODS to reduce total sulfur in light oil to less than 0.1 ppm of sulfur while recovering the sulfur organic compounds.

Dasgupta et al 2009, used hydrogen peroxide-formic acids as an oxidizing reagent to desulfurize a 500 ppm diesel fuel. The results showed a complete conversion of the DBT into DBT-sulfones where the DBT-sulfones can be removed easily by extraction or adsorption.

ODS has the advantages of ambient operating conditions and the absence of hydrogen. Furthermore, ODS has the ability to reduce sulfur content to less than 1 ppm of sulfur in liquid fuels which allows them to potentially used as a feed for fuel cell applications. On the other hand, the ODS limitation is economic feasibility. The use of hydrogen peroxide as an oxidant is affecting the economic factor of the process. Moreover, it is important to consider the other factors such as, manufacturing, concentrating, transporting, and storing oxidizers. All of these factors with varying severity can influence the economy of the process.

Although ODS shows some economic feasibility limitations, it is widely developed for commercial use. There are three commercial processes reported in the literature. Petro Star, Inc. reported an ODS process where peroxacetic acid is used as an oxidant followed by solvent extracting. Peroxacetic acid is formed by mixing hydrogen peroxide and acetic acid. Unipure Corp and ChevronTexaco developed the ASR-2 process which is based on two liquid phase reactive extraction using an organic acid mixture containing hydrogen peroxide. The extraction of the sulfones is accomplished by methanol which separated from the methanol-sulfone mixture using flash distillation (Levy 2002). Alumina is used to neutralize any remaining sulfones in the treated diesel. SulphCo, Inc. licenses the third ODS technology. The process involves the in situ generation of hydroxyl radicals by ultra-sonication of water-oil emulsion in the presence of proprietary hydrogen peroxide

generating catalyst but the selectivity in this process is likely to be low. In this process, the hydroxyl and atomic hydrogen radicals react with hydrocarbons in high temperature and pressure center of imploding cavitation.

2.3.2. Biological desulfurization

Biodesulfurization (BDS) has a growing interest due to its "Green Chemistry" advantages (Grossman et al 1999; McFarland et al 1998; Qi et al 2007). The target of biodesulfurization is that microorganisms remove sulfur compounds selectively from hydrocarbon fuels at mild conditions. In other words, the BDS has to remove the organo-sulfur compounds present in the fuels without altering the carbon structure. (Kertesz 1999) proved that some microorganisms have the ability to selectively consume sulfur in the thiophenic compounds and thus reduce the sulfur content in the fuel. Furthermore, (Bassi et al 2007; Nair 2010) illustrated that both aerobic and anaerobic microorganisms are effective in the desulfurization process while protecting the aliphatic and aromatic contents of the fuel. Therefore, the major challenge of BDS is the isolating or designing a microbial strain that can be used to produce ultra-low sulfur content liquid fuel and be characterized with higher efficiency. Several literature papers considered the application of BDS for the removal of sulfur organic compounds especially the least reactive ones in the HDS including the sterically hindered alkyl-DBTs (Ball and Mahebali 2008; Monicello 2000). Some researchers recommended BDS to be used as a complementary step to HDS in order to accomplish the removal of the remaining sulfur compounds especially the ones that are least reactive toward HDS. Other researchers proposed employing BDS before HDS in order to reduce the hydrogen consumption (Monicello 2000).

The BDS method has several challenges that need to be improved in order to be practical. The first challenge is the slow sulfur compounds metabolism. For example, it takes the sulfur metabolizing bacteria 24 hours to reduce the sulfur content of diesel fuel from 535 ppm to 75 ppm (Li 2003). In addition, the biological system must be kept alive in order for the desulfurization process to a function which is difficult in the conditions found in most refineries. pH, temperature, and dissolve oxygen concentration have a strong effect on the desulfurization rate. (Olmo 2005). Also, another BDS challenge is the immobilized cells activity and lifetime is limited (Borole 2002; Gray et al 2003). The major drawbacks of biocatalyst are the low activity and low stability. (Kertesz 1999; Bassi et al 2007; Nair 2010). All of these factors must be studied and improved to make the BDS a practical desulfurization approach.

2.3.3. Extraction desulfurization: ionic liquid (ILs), organic solvent

Extraction desulfurization (ILs) is another promising approach that can be used for the production of ultra-low sulfur diesel. Extractive desulfurization is considered a promising desulfurization approach because of the low operation cost. Extractive desulfurization operates at ambient conditions where no hydrogen is consumed. Furthermore, extraction desulfurization can be applied to all middle distillates using convention extraction solvents or Ionic Liquid distillates. Extraction desulfurization can be conducted by ILs.

Extraction desulfurization using conventional solvent is used to remove the sulfur compounds from liquid fuels by applying a solvent that has higher solubility toward the organo-sulfur compounds contained in the fuel than the hydrocarbons. There are several factors that govern the process: selecting the appropriate solvent, melting point, boiling

point and surface tension. There are several solvents that have been examined for the sulfur organic removal including acetone, carbon disulfide, ethanol, dimethyl sulfoxide (DMSO), n-butyl alcohol, methanol, lactones (i.e., gamma butyrolactone), N-containing solvents and water (Dastgheib et al 2012; Aida and Funakoshi 1998; Forte 1996). Due to the slight polarity difference between the sulfur organic compounds and the aromatic hydrocarbons, the sulfur organic removal capacity of the extractive desulfurization process is poor. The sulfur removal capacity can be improved significantly when the sulfur compounds are oxidized then extracted. (Topalova and Toteva 2007) used a two-stage extraction process using a dimethylformamide as a solvent. The results indicated 83.5 % sulfur removal. (Bailes 1981), examined the sulfur organic compounds and aromatics extractability by examining several solvents like DMSO, acetonitrile, and tetramethylenesulfone at ambient conditions. Among these solvents, acetonenitrile was the most suitable solvent for light oils and distillates.

Extraction desulfurization using Ionic Liquids is another approach that proven to be more efficient in removing sulfur organic compounds. The definition of Ionic Liquids (ILs) is salt in the liquid state. ILs have the flexibility advantage of modulating the hydrophobic or hydrophilic nature by altering the cations and anions. Datsevich et al 2001 tested several ILs like tetrafluoroborate, Chloroaluminate, and hexafluorophosphate are for the deep diesel desulfurization. The results showed that these ILs are efficient in the extraction of DBT derivatives contained in diesel oil. The extraction achieved 80% of the sulfur organic compounds were successfully removed by using a five-stage-extraction process operated at a temperature of 60 °C.

ILs hydrolytic instability makes the application difficult and several kinds of literature considered the use of stable ILs. In addition, ILs regeneration is another major challenge. The conventional regeneration using distillation or stripping was inefficient due to the low vapor pressure of the sulfur compounds contained in the ILs. The best results were obtained when combining the ILs approach with the oxidative desulfurization approach and it was reported that 96.1% desulfurization rate was achieved using the combined approaches (Zhu et al 2009).

2.3.4. Photochemical Desulfurization

In the photochemical desulfurization process, liquid extraction using a polar solvent such as water or acetonitrile is applied to remove the sulfur compounds. Afterward, the photochemical oxidation is carried out in the solvent phase that accumulates sulfoxides and sulfones in the polar phase (Thomas2008).

2.3.5. Adsorption desulfurization: definition and Challenges

Adsorptive desulfurization is a promising method that has the potential to produce Ultra Low Sulfur fuels at 1 ppmw for liquid fuels and fuel cell applications. The researchers worldwide have worked in developing adsorbents material that can be used to achieve ultra-low sulfur levels at 1 ppmw of sulfur in liquid fuels for fuel cell applications. Adsorptive desulfurization uses a solid adsorbent material that has a selectively adsorb sulfur compounds from fuel feeds. It is one of the most economical ways for removal of sulfur compounds from liquid fuels where it can be operated at room temperature and under atmospheric or low pressure. Adsorptive desulfurization process can be applied to produce high-quality fuel oils with low sulfur content. Furthermore, It can be used as a

complementary process to hydrodesulfurization in removing efficiently refractory sulfur compounds from the liquid fuels such as benzothiophene (BT), dibenzothiophene (DBT) and 4,6-dimethyldibenzo-thiophene (4,6-DMDBT) which are difficult to be removed by conventional methods. Adsorptive desulfurization can be used for the removal of sulfur organic compounds in efficient and economical manners due to: low energy consumption, ambient temperature, no pressure operations, little or no hydrogen consumption, the feasibility of adsorbent regenerations, and the availability of a broad range of adsorbents. There are a lot of adsorbents materials that are under research and development worldwide such as zeolite, microporous coordinated polymers, activated carbon, nickel based adsorbents, and metal sulfide based adsorbent.

2.4 Adsorption theory

Adsorption is a process of accumulation of one substance over another. Adsorption desulfurization involves the utilization of a solid material (adsorbent) with the aim of selectively adsorb sulfur compound from liquid fuels. There are two types of adsorption desulfurization: reactive and non-reactive. In the reactive adsorption type, the adsorbent is used to strip of the sulfur atom from the organosulfur compounds while the rest of compound (hydrocarbon) is recovered. This type involves Chemisorption that includes ê transfer leading to bond cleavage and formation. For the other type of adsorption (non-reactive), the adsorbent accumulates the organosulfur compounds on the surface (physisorption) as a whole at mild operating conditions (<100 °C). Then, when the adsorbent is saturated, the organsosulfur compounds will be desorbed using high temperature or solvent and the adsorbent will be regenerated.

A detailed comparison between the two types of adsorption: chemisorption and physisorption are shown in Table 2. The physisorption is due to Van der Waals forces and electrostatic forces in permanent dipole moment molecules. These types of physical forces are a relatively weak, attract a molecule to the surface without altering the adsorbate molecule. The chemisorption involves the formation of a strong chemical bond between adsorbate molecules and the surface, unlike the physisorption. Due to the covalent bonds are broken between atoms at the surface of the adsorbent, the surface of the adsorbent has at least one free valence that leads to force unevenness at the surface and the free valences net surface energy. The chemisorption involves molecular interactions with these free valences. Thus, the adsorbent surface is covered with monolayers. If the chemisorption involves the dissociation of the adsorbed molecules, it is called dissociative adsorption. It is important to note that some molecules adsorb chemically through π-electrons and lone pair electrons with undergoing dissociation. They only participate in free valences through non-dissociative adsorption (Bond, 1987).

Table 2. Comparison of chemisorption and physisorption.

Trait	**Chemisorption**	**Physisorption**
Enthalpy of adsorption	40-800 kJ/mol	8-20 kJ/mol
Activation Energy	Small	Zero
Temperature	Depends on E_a ,usually low	Depends on Boiling point, usually low
No. of layers adsorbed	One	One or more
Trends	Activated, may be slow or irreversible, involves e-transfer leading to bond formation	Rapid, non-activated, reversible, van der Waals forces, electrostatic interactions

The target of the adsorption process is to produce ultra-low sulfur fuels using an adsorbent that selectively removes the sulfur compounds particularly refractory sulfur compounds without altering the qualities of the fuel. The main challenge of the adsorption desulfurization is to Synthesize the ideal adsorbent that contains several qualities. First, the ideal adsorbent should have a significant adsorption capacity. In addition, the operating condition for the perfect adsorbent should be mild temperature and pressure. The adsorbent should be regenerated easily and environmentally friendly. Finally, the cost of the adsorbent is preferably low and has high selectivity towards sulfur compounds.

There are a few successful adsorption desulfurization processes that are applied commercially. Black and Veatch Pritchard Engineering Company have developed the IRVAD process to remove sulfur organic species from FCC gasoline via reactive adsorption with consuming hydrogen. The adsorbent beds are adsorbed and regenerated continuously using moving bed technology. The process employs multi-stage absorber with alumina based adsorbent under the operating condition of 240°C and low pressure with no hydrogen.

The S-zorb process, which was developed and commercialized by Conoco Philips, is a reactive adsorption process that process low sulfur gasoline (ConocoPhillips, 2008). The S-Zorb process operating conditions are between 340-420° C in terms of temperature and hydrogen 30-300 psi in terms of hydrogen pressure. The thiophenic compounds in gasoline are removed in a fluidized bed using a solid adsorbent that is made up of zinc oxide, alumina, silica, and nickel oxide (Ma et al 2005; Babich and Moulijn 2003). Regeneration

of the spent sorbent is conducted using nitrogen then oxidized with air. (Hernandez-Maldonado and Yang 2004).

Another commercial method is the Research Trinagle Institue (RTI) developed the TReND (Transport Reactor Naphtha Desulfurization) which is mainly used for FCC naphtha desulfurization. The TReND process is very similar to the S-zorb with the differences of using a metal oxide of iron or copper promoted by Al_2O_3-ZnO sorbent at high temperature (>400 °C). The process uses a high-throughput transport reactor.

In brief, sulfur occurs in the forms of several compounds including H_2S, sulfides, thiphenes, benzothiophenes, and dibenzothiphenes. As the boiling point of the petroleum distillate fraction increases, as the complexity of the sulfur compounds increases significantly. Hydrodesulfurization is the conventional method of desulfurization and it remains the refiner~~'s~~ choice worldwide. Nevertheless, HDS is expensive and inefficient in producing ultra-low-sulfur diesels. There are several desulfurization methods that are being studied with the intentions of replacing HDS or adding the process as a complementary step. Adsorptive desulfurization is a very promising method due to its simplicity and cost-effectiveness. However, adsorption desulfurization needs to be selective toward sulfur compounds because the process leads to the removal of the aromatic component in the feed. Biological desulfurization has a minimum energy requirement which makes it desirable. However, it is not a feasible process due to the microbial wastes disposals requirements and the storage and handling of bacteria in the industrial harsh environments. Oxidative desulfurization can work with a wide range of sulfur compounds but the need to removal the oxidized products in an addition step separately and the complex chemistry of the process is a major shortcoming.

2.5 Adsorption by activated carbon theory and types

Several materials were used in the literature for the adsorption desulfurization as illustrated in Figure 8, including but not limited to zeolite, microporous coordinated polymers, activated carbon, reduced metals, metal oxides, alumina, metal sulfides, silica, transition metals and metallic organic frames. Among all of these, activated carbon is the adsorbent that is intended to be studied in this thesis. The activated carbon surface is modified with metal oxides, transition metal oxides, and bimetallic oxide mixture.

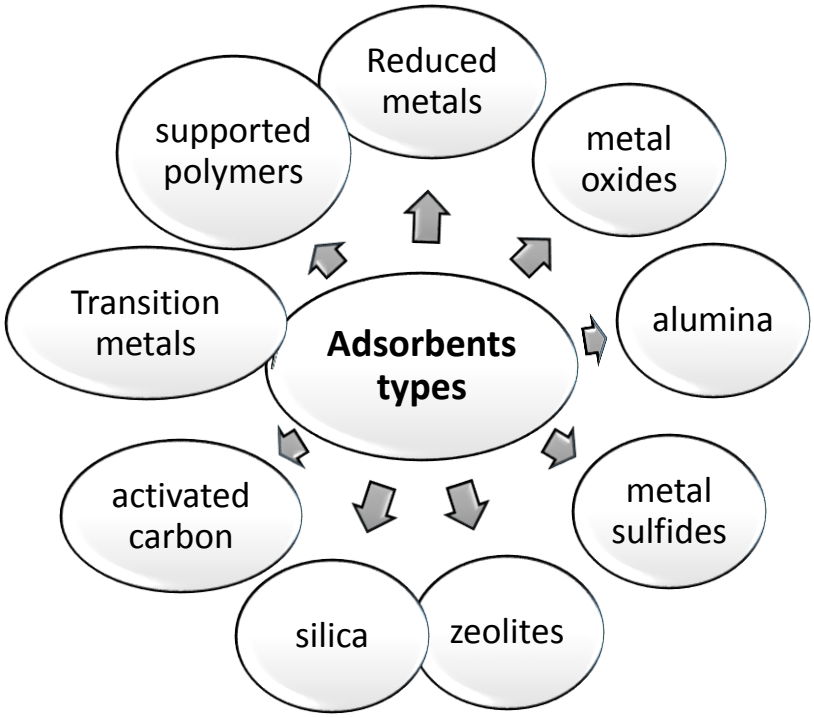

Figure 8. Examples of adsorbent types reported in the literature.

Activated carbon covers a wide range of amorphous based carbon materials that is prepared to exhibit a high degree of porosity, large surface area, and a high degree of surface and variable characteristics of surface chemistry (Dias et al, 2007). All of these criteria make the activated carbon a very effective adsorbent candidate material. Furthermore, activated carbon has been also studied and used as a catalyst and catalyst supports (Derbyshire et al 2001). Several applications already use activated carbon material in the industry including water purifications, dye removal, and wastewater treatment. In the oil and gas industry, activated carbon is used extensively for aromatics removal of benzene, toluene ethylbenzene xylene (BTEX). The research of using activated carbon as an adsorbent for sulfur organic compounds of refractory compounds, in particular, has grown substantially in the recent years. Activated carbon has several criteria that are attractive for the field of adsorption desulfurization. Activated carbon is an efficient and economically feasible adsorbent. Furthermore, activated carbon has low operation cost because it operates at ambient temperature and pressure without the need to hydrogen gas. Activated carbon can be easily regenerated by using high temperature or polar solvent desorption. Due to porous nature, high surface area and large pore volumes, activated carbon can be used in the desulfurization of liquid fuels especially in the removal of refractory sulfur compounds and reduce sulfur levels to below 1 ppm. Activated carbon showed high effectivity in the removal of sterically hindered sulfur organic compound such 4,6 DMDBT from hydrotreated middle distillate at 100 ^{0}C (Savage et al, 1995, Kim et al, 2006, and Zhou et al, 2009)

Several adsorbents of sulfur compounds from liquid fuels have been studied by (Babich and Mouling, 2003). Most adsorbents carry out the adsorption based on the polarity

principal. Activated carbon adsorption is carried out based on more than one mechanisms. There are several complexes or multiple adsorption mechanisms that can be carried out on the activated carbon based on the metallic oxide impurity and the surface functional groups on the carbon. With regard to polarity, the sulfur organic compounds are more polar than hydrocarbons which can be used as a base for separation. Nevertheless, the adsorbents work purely on polarity have low breakthrough capacity. (Shen et al 2001)

The electronic structure of sulfur organic molecules strongly influences its adsorption. The atom has more lone pairs and π-bonds, it will have more negative electrostatic potential. Figure 9 illustrated the order of the electrostatic potential: naphthalene (Nap) < 1-methylnaphthalene (1MNap) < DBT <4,6-DBDBT. When electron donors groups are added to an aromatic ring, they increase the overall electrostatic potential of the molecule. The thiophene electrostatic potential is relatively high. When two aromatics rings are added, the electrostatic potential increases further like the case for DBT. The order of the electrostatic potential and polarity is T > BT > DBT > 46DBT. (Kim et al 2006). The electrostatic potential effect is similar when methyl groups are added to the core organic sulfur molecule since the methyl groups are considered electron donors groups.

There are two types of interaction proposed between the sulfur compounds and the adsorbents: Sulfur metal interaction and π complexation (Shen et al 2011). The π complexation or interaction is a non-covalent interaction that involves π systems. The π system has the ability to interact with metal, an anion, another molecule and another π system on the basis of electrostatic interaction where a region of negative charge interacts with a positive charge. (Anslyn 2005).

DBT can act either as an n-type donor by direct S–M σ bond or as a π -type donor by π complexation bond. The direct S–M σ bond can be achieved by donating the lone pairs of electrons that lies on the plane of the rings on the sulfur atom to the metal. The π complexation bond can be achieved by donating the delocalized π electrons of the aromatic ring to form π-type complexation with the metal ion or the activated carbon. The π complexation mechanism explains the low selectivity for sulfur compounds that is due to the competitive adsorption of the aromatic compounds. The direct sulfur-metal interaction explains the high selectivity for sulfur compounds and the difficulty to remove sterically hindered sulfur compounds e.g. DMDBT.

Furthermore, the activated carbon adsorption capacity and selectivity can be improved by modifying the adsorption surface active sites including Lewis acid sites, useful functional groups, electronic defect centers, micro-structural defects (Shen et al 2011). High dispersion of metallic centers, the presence of surface acidic groups, and strong interaction of metals with DBT via S-M σ bonds or with disturbed π- electrons of aromatic rings of DBT can all enhance the adsorption of DBT over activated carbon adsorbents (Seredych and Bandosz 2007). Therefore, in order to increase the adsorption capacity of activated carbon, the structure can be altered by impregnating metal oxides. In addition, the acidic active sites can be increased by acidic treatment which enhances the desulfurization performance.

During the survey of the literature, the interaction between organometallic complexes and thiophene is studied by PSU-SARS (Song and Ma 2004; Song 2002; Ma et al 2002; Velu et al 2005). Thiophenic molecule participation in bonding can be through the two lone pairs of electrons that are located in the sulfur atom where one pair is on the plane of the

ring and the other pair is on the π-system. The case of the DBT is similar to the thiophene yet DBT has higher electrostatic potential due to the presence of two aromatic rings. The sulfur and metal can interact directly via the lone pair of electrons on the sulfur atom and/or by forming π-complexation with the metal.

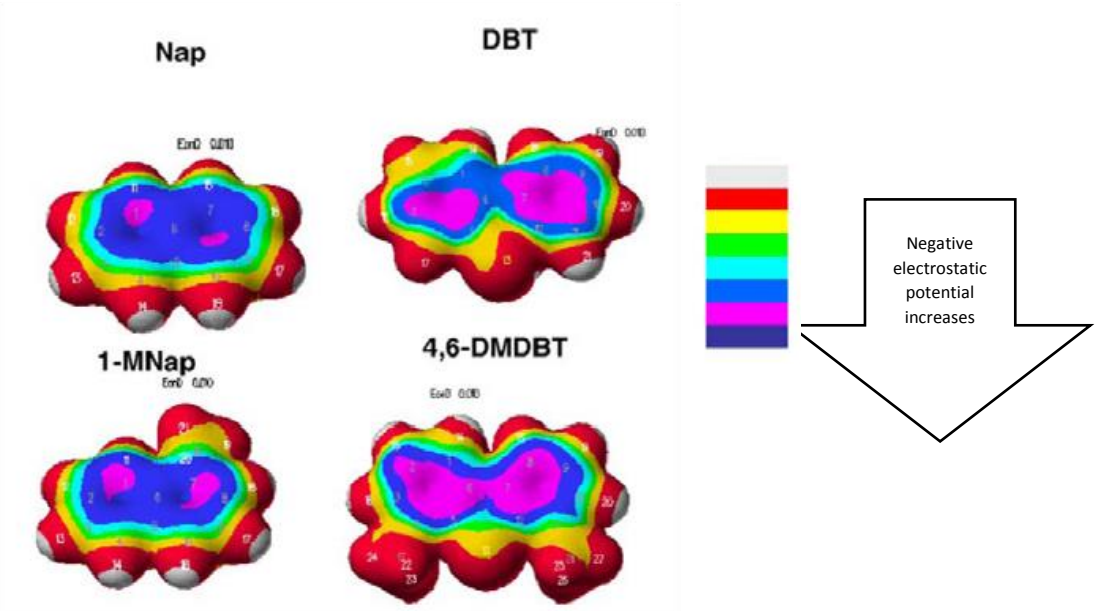

Figure 9. Electrostatic potential on electron densities for aromatics and organic sulfur compounds(Kim et al 2006).

The sulfur-organometallic complex interaction can occur via several coordination geometries. Figure 10 shows several interacting geometries studied by PSU for SARS which stands for selective adsorption for removing sulfur process at ambient temperature and pressure with hydrogen consumption. Figure 10 shows that Geometries η^1S and S-μ3 represents the direct sulfur-metal interaction. The four η^1C, η^2, η^4, and η^5 geometries represent the π-π complexation interaction mode which is via one or more C=C double

bond. The two configuration η^4, S-μ2, and η^4, S-μ3 involve both types of interaction the π-complexation and direct Sulfur-Metal interaction.

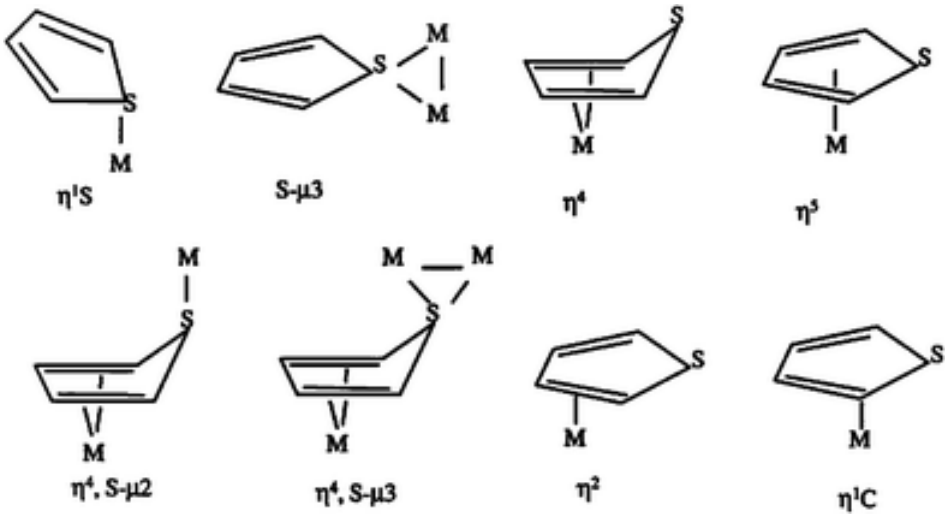

Figure 10. Coordination geometries for thiophene with metal species in organometallic complexes (Ma et al 2002).

Activated carbon has a high selectivity for 4,6-DMDBT which is the opposite trend for adsorbents that perform through a direct sulfur-metal interaction. On the other hands, activated carbon has a high selectivity for molecules with a more negative electrostatic potential. Hernandez-Maldonado et al 2003) claim that activated carbon adsorption can be explained by Van der Waals and electrostatic interaction and thus activated carbon is selective to larger molecules with high polarizabilities over thiophenic compounds. This is not the case for nitrogen compounds. Therefore, the electrostatic potential property alone cannot explain the mechanism. (Yang 2003) used activated carbon guard bed to adsorb

aromatics and large sulfur molecules which increase the adsorption capacity of Cu(I)-Y-zeolite for smaller sulfur molecules. (Haji and Erkey 2003), studied the adsorption of DBT and Naphthalene used carbon aerogel adsorbent with different pore sized. They concluded that at larger pore size (21 nm vs. 4 nm), the DBT showed a higher capacity and higher sulfur adsorption rate. Anie and Bandosz, 2005 concluded that an important role is played by the chemistry of the carbon surface in the sulfur organic compound adsorption. The sulfur capacity has increased by increasing the oxygen-containing functional metal groups (e.g. NiO) and they are several surface chemistry parameters that play a role in the adsorption of DBT over activated carbon from liquid fuels. Surface functional groups, the density of acidic sites, carbon pore sizes, and surface chemistry of activated carbon are parameters that can be optimized to enhance the activated carbon capacity.

Ma et al 2005 emphasized the activated carbon adsorption mechanism using the π-complexation concept is not sufficient due to the competition between the refractory sulfur organic compounds, aromatics and olefins for the activated carbon active site. (Zhou et al 2006) conducted a study for the activated carbon selectivity trend. Using different carbon material types, the order of the selectivity remained the same and adsorption selectivity was: BT < naphthalene < 2-methylnaphthalene < DBT < 4-MDBT < 4,6-DMDBT. They found the selectivity trend is opposite to that of Ni-based adsorbents. Methyl groups increase the selectivity for activated carbon to sulfur adsorption, they suggested the electron donors to the aromatic ring are increased with π-electron density and the electrostatic potential.

Huntley et al 1996 conducted another study on the adsorption and decomposition of thiophene on nickel metal oxide adsorbents at ambient conditions. Based on this study, they suggested that thiophene adsorption on nickel was through direct sulfur-metal and π-π interactions. This is relevant to another study (Ma et al 2002) because several metal oxides including nickel have been loaded on the activated carbon. As illustrated in Figure 10, the direct sulfur-to-metal (S-M) interaction could occur via two coordination geometries η_1S and S-μ3. In addition, as per the molecular orbital π-calculations, it is suggested the highest occupied molecular orbital (HOMO) on the sulfur atom can interact with the lowest unoccupied molecular orbital (LUMO) of the metal species. The HOMO for thiophene (T), benzothiophene (BT), and dibenzothiophene (DBT) is on the sulfur atom, but the HOMO for aromatics benzenes and naphthalene is on the six-member ring. This explains the selectivity of activated carbon impregnated with metal oxides toward organosulfur compounds.

Tatarchuk 2011 concluded that the metal oxide~~s~~ support materials in general, TiO_2, in particular, contributes to the adsorption sulfur capacity. It is postulated that during calcination of the adsorbents, active sites that include some surface acid functional group were formed. TiO_2 acts as an electronic promoter in different catalytic processes (Ramirez et al 2004; Rana et al 2003)

In conclusion, multiple mechanisms are carried out for the activated carbon adsorption of organosulfur compounds in the model or liquid fuels. The mechanisms that govern sulfur adsorption with many adsorbents material including activated carbon are not yet well understood (Kim et al 2006; Bhandari et al 2006). Several mechanisms can explain the enhancement of activated carbon performance. In summary: polarity, surface chemistry,

the π-complexation, direct sulfur-metal interaction, Lewis acid sites, useful functional groups, electronic defect centers, are micro-structural defects important factors for material to be understood. High dispersion of metallic centers, the presence of surface acidic groups, and strong interaction of metals with DBT via S-M σ-bonds or with disturbed π-electrons of aromatic rings of DBT can all enhance the adsorption of DBT over activated carbon adsorbents in particular and organosulfur compounds over adsorbents in general. Each parameter can be studied by selecting different conditions and observe the desulfurization performance changes.

Further effort was conducted in order to summarize the literature review based on the adsorption desulfurization by using fixed bed absorber process are listed in Table 3. It is noted that so several materials were used as adsorbents including activated carbon, zeolites, metal oxides, metallic organic frames, nickel-based adsorbents, and silica gel. The fixed bed absorber process tested by different conditions ranging from ambient temperature to 200 ^{0}C. Most of the testing for activated carbon adsorption was conducted using the batch process as seen in Table 4. In addition, the model fuels contained several aromatic contents and some authors included olefins to mimic their behavior in liquid fuels some literature papers added nitrogen compounds to study their interferences during the adsorption process. Some authors used model fuels while others used real fuels. It is noticed that the breakthrough capacity of the adsorbent differs significantly between real fuels in comparison with model fuels. This indicates that the model fuels used are not reprehensive of the real fuels. Therefore, in this study, the effect of the model fuel composition on the adsorbent performance is studied.

Table 3. Literature Summary of fixed bed adsorption desulfurization.

Author	Feed and Spec.	Reactor Condition	Adsorption material	Product and Finding
Zhang, 2015	Model diesel ([S]=300 ppm, BT, DBT, DMDBT in n-octane) Diesel 187.2 ppmw	Fixed bed at STB Flow=1.0ml/40 min	Ag/Al-SBA-15, Ni/Al-SBA-15, Ce/Al-SBA-15	Desulfurization capability of Ni/ASL60-4 can be enhanced a total of 250% compared to Ni/AS20-1
Xu, 2014	Jet-A fuel 1037 ppm S	Fixed bed	10NiO–CeO2/7.5Al2O3–SiO2	1.98 mg S/g
Sarda, 2012	Commercial diesel 325 ppm S	At STB, flow rate 0.1-2 ml/min.	Ni/Cu loadings onto ZSM-5 (Si/Al = 20) and activated alumina	496 mg S/kg
Bu, 2011	Diesel Mono aromatic 30.9 % Di aromatic 5.3 % Tri aromatic 1.4 % PASH 0.26 % 398 ppm S Model diesel Hexadecane79.74 N-Heptylbenzene= 20% 4.6DMDBT=0.27 5	75 °C 6-15 g of AC V of acsorbent= 26 cm^3 LHSV=0.5 h^{-1}	Activated carbon materials obtained from different sources	adsorption selectivity increases as follows: naphthalene < fluorene < dibenzothiophene < 4,6-dimethyl dibenzothiophene < anthracene < phenanthrene
Teymouri, 2013	ULSD, 300 ppmw of 4-MDBT.	Fixed bed at 200 °C, 0.3 mL/min of feed flow rate	palladium containing MCM-41	adsorption capacity and total sulfur adsorption capacity: 1.67 and 2.35 mg sulfur/g adsorbent
Kim, 2006	Model diesel 10% aromatic Sulur and nitrognent=687, 303 ppm, respectively.	At STB. (LHSV) of 4.8 h-1.	(AC, activated alumina and nickel-based adsorbent	AC:7.15 mg S/g ads. activated alumina 1.57mg S/g ads. nickel-based adsorbent 2.18mg S/g ads.

Ma, 2002	model diesel: 0.167 wt.% of DBT and 0.196 wt.% of 4,6-DMDBT. 12 wt.% of aromatics 4.7 wt.% olefin real diesel and JP-8 Jet fuel	Fixed bed at STB	5.0 % transition metal supported on silica gel.	The saturated adsorption capacity is 0.123 mol of sulfur per mol of the metal compound
Song, 2013	Model gasoline: 1-octane solution of refractory sulfur compounds (T, BT) and toluene, pyridine or cyclohexene	Fixed bed at STB	Cu–Ce bimetal ion-exchanged Y zeolite	Adsorption selectivity: BT > T. Effect on the metal ion-exchanged Y zeolites for sulfur removal was in the order: pyridine > cyclohexene > toluene.

Table 4. Literature review summary of adsorption desulfurization using activated carbon based material.

Author	Feed and Spec.	Reactor Condition	Adsorption material	Product and Finding
Alhamed and Bamufleh 2009	Model diesel DBT, in n-octane)	Batch process for 48 hours.	Granular activated carbon particle size 1.71 mm.	92.6 % sulfur adsorption.
Loh et al, 2001	real diesel 398 ppmw model diesel oil 400 ppmw of S (prepared by adding sulfur compounds, such as 4,6-dimethyldibenzothiophene, and various mono-aromatic, di-aromatic and tri-aromatic compounds to hexadecane	Batch and fixed-bed adsorption systems	Commercial activated carbon	96 % sulfur adsorption. Adsorption selectivity increases as follows: naphthalene< DBT< 4,6-DMDBT< anthracene < phenanthrene.
Chandra and Kumar 20120	DBT dissolved in iso-octane	C0: 100–900 mg/L), adsorbent dosage (m: 2–22 g/L), time of adsorption (t: 15–735min) and temperature (T: 10–508oC)	commercial activated carbon (CAC)	Highest removal was achieved at these conditions: m=20 g/L, t=6hr and T=308 oC.
Al-Zubaidy et al 2013	Diesel 410 ppmw of S	Batch process At STB	CAC and Carbonized date palm kernel powder	54% sulfur removal.

Zhou et al , 2009	model diesel fuel (MDF)containing 400 ppmw S in a 50:50 mixture of decane and dodecane 100 ppmw of each of the following: BT, DBT, 4-MDBT, and 4,6-DMDBT	Fixed bed LHSV=4.8 at STB.	Calgon AC (1800 m2/g) and Westvaco AC(900)m2/g NHNO3 treated AC	Breakthrough capacity is 6.4 mg/g for Calgon AC and 3.8 mg/g for Wesvaco AC. Mild HNO3 treatment increased the sulfur capacity by over 200 %.
Kim et al, 2006	model diesel fuel containing 687 ppm of S	Fixed bed at STB	commercial activated carbon (1800 m2/g	6.3 mg S/g sorbent prior to breakthrough at around 1 ppmw

CHAPTER 3 EXPERIMENTAL WORK

3.1 Research methodology

The objective of this work is to develop nano-based activated carbon adsorbents that can improve the quality of liquid fuels via reducing the sulfur content suing adsorptive desulfurization. The experimental work will cover the adsorption desulphurization of the liquid fuel by different types of commercially available and synthesized adsorbents. Then, using model diesel fuel, each adsorbent is tested using fixed bed absorber process at ambient temperature and pressure. Once the breakthrough curve is obtained, the total sulfur breakthrough capacity is used to carry out the investigation of the liquid fuel sulfur compounds modifications and the different adsorbent capacity for comparisons. The breakthrough concentration used is 1 ppm of total sulfur.

3.2 Material

The chemicals used or model diesel are: DBT: dibenzothiophene with 98 % purity from Sigma Aldrich., Isooctane: HPLC grade obtained from Fisher Scientific, Toluene HPLC grade obtained from Fisher Scientific. The material and chemical used in the adsorbents fixed bed are activated carbon and H-Y-zeolite (SiO_2/Al_2O_3 ratio of 20:1). The activated carbon is synthesized in-house from tires. The iron (III) nitrate nonahydrate $(FeNO_3)_3 \cdot 9H_2O$) (purity 98%), nickel (II) nitrate hexahydrate (purity 98.5%) and lanthanum (III) chloride hydrate (purity 99.9 %), tungstic Acid (H_2WO_4) (purity 99%) are all obtained from sigma Aldrich.

3.3 Evaluation of Adsorbents

All the adsorbents were tested using the fixed-bed absorber dynamic adsorption experiments. The fixed bed apparatus is illustrated schematically and ł picture in Figure 11 and 12. First, the piping started from the pump through the fixed bed column until final transfer lines are cleaned with chloroform then hexane. Then the lines are purged with nitrogen to flush out any contaminants. The volume of tested adsorbent that was loaded into the column is 1 mL. The adsorbent is weighed and loaded into a vertically configured stainless steel column as shown in Figure 11. The column internal parameters and length are 4.6 mm and 250 mm. The adsorbents were bracketed between two layers of glass walls inside the column. All the experiments were conducted without the consumption of hydrogen and carried out at ambient pressure and temperature.

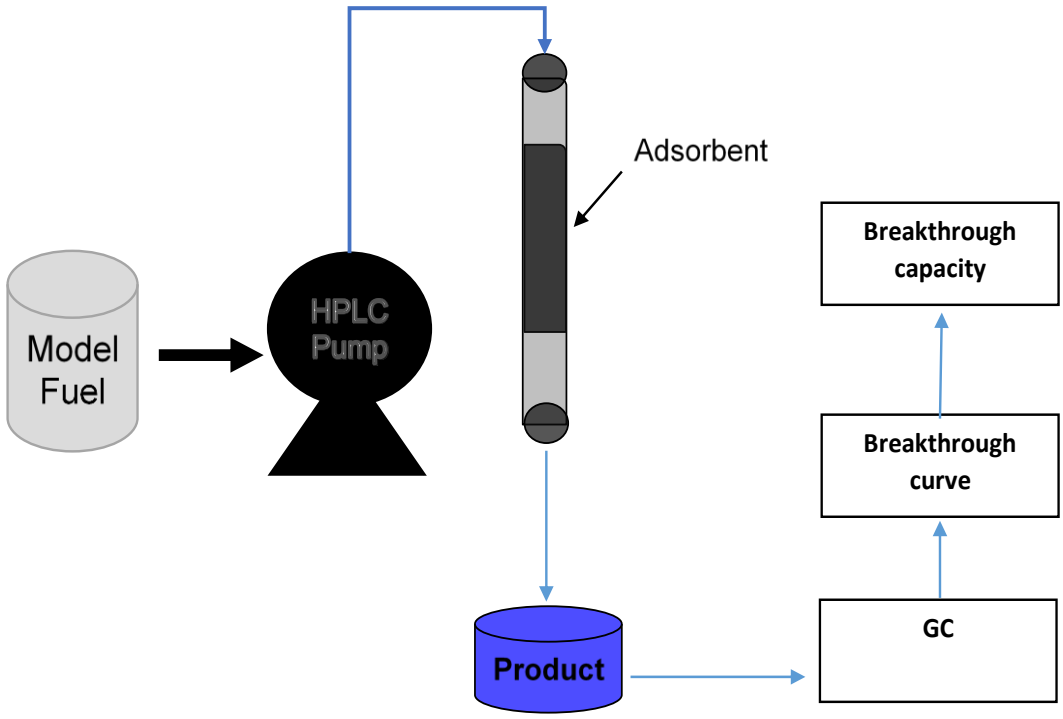

Figure 11. Schematics that represents the fixed bed absorber dynamic process.

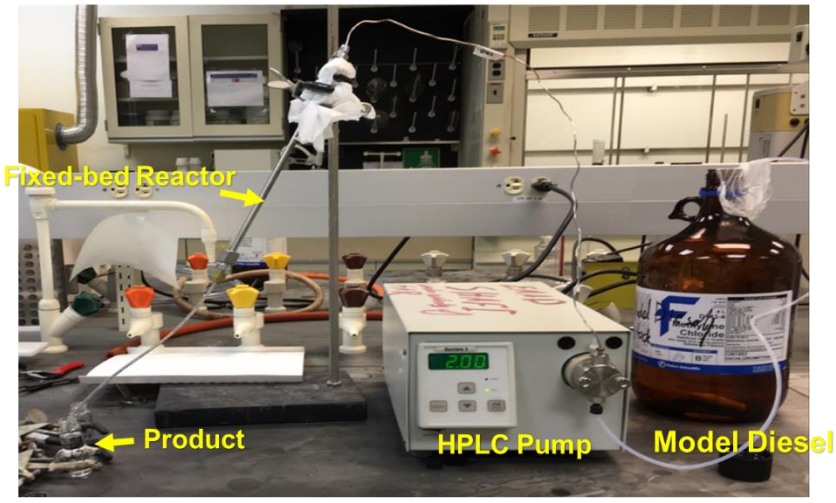

Figure 12. Picture of the fixed bed absorber dynamic process at STB. Fixed bed Absorber experimental conditions: Flow rate=2 ml/minute LHSV=120h^{-1}, Adsorbent volume: 1 mL.

The model fuel was pumped downward into the column at a flow rate of 2 mL/minute. The liquid hourly space velocity (LHSV) is 120 h^{-1} which corresponds to a residence time of 0.5 minute. The pump was calibrated before every experiment to ensure the accuracy of the flow rate. The treated model fuel (product) was collected in vials in regular intervals then weighed to ensure accurate mass balance. Afterwards, the product is analyzed for DBT concentration using GC-FID or GC-SCD. The experiment is carried out until the DBT concentration reaches the initial concentration of the model fuel which depends on the type of model fuel used.

The breakthrough curve for each adsorbent test is constructed by plotting the concentration of the DBT in ppm of each product against the treated mass of the model diesel in gram. The breakthrough point indicates the amount of fuel that can be treated before any detectable sulfur is measured at the outlet. To ensure the reproducibility of the experiment,

the breakthrough concentration is 1 ppm of sulfur. The breakthrough curve, or outlet sulfur concentration as a function of the amount of treated fuel, can be determined experimentally with a fixed-bed flow column the breakthrough capacity is defined as the mass of the model fuel treated to below 1 ppm of sulfur which corresponds to 5.74 ppm of DBT. Figure 13 illustrates the breakthrough curve for activated carbon using model diesel no. 1 (MD-1) which contains 96 ppm of DBT, 16 % toluene, and 84 % isooctane. The breakthrough capacity is calculated using equation (1):

$$q_b = \frac{m_b\, C_0}{1000\, m_{ads}} \qquad \text{Eq. 1}$$

Where $q_b$is the breakthrough capacity in mg DBT/g is adsorbent, C_0 is the initial DBT concentration in ppm, m_b is the model fuel mass at the breakthrough concentration (1 ppm of sulfur which is equivalent to 5.74 ppm of DBT), and m_{ads} is the mass of the adsorbent in g.

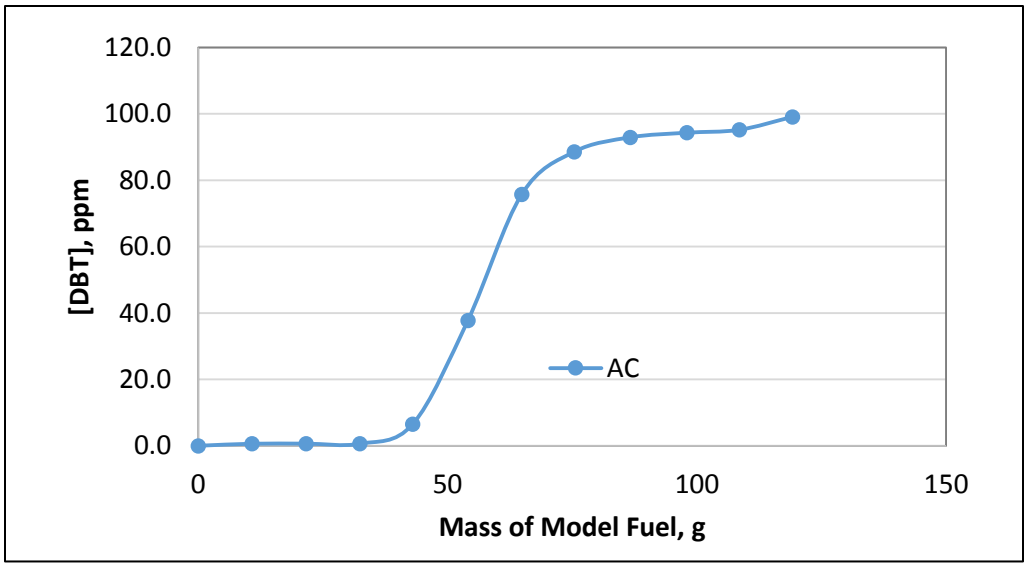

Figure 13. The breakthrough capacity curve for Activated carbon using MD-1.

As shown in Figure 13, the DBT was adsorbed and then detected until 42 g of the MD-1 has been treated. Then, the amount of DBT is measured at each point using GC-SCD or GC-FID. The amount of DBT onward is increasing until saturation and possibly desorption. The breakthrough capacity is calculated using equation 1 and the data are shown in Table 5. The activated carbon voidage and pores are expected retain 3-7% of total volume model diesel during the adsorption process but the selectivity towards desulfurization is maintained. The material balance of model diesel is measured by peak area of toluene and iso-octane after and before adsorption. The result showed the activated carbon retained in voidage and pores about 6% of total toluene and iso-octane. However, Activated carbon impregnated with 2% Fe/AC and 2% Ni/AC showed the 3.8% of toluene and iso-octane were retained in voidage and pores lower than the activated carbon due to the Fe oxide or Ni oxide encountered inside the pores and reduced the texture property of total surface area.

Table 5. The breakthrough capacity of activated carbon in mg DBT/g ads and mg S/g ads.

Ads	**Breakthrough capacity mg DBT/g ads**	**Breakthrough capacity mg S/g ads**
AC	9.25	1.61

3.4 Adsorbent preparation:

The activated carbon used as a support is synthesized using the method reported in the literature (Saleh and Danmaliki, 2016) and (Saleh, 2011). The activated carbon was

obtained by processing waste rubber tires: first, the waste rubber tires were cleaned and dried in an oven at 110 C^0. Afterwards, the produced oil, distilled diesel oil, and black tire crude oil are isolated from the tires by heating at 300 ^{0}C. Then, the materials were placed in a muffle furnace at a temperature of 500 C^0 for five hours for the carbonization to remove the ash and the carbon black. The materials obtained from the previous step were treated with an H_2O_2 solution to oxidize adhering organic impurities. Next, the materials were washed, dried and then activated at 900 C^0 for five hours. Deionized water was used to wash the activated carbon and then the activated carbon was dried in an oven overnight. In order to develop surface acidic functional groups for adsorption enhancement (Saleh, 2015), 4 M HNO_3 was used to treat the activated carbon at a ratio of 1 g AC: 15 ml HNO3 at 90 ^{0}C for three hours. Finally, the activated carbon was washed and dried in an oven at 110 ^{0}C for 24 hours.

Then, the activated carbon structure is modified by metal impregnation in order to enhance the adsorption capacity. The impregnation of metals on activated carbon is accomplished using two different methods: wet impregnation method by precipitation and wet impregnation by ion exchange method.

3.4.1. Wet impregnation by precipitation method:

The wet impregnation method by precipitation uses the steps as shown in Figure 14. First, the metal salt or acid, which depends on the intended metal for impregnation, is diluted with deionized water. Nickel(II) nitrate hexahydrate , iron nitrate, iron impregnation,

tungsten acid and lanthanide chloride were used for impregnation on activated carbon. The concentration of the salt or acid was adjusted according to the desired metal loading on the activated carbon. Then, activated carbon is added after metal salt dissolved in D.I water and mixed for 3 hours at room temperature. Afterward, the precursor is dried in an oven at 80 ^{0}C overnight. Finally, the metal impregnated activated carbon is calcined as shown in Figure 16 under a nitrogen flow of 100 ml/min at 450 ^{0}C for five hours.

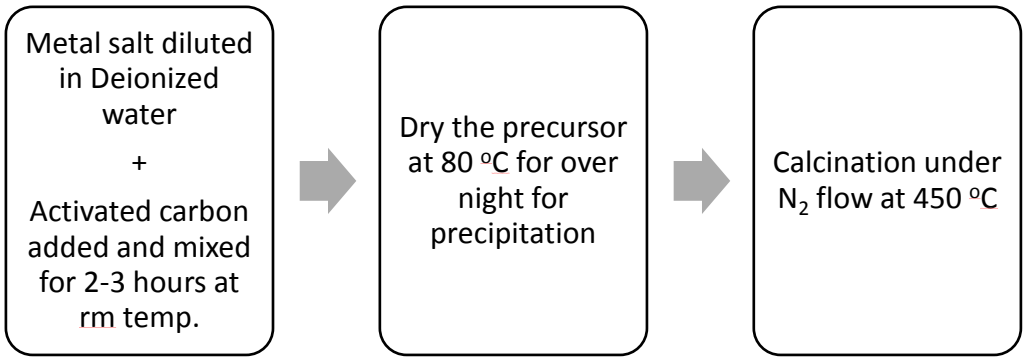

Figure 14. Illustration summary of the Wet Impregnation Method procedure.

3.4.2. Metal impregnation using the ion exchange method:

Figure 15 illustrates a summary of the metal impregnation by using ion-exchange method. First, the weighted metal salt or acid is diluted in 0.5 N NH_3OH and then mixed with Activated carbon for 12 hours at 60 °C. Then, the precursor is washed with deionized water in order to remove the ammonia and the undissolved salts to remove the participation in

the porosity of the activated carbon. The washing can only be stopped when the pH reaches 7. The precursor is dried at 80 ^{o}C for overnight. Finally, the metal impregnated activated carbon is calcined as shown in the Figure under a nitrogen flow of 100 ml/min at 450 ^{0}C for five hours.

The calcination procedure for both methods is the same. First, the adsorbent is placed inside the tube furnace. Then, the temperature is adjusted at 450 ^{o}C under a nitrogen flow of 100 ml/min for 5 hours. Then, the temperature is cooled down slowly to room temperature under the nitrogen flow. When the temperature has cooled down to room temperature, the nitrogen flow is stopped and the adsorbent is removed from the tube and collected. The purpose of the calcination is to increase the amount of oxygen surface groups and modifies the distribution of these groups which increases the surface activity and thus the activated carbon capacity (Zazo et al 2009)

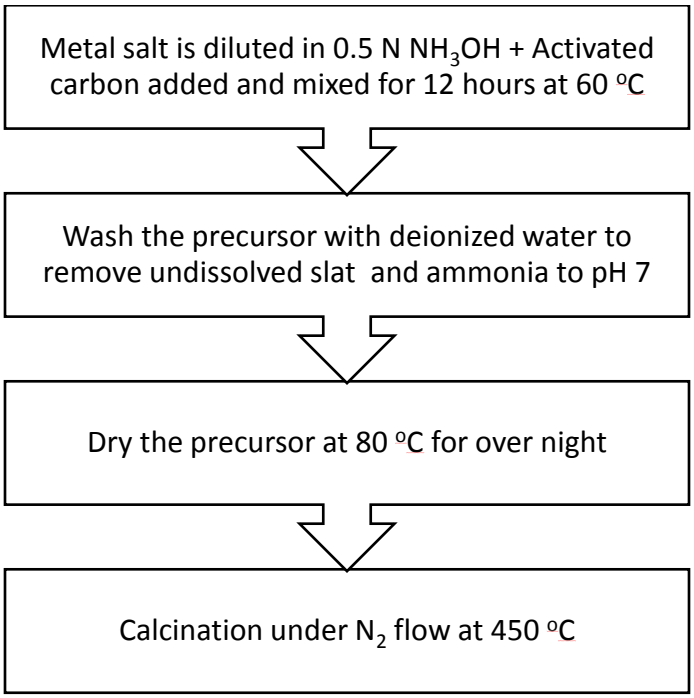

Figure 15. Illustration summary of the ion exchange Method procedure.

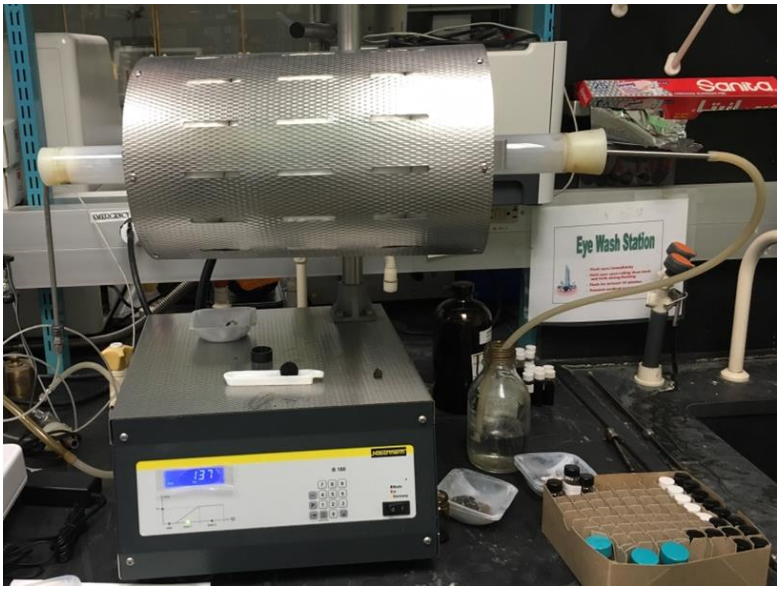

Figure 16. The tube furnace used for activated carbon calculations at nitrogen flow.

The precipitation method is a simpler process than the ion exchange. It involves fewer steps and can provide more concentration loading of the metal oxides intended for impregnation. However, the method can lead to extreme pores blockage of the activated carbon. Moreover, it is difficult to form monolayers. Also, and the surface area of the activated carbon can be reduced due to metal load inside pores from the precipitation. The ion exchange method is more complicated and it involves more steps and chemical preparation. It can lead to no pore blockage and thus it does not reduce the surface area of the activated carbon. The metal oxide concentration loading is limited compared to the precipitation method.

Another objective of the model fuel is to synthesize a fuel that can be used for the adsorption experiments of the nanomaterials while simulating the real fuels. The model fuel should be easily characterized and any changes that it undergoes should be easily monitored. For example, real diesel requires long GC analysis while model diesel can be characterized by real time. The main model diesel no.1 (MD-1) used for this study consists of 96 ppm of Dibenzothiophene (DBT), 16 % toluene, and 84% isooctane. The DBT mimics the sulfur compounds in real diesel, the toluene mimics the aromatics, and the isooctane represents the saturates. The model undergoes fixed bed absorber process that is a dynamic process to provide breakthrough capacity curves that can be used to compare different adsorbent using the adsorption capacity parameter. Based on the adsorption capacity parameter, the adsorbents are indexed based on their desulfurization efficiency.

3.5 Analytical methods

3.5.1. Gas chromatography –Sulfur Chemilumniescence Detector (GC-SCD):

Gas chromatography is used in various industries for hydrocarbon measurement and provides qualitative and quantitative information. GC involves the separation of the different compounds in the sample based on their boiling points and structure than detect them using the various types of detectors equipped with the instrument. The detector used for the analysis is the sulfur chemilumniescence detector (SCD) which is selective toward sulfur compounds. The SCD detector uses the combustion of sulfur compound to form sulfur monoxide and the resulted chemilumniescence produced from the reaction of the sulfur monoxide and the ozone as shown in the following reaction equations 2 and 3. Afterwards, the light produced by the reaction passes through an optical filter and a photomultiplier tube. Finally, this light (400 nm UV) can be used for the detection of sulfur compounds selectively.

$$\text{S-compound} + \tfrac{1}{2}\,O_2 \rightarrow SO + \text{Other Products} \qquad \text{Eq. (2)}$$

$$SO + O_3 \rightarrow SO_2 + O_2 + h\nu \qquad \text{Eq. (3)}$$

Agilent 6890II N gas chromatograph, equipped with an autosampler and computer with HP Chemstation. The analytical column used is wall coated open tubular (WCOT) capillary column DB1, 60 m, 250 µm ID and film thickness of 0.25 µm or equivalent. The GC conditions are summarized in Table 6. The sulfur chemiluminescence detector which is a detector selective for sulfur compounds is checked before every experiment by injecting a sample that contains 20 ppm of benzothiophene and 29 ppm of DBT to ensure it has the following requirements: linearity of 10^4, 5 pg sulfur/s minimum detectability,

approximately equimolar response on a sulfur basis, and no interference or quenching from co-eluting hydrocarbons at the used GC sampling volume.

Table 6. Summery GC-SCD conditions.

Chromatography	HP 6890 equipped with SCD and autoinjector
Column	DB-1, 60 meter, 250 µm ID, film thickness 0.25 µm film
Carrier gas	He, constant flow, 1.2 mL/min
Oven temperature	50°C then ramp temperature at 30°C/min to 310°C hold for 0.5 minute.
Injector	280°C and split ratio of 50:1
Injection volume	1 µL
Detector type	sulfur chemiluminescence detector
Detector parameters	SCD furnace 800°C, H_2 40 mL/min, air 5 – 6 mL/min, pressure 300 – 420 mbar
Integration	Chemstation method parameters with operator check

The DBT was identified by matching its retention time with that of pure DBT sample. Five calibration points were the concentration of the DBT is ranging from 0.85 ppm to 123 ppm. The limit of detection (LOD) and the limit of quantification (LOQ) were measured as three times the noise and ten times the noise, respectively. Their values are illustrated in Table 7. If the DBT concentration is above the method range, the sample is diluted until it is within the range of the method.

Table 7. Limit of detection and limit of quantification for DBT using GC-SCD.

Compound	LOD	LOQ
DBT	0.24 ppm	0.85 ppm

Three quality control (QC) samples covering the range of the method were prepared by accurately weighing a known amount of DBT in toluene using a certified balance. Table 8 illustrates the concentrations of the QCs. Then, they were injected with the sequence to ensure the validity of the method. During the method development, each QC is injected 10 times and the concentrated of the DBT was measured against the reference. All the QC's errors were less than 10 %.

Table 8 . The QC concentrations that are used for the method validation.

QC	[DBT] True Value Ref, ppm
QC-1	10.50
QC-2	51.30
QC-3	102.90

The [DBT] was determined using GC-SCD for the three QC samples. The method is validated by applying statistical validation tests where each test is used to validate criteria in the method. The [DBT] was measured ten times and compared to the true value (in-house prepared QC) to validate the method. In order to determine the accuracy of the method, the percentage (%) relative error was calculated against the reference value using the following equation (4):

$$relative\ error\ \% = \frac{MV-TV}{TV} * 100 \qquad \text{Eq. (4)}$$

Where MV, is the mean value and TV is the true value. The reference value is used as the true value. The % relative error is measured and the results for the three QCs are shown in Table 9.

Table 9. The % relative error results of the QCs used for the method validation.

QC	[DBT] True Value Ref, ppm	Average [DBT], ppm measured	Relative error %
QC-1	10.50	10.80	2.9
QC-2	51.30	51.57	0.5
QC-3	102.90	104.42	1.5

The Q-test (Dixon Rules) was applied to detect any outliers using the following equation (5) where X_a is suspected value and X_b is the nearest value to the suspected value

$$Q_{test\ Calculated} = \frac{X_a - X_b}{Range} \qquad \text{Eq. (5)}$$

The Q- test is applied at 99.0 % confidence interval was for the suspected outliers. The highest and the lowest measured concentration were tested for suspecting outliers for each QC**.** The $Q_{test\ Calculated}$ for both data points are less than $Q_{critical}$ at 99 % confidence interval. Therefore, no outliers observed in the collected data as shown w in Table 10.

Table 10. Q_{test} results for the suspected outliers.

QC	Suspected outliers	$Q\ Test\ Calculated$	$Q_{critical}$
QC-1	11.4 ppm	0.04	0.6
	10.1 ppm	0.2	0.6
QC-2	55.5 ppm	0.3	0.6
	48.3 ppm	0.1	0.6
QC-3	110.6 ppm	0.2	0.6
	98.7 ppm	0.1	0.6

The student test (T-test) is applied to proof that the analytical method measurement has no significance systematic errors which indicate that the average of the [DBT] measured results has a real difference against the reference value. The $T_{calculated}$ is calculated using the following equation (6):

$$T_{calculated} = \left| \frac{X' - \mu}{\frac{s}{\sqrt{n}}} \right| \qquad \text{Eq. (6)}$$

Where X' is the average value, μ is the reference value, s is the standard deviation and n is the number of measurements. After calculating the$T_{calculated}$, it is compared with $T_{critical}$ from the T-test Table. At 99 % confidence interval, the value of $T_{calculated}$ is less than $T_{critical}$, therefore; method showed no significance systematic errors. Table 11 shows the parameters that were used to apply the student test. The $T_{caluated}$ is measured to be than $T_{critical}$ at 99.0 % confidence interval for all QCs. Hence, the method has no significant systematic errors.

Table 11. The Student test parameters used for the validation.

Parameters	QC-1	QC-2	QC-3
Average	10.8	51.6	104.4
Reference Value	10.5	51.3	102.9
Number of measurements	10	10	10
Samples Standard Deviation	0.4	2.1	3.9

The standard error of the mean is calculated using the following equation (7) where the X_i is the reported value for the [DBT]. At 99.0 % confidence interval, X_i, estimated uncertainty, and the range are reported for each QC as shown in the Table 12.

$$X_i = X' \pm \frac{S}{\sqrt{N}} \qquad \text{Eq. (7)}$$

Table 12. QC method results.

Parameters	QC-1	QC-2	QC-3
X_i	10.8	51.6	104.4
Estimated uncertainty	0.1	0.6	1.2
Range	10.7-10.9	51.0-51.9	103.2-105.6

The statistical method validation has proven, the method has no significance errors (systematic errors) with an estimated uncertainty of a maximum of ± 1.2 ppm. Therefore; the method fits for the purpose.

3.5.2. Gas Chromatography-Flame Ionization Detector (GC-FID):

In case the GC-SCD is not available or under troubleshooting to meet the specifications of the detector, GC-FID is used as a replacement. The FID is not as sensitive as the SCD. Therefore, special adjustments were conducted to increase the sensitivity. The parameters for the FID are illustrated in the table below. The calibration was conducted with five calibration points and checked with the same QCs applied for the GC-SCD.

Table 13. Summery GC-FID conditions.

Chromatography	HP 6890 equipped with FID and autoinjector
Column	DB-1, 60 meter, 250 µm ID, film thickness 0.25 µm film
Carrier gas	He, constant flow, 1.3 mL/min
Oven temperature	50°C then ramp temperature at 30°C/min to 310°C hold for 0.5 minute.
Injector	280°C and splitless
Injection volume	1 µL
Detector type	Flame ionization detector

Detector parameters	The detector temperature shall be set at 300 °C. The flow rate for hydrogen is 30.0 mL/min, for air is 400.0 mL/min, and the makeup flow of nitrogen is 25.0 mL/min.
Integration	Chemstation method parameters with operator check

3.6 Characterization

3.6.1. X-ray diffraction (XRD)

The X-ray diffraction (XRD) was used to verify the crystal structures of the adsorbent and also used for fingerprinting the crystal structure formation of the metals loaded on the activated carbon. X-ray diffraction crystallography involves exposing a crystalline to a monochromatic collimated x-ray beam at an angle **θ**. As the X-ray source is scanned through a range of **θ** values, the intensity of a reflected beam at a reflected angle **θ** is measured. The diffractogram is a plot of the intensity of the reflected beam against **2θ** (the angle through which the X-rays are deflected). Intense reflections are detected at angles at which there is constructive interference from X-rays reflected from series of adjacent of atomic planes. There are many sets of planes in any crystal that can cause reflection and each set is described by its Miller indices, **h**, **k,** and **l**. The angle is related to the spacing **d** between the planes by Bragg's Law (equation 8):

$$n\lambda = 2d \sin \theta \qquad \text{Eq. (8)}$$

θ is the angle of the diffracted X-ray, **λ** is the wavelength of X-ray radiation, **d** is the spacing of atomic/crystal planes, and **n** is an integer (usually 1). The d-spacings of planes is related to their Miller indices so diffraction is detected at different angles for planes with different Miller Indices. The powder X-ray diffraction pattern of a particular salt, therefore, contains a series of maxima (lines) at angles that are characteristic of the material, and at a series of relative intensities that are also characteristic. The overall pattern can, therefore, be used as a fingerprint of a crystalline material. Crystallite size can be determined from the width of X-ray different peaks using the Scherrer equation (equation 9)

$$L_{2\theta} = \frac{K\lambda}{\beta cos\theta} \qquad \text{Eq. (9)}$$

where **L** is the crystallite dimension, **β** the line width at half height, **θ** is the diffraction angle and **K** is a constant. In the work in this thesis, crystallite sizes were attempted to be determined for metallic oxides spiked on the activated carbon using the major peak for planes with Miller Indices. However, due to the low concentration of the metallic oxides, such calculation couldn't be achieved.

A Panalytical X'Pert PRO Diffractometer instrument was used for XRD analysis throughout this study. The XRD instrument is controlled by computer software (XRD Control System) to convert peak positions as 2**θ** values to **d**-spacings. The catalysts' XRD patterns are compared with the Powder Diffraction Files (PDF) of the International Centre for Diffraction Data (ICDD). The analysis was conducted from 4^{o} to 80^{o} degrees 2**θ**. The measurement parameters used for catalyst XRD characterization are shown in Table 14.

Table 14. XRD pattern measurement condition.

Name	**Description**
Instrument	PANalytical X′PERT PRO MPD
Radiation	copper-anode tube operated at 40 kV and 100 mA Wavelength: = 1.5418 Å
Acquisition	Angular range in 2θ: 4° - 80° Step size: 0.04° and 0.4° Scanning step time: 9.7282 s

3.6.2. Texture properties

The texture properties were used the nitrogen adsorption analysis was conducted to determine porosities and surface areas. The calcined adsorbents were analyzed using a Micromeritics ASAP 2420 instrument to measure the nitrogen adsorption/desorption isotherms at liquid nitrogen temperature (77 K). The surface area was calculated from the adsorption isotherm by using the B.E.T equation and the total volume of pores was determined from the amount of N_2 desorbed at STP. The pore size distribution was calculated using the Kelvin equation modified with the B.J.H method. A catalyst weight of 200-500 mg was introduced into the sample tube. The catalyst was heated to 150 ^{o}C for 1 hour at the degassing condition of vacuum at 10^{-4} Torr before measurement. There are six major isotherm types recognized by IUPAC for gas physisorption as seen in Figure 17. Solid metal oxides activated carbon types are known to be mesoporous and normally exhibit type of IV isotherms with hysteresis loops.

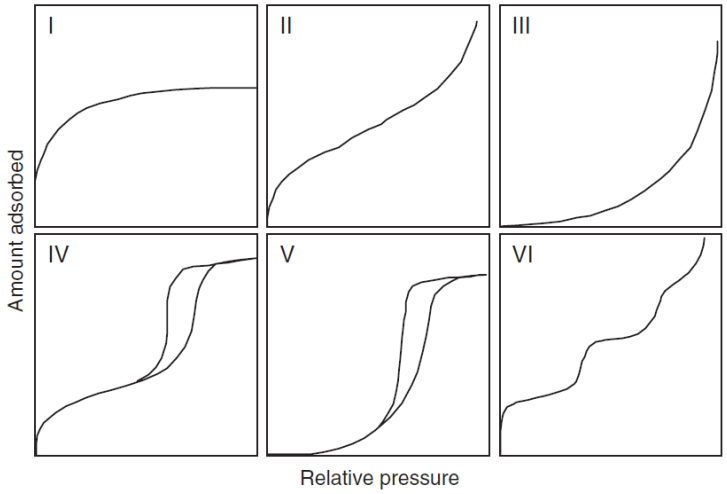

Figure 17. Isotherms diagrams according to IUPAC classifications.

3.6.3. Scanning electron microscope (SEM) and energy dispersive x-ray (EDX/EDS)

The SEM and EDX analytical techniques were used to characterize the surface morphology of selected activated carbon based adsorbents. The microscope (Figure 15) is an environmental scanning electron microscope (ESEM) which has an advantage over a conventional SEM by examining non-conductive samples without coating. The ESEM is operated at 20 kV and at an overpressure of 0.23 torr. The objective of the ESEM measurement was to determine the homogeneity of catalysts, and the size and shape of particles. In addition, energy dispersive X-ray microanalysis (EDX) characterization was acquired from different parts of the catalyst surface to obtain semi-quantitative elemental composition data (Table 15). In addition, few samples were tested by using the SEM of King Fahd University of Petroleum and Minerals (KFUPM) as a backup for surface

morphology. The instrument is made from Tescan (VEGA 3 LMU) and several adsorbents were coated by using carbon coater before testing.

Figure 18. ESEM instrument FEI Quanta 400.

Table 15. EDX parameters for adsorbent analysis by ESEM.

Detector	**EDX liquid-nitrogen cooled detector**
Operating Voltage	20 kV
Spot Size	4 nm
Working Distance	10 mm
Acquisition Time	60 s
Amplification Time	26.5 μs
Counts per second	2500 CPS
Dead time	25%

CHAPTER 4 RESULTS AND DISCUSSION

The target of this work is to evaluate the desulfurization performance of several materials and study the factors that can affect their performance. In this study, an emphasis was placed on the material characterization and performance in addition to the model fuel composition. First, a comprehensive characterization of the materials used was conducted using BET, ESEM, and XRD. Then, the material support for desulfurization was selected by comparing the desulfurization performance on the basis of breakthrough capacities of H-zeolites and activated carbon. Subsequently, the effect model fuel composition was studied by varying the total sulfur and aromatics of the model fuel and determine their effect on the sulfur breakthrough capacity. Then, the effect of metal loading types on activated carbon is studied using two different model fuels. Formerly, the effect of metal loading amount and preparation method effect on the desulfurization performance of the materials used is studied. Finally, the effect of bimetallic oxides loading on the adsorbent sulfur capacity is evaluated.

4.1 Characterization of catalyst and support:

The adsorbent materials had been characterized in order to understand the adsorbent loaded and preparation methods to activated carbon support and correlated with the performance of material for desulfurization. Different analytical techniques were used to characterize and describe the materials properties.

4.1.1. Scanning electron microscope (SEM)

The SEM was utilized to study the topography of the metal loaded to the activated carbon support and also used EDS applications to analyze the metal content. The EDS analysis is semi-quantitative and was conducted on 3-5 spots of the adsorbent in order to determine the final metal content. The metal content of the adsorbent is an indicator of metal loaded according to the preparation method. Figure 19 shows the topography of the activated carbon support and it is round shape and well distributed. Table 16 lists the element content of activated carbon that is mainly of carbon and oxygen. Interestingly, after desulfurization of model diesel, the activated carbon tested by EDS and data showed an indication of sulfur element adsorbed in the activated carbon support in the range of 0.82%.

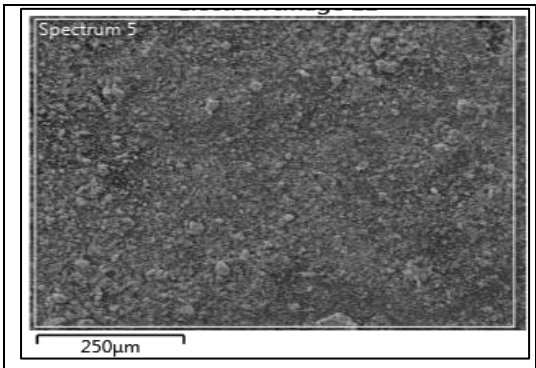

Figure 19. The topography of the activated carbon support.

Table 16. Element content of activated carbon support before and after desulfurization.

	C %	O%	S%
Before desulfurization	85.26	14.74	0
After desulfurization	85.44	13.74	0.82

Table 17 showed the element analysis of selected adsorbents prepared by two different methods in order to determine the deposition of metal during preparation. The ion exchange method is expected to have a lower metal loading of 2% Fe/AC ad 2% La/AC to activated

carbon as shown in Table 17. Ion exchange method is only the bonding metal salt will be incorporated with AC and undissolved metal salt will be removed by water during salt washing step from support. In contrast, the wet impregnation method does not require water washing from undissolved metal salt removal, it usually contained higher metal loading to salt.

Table 17. EDS analysis of selected adsorbents prepared by different catalyst method.

Catalysts method	**Catalyst synthesis preparation recipe, metal ratio (w/w %)**	**Metal content detected by EDS (wt/wt %)**
Ion exchange	2% Fe/AC	1.3% Fe/AC
Ion exchange	2% La/AC	0.8% La/AC
Wet impregnation high loading	15%Fe-15% Ni/AC	9.9% Fe-8.7% Ni/AC

Other examples of high loading vs. low loading are shown in tables 18-21 and figures 20-27 for selected adsorbents. 1%Ni/1%Fe/AC and 15%Ni/15%Fe/AC are two different adsorbents loaded with different amounts of metal loading. Also, 1%W/1%Fe/AC and 15%W/15%Fe/AC were shown as examples for high vs. low metal loading. The general trend observed is that loading metals using ion exchange method impregnate fewer metals than when using the precipitation method. Moreover, low loading provides more uniform impregnation and less aggregation comparing with the high loading for all the examples.

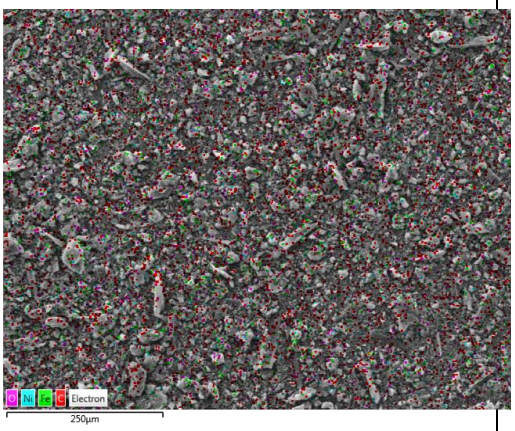

Figure 20. SEM elemental mapping of 1%Ni/1%Fe/AC adsorbent.

Table 18. Element content of 1%Ni/1%Fe/AC.

Ads.	**C %**	**O%**	**Fe%**	**Ni%**
1%Ni/1%Fe/AC	76.3	20.9	1.7	1.2

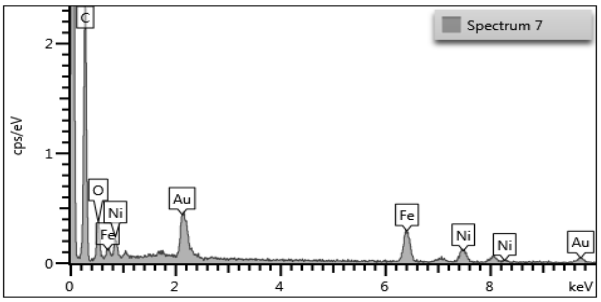

Figure 21. EDS spectrum of 1%Ni/1%Fe/AC adsorbent.

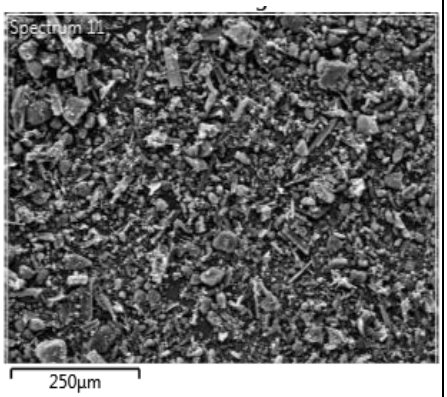

Figure 22. SEM elemental mapping of 15%Ni/15%Fe/AC adsorbent.

Table 19. Element content of 15%Ni/15%Fe/AC.

Ads.	C %	O%	Fe%	Ni%
15%Ni/15%Fe/AC	69.4	14.9	9.9	5.9

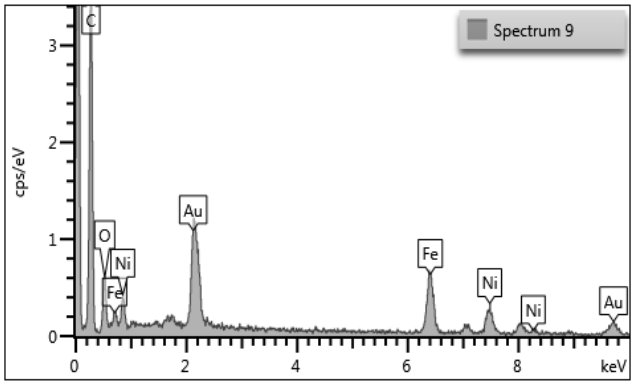

Figure 23. EDS spectrum of 15%Ni/15%Fe/AC adsorbent.

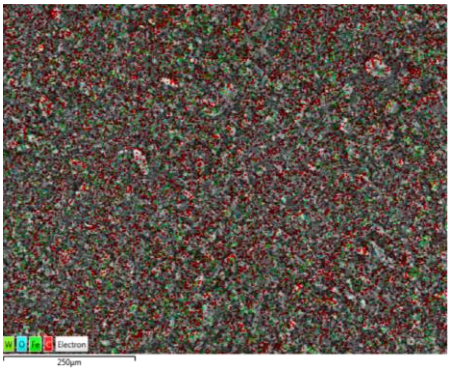

Figure 24. SEM elemental mapping of 1%W/1%Fe/AC adsorbent.

Table 20. Element content of 1%W/1%Fe/AC.

Ads.	C %	O%	Fe%	W%
1%Ni/1%Fe/AC	78.7	4.8	0.8	1.6

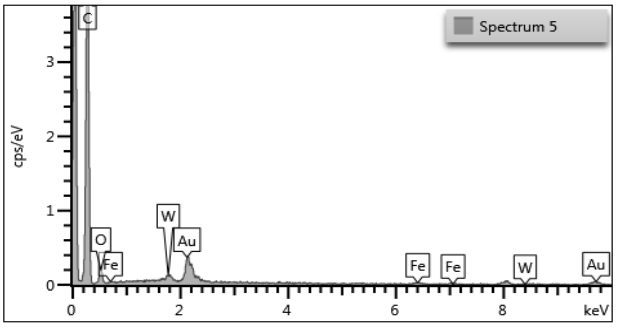

Figure 25. EDS spectrum of 1%Ni/1%Fe/AC adsorbent.

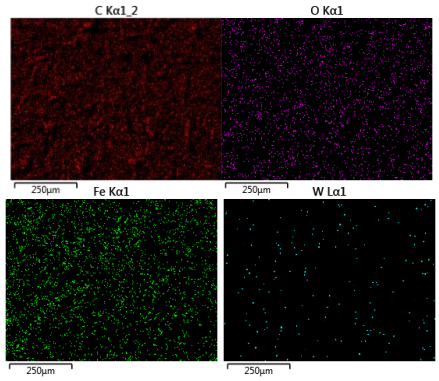

Figure 26. SEM elemental mapping of 15%W/15%Fe/AC adsorbent.

Table 21. Element content of 15%W/15%Fe/AC.

Ads.	**C %**	**O%**	**Fe%**	**W%**
15%Ni/15%Fe/AC	67.1	17.0	10.4	5.5

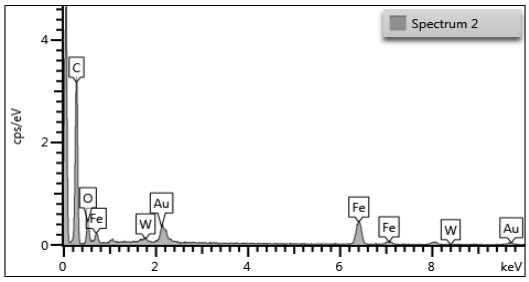

Figure 27. EDS spectrum of 15%W/15%Fe/AC adsorbent.

The SEM data for 2%Ni /AC, 2%La /AC, 2%W /AC and 2%Fe(IE) /AC are shown in figures 28-35 and tables 22- 25 below. Each adsorbent is presented with an SEM elemental mapping, EDS spectrum, and EDS elemental content table. All of these adsorbents were prepared by ion exchange with a relatively uniform metal distribution on the surface of the activated carbon.

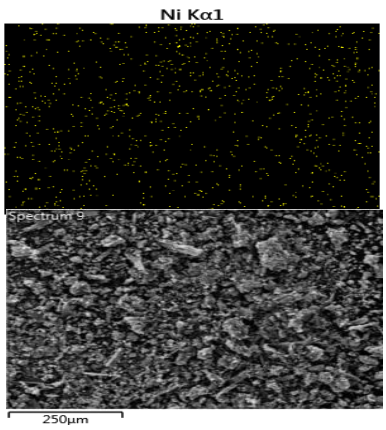

Figure 28. SEM elemental mapping of 2%Ni/AC adsorbent.

Table 22. Element content of 2%Ni/AC.

Ads.	**C %**	**O%**	**Ni%**
2%Ni/AC	81.3	16.8	1.9

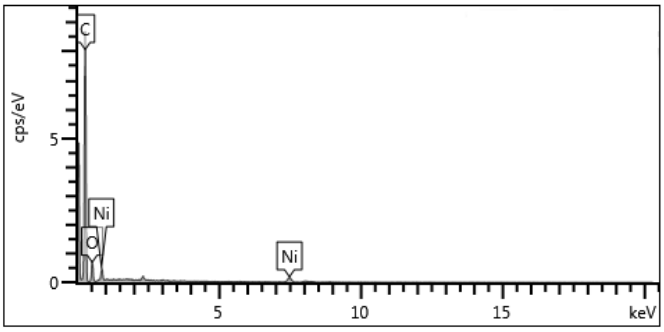

Figure 29. EDS spectrum of 2%Ni/AC adsorbent.

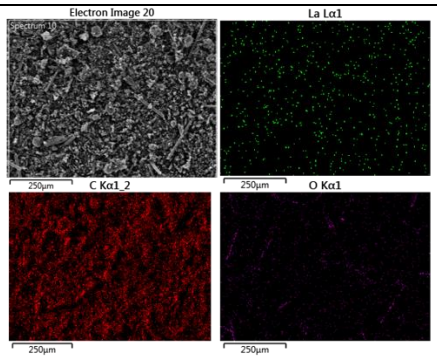

Figure 30. SEM elemental mapping of 2%La/AC adsorbent.

Table 23. Element content of 2%La/AC.

Ads.	**C %**	**O%**	**La%**
2%La/AC	86.6	12.6	0.8

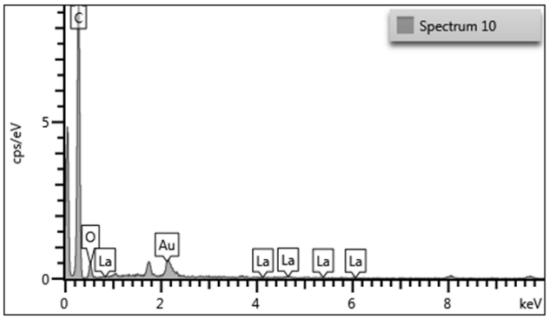

Figure 31. EDS spectrum of 2%La/AC adsorbent.

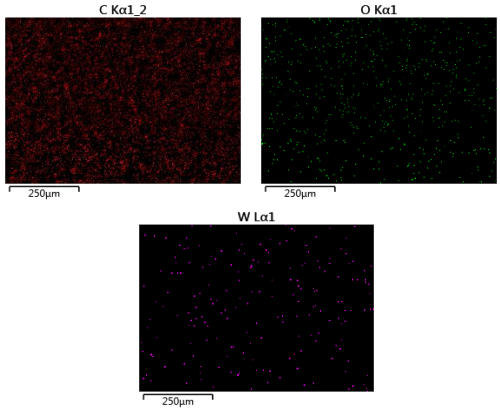

Figure 32. SEM elemental mapping of 2%W/AC adsorbent.

Table 24. Element content of 2%W/AC.

Ads.	C %	O%	W%
2%W/AC	87.7	9.9	2.4

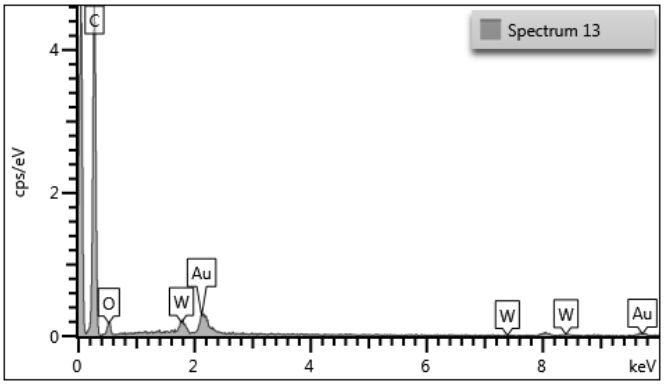

Figure 33. EDS spectrum of 2%W/AC adsorbent.

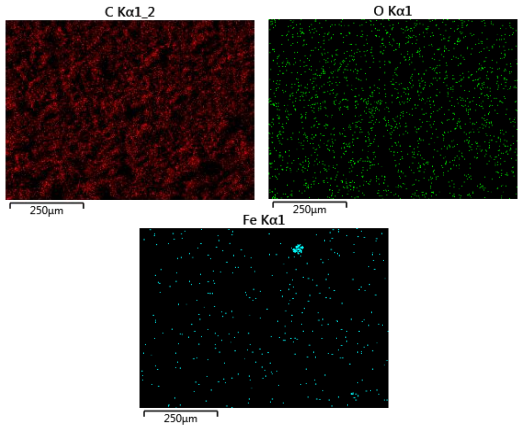

Figure 34. SEM elemental mapping of 2%Fe(IE)/AC adsorbent.

Table 25. Element content of 2%Fe (IE)/AC.

Ads.	C %	O%	Fe%
2%Fe (IE)/AC	87.8	10.9	1.3

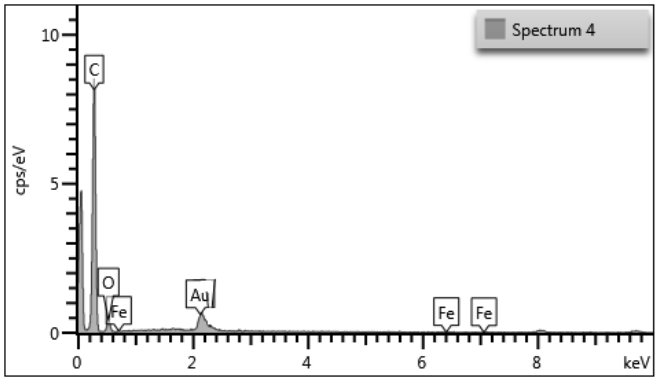

Figure 35. EDS spectrum of 2%Fe(IE)/AC adsorbent.

4.1.2. Nitrogen adsorption analysis

Table 26 lists the surface areas, pore volumes and pore sizes for adsorbents of activated carbon prepared by ion exchange and wet impregnation methods. In general, the activated carbon support has the highest surface area and pore volume were reduced by loading metal oxides by the two methods. The method of wet impregnation was applied for low and high loading. This method shows a higher reduction of surface area and pore volume compared to the other adsorbents prepared by using ion-exchange method. The pore size of the adsorbents and support indicated mesoporous pores as shown in Table 26. The pore size diameter has increased by the metal loading using method of wet impregnation compared to the ion exchange method.

Table 26. Surface area and porosity data for adsorbents made by wet impregnation and ion exchange methods.

sample	Catalysts preparation	BET Surface Area, m^2/g	Pore Volume [(i)], cm^3/g	Pore Size [(ii)], Å
Activated carbon	Support	556.3	0.77	112.5
1%Ni-1%Fe/AC	Ion exchange	494.8	0.69	119.3
2%Ni/AC	Ion exchange	490.1	0.69	121.1
1%W-1%Fe.AC	Ion exchange	486.3	0.68	119.2
1%Ni, 1%Fe/AC	Ion exchange	482.9	0.66	114.5
2%La /AC	Ion exchange	430.5	0.74	117.5
2%W AC	Ion exchange	478.4	0.65	116.6
2% Fe/AC	Ion exchange	515.6	0.73	119.5
15% Fe/AC	Wet impregnation high loading	421.1	0.64	**120.5**
2% Fe/ AC	Wet impregnation low loading	425.7	0.70	**131.7**
15% W-15%Fe/AC	Wet impregnation high loading	446.1	0.69	**131.6**
15%Fe-15% Ni/AC	Wet impregnation high loading	388.2	0.60	**122.8**

(i) BJH Adsorption cumulative volume of pores, (ii) BJH Adsorption average pore width

The isotherm plots of catalysts and support of activated carbon are in Figure 36, 37 and 38. The isotherm of these adsorbents and support are in the type IV isotherms according to IUPAC, with hysteresis loop associated of nitrogen desorption. Due to a slight changed of the texture priority of wet impregnation method, the isotherm plots showed also a slight reduced of nitrogen adsorbed from the catalysts loading compared to the activated carbon support (used as reference) as shown in Figure 36. On the other hand, the adsorbents prepared by the ion exchange with single metal oxide showed the isotherm plot similarity with the nitrogen adsorbed with the activated carbon support as shown in Figure 37. Slightly change of the nitrogen adsorbed with two metals loading to activated carbon by using ion-exchange method as shown in Figure 38. It is clear that the isotherm plot showed the nitrogen adsorbed has been affected by the preparation method and the quantity of metal loading.

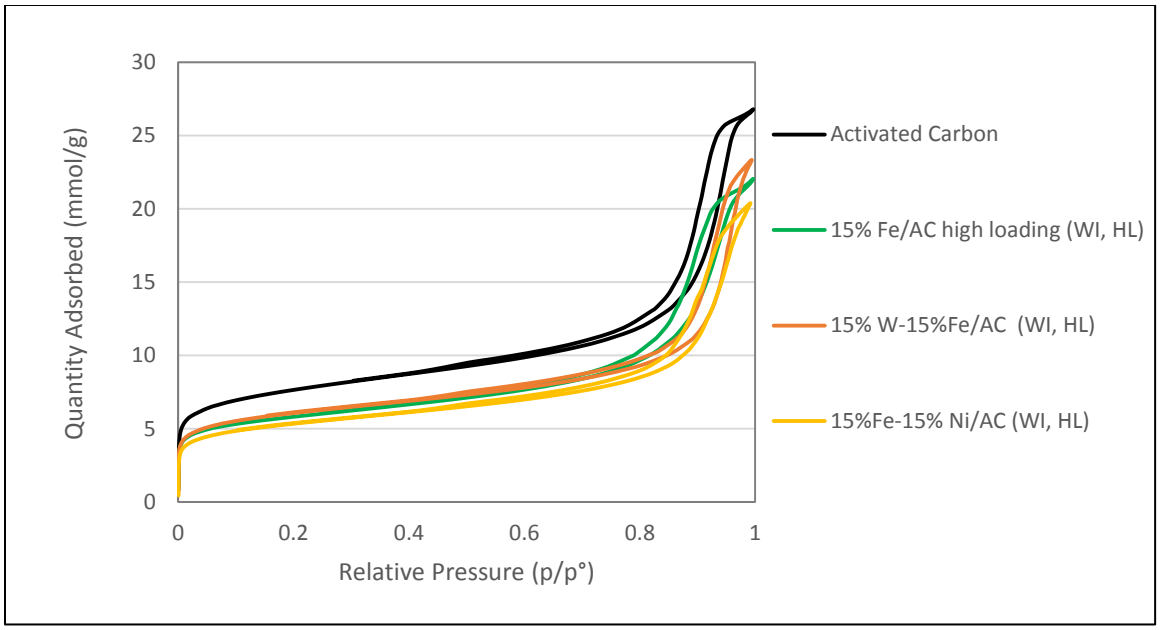

Figure 36. Isotherm of wet impregnation method compared to activated carbon support.

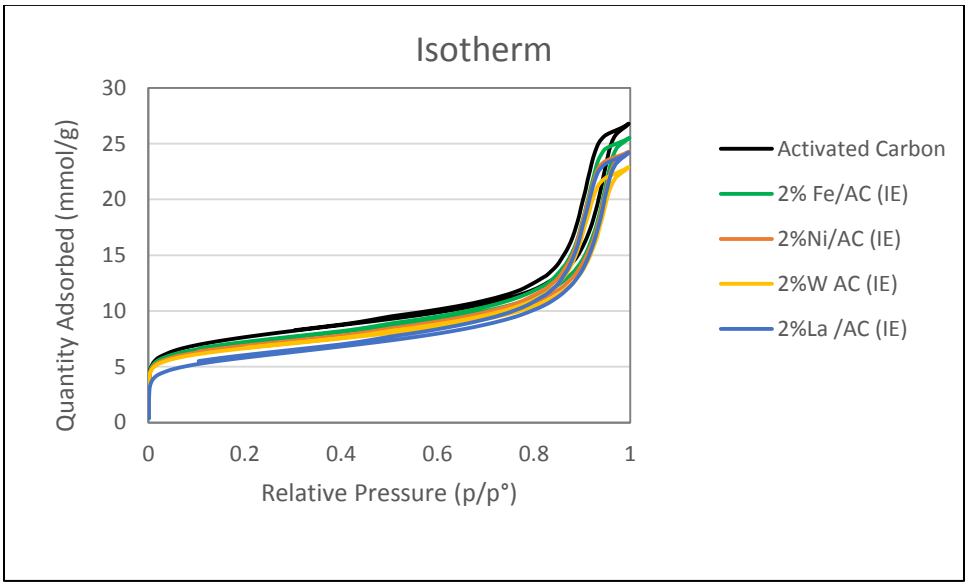

Figure 37.Isotherm of ion exchange method of single metal compared to activated carbon support.

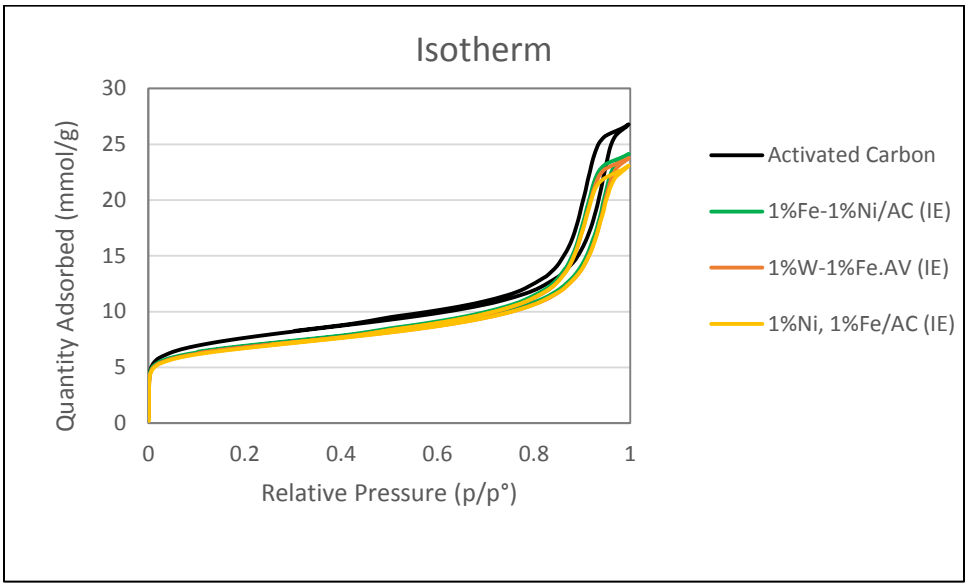

Figure 38. Isotherm of ion exchange method of bi-metallic metal compared to activated carbon support.

4.1.3. X-ray diffraction (XRD)

Diffraction patterns are presented for activated carbon in Figure 39 showed the amorphous phase of the activated carbon support. The ICDD and Miller indices 2**θ** of carbon are shown a broad peak at 26. The adsorbents that were prepared by the ion exchange showed no diffraction peaks due to the low metal loading content and the amorphous phase of carbon as shown in Figure 39 and 40. On the other hand, the wet impregnation method showed XRD peak of the amorphous phase of Fe at 2**θ** of 35, 41 and 51 as shown in Figure 41 are matched with ICDD and Miller indices. The bimetallic of 15% FeO and 15% NiO showed in Figure 42 are amorphous phases and NiO peak located in the broad peak with FeO.

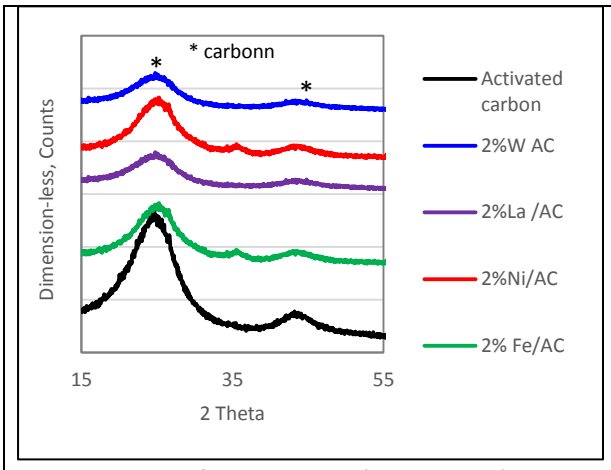

Figure 39.XRD of ion exchange (single metal) catalysts and support showed amorphous phase.

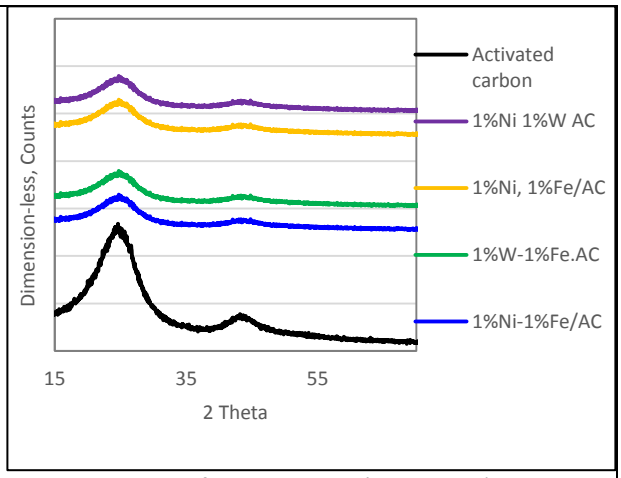

Figure 40. XRD of ion exchange (bi-metallic) catalysts and support showed amorphous phase.

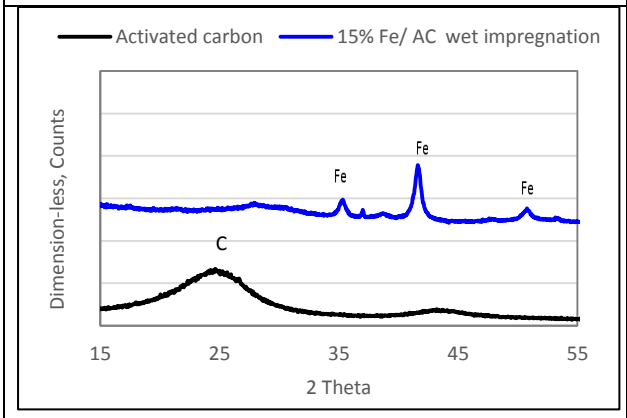

Figure 41. , XRD of wet impregnation catalysts and support showed the amorphous phase of iron oxide.

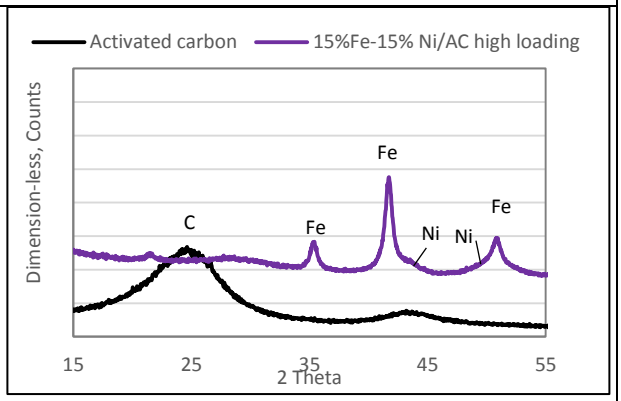

Figure 42. XRD of wet impregnation catalysts and support showed the amorphous phase of iron and nickel oxides.

4.2 Material support selection for desulfurization

There are several materials that have been used as a support for adsorbents. Activated carbon and Y-zeolite have been used by various authors (J. Hernandez-Maldonado et al 2005; Takashi et al 2002; Liu, 2009; Jin, 2009; Kim et al 2006). Initially, H-Y-zeolite and in-house prepared activated carbon were tested using the model fuel in order to determine the breakthrough capacity for each and then decide the best adsorbent support. Figure 43

shows the breakthrough curve for the activated carbon and H-Y-zeolite. Table 27 shows a comparison between the breakthrough capacity for activated carbon and H-Y-zeolite. The results showed that the activated carbon is superior to the H-Y-zeolite for the adsorptive desulfurization of model fuel at room temperature and pressure. Therefore, the activated carbon has been selected as a support for all the adsorbents in this study. Activated carbon was spiked with several metals: iron (Fe), lanthanide (La), tungsten (W) and Nickel (Ni).

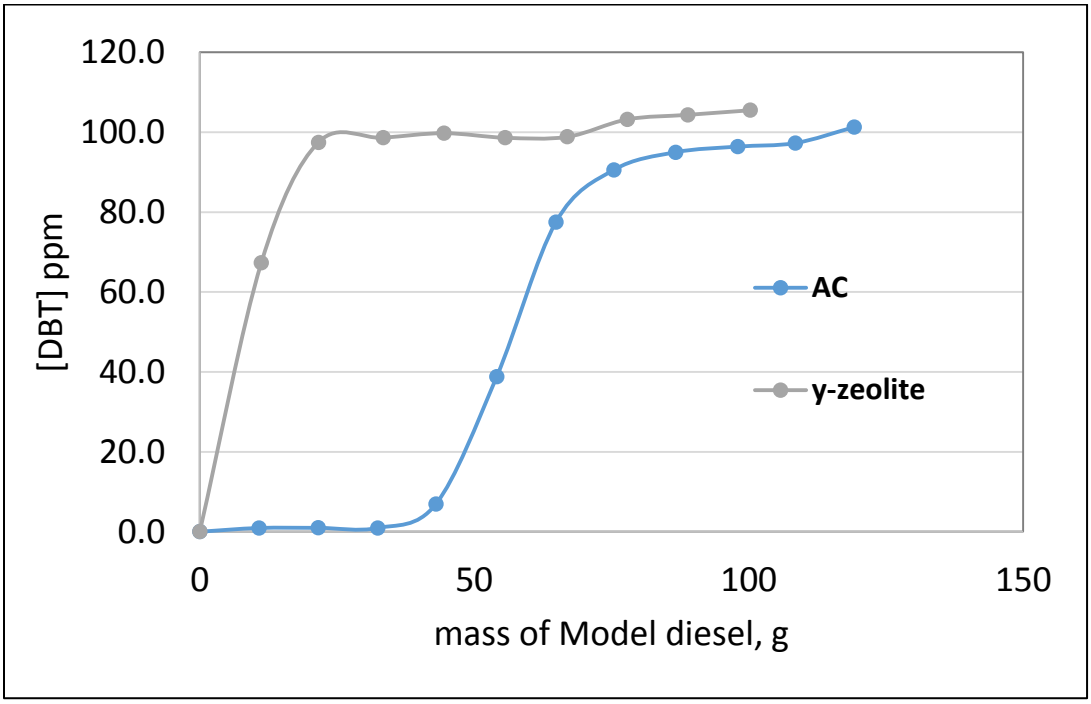

Figure 43. The breakthrough capacity curve for Activated carbon and H-Y-zeolite using MD-1 at room temperatreu and pressure.

Table 27. Comparison between activated carbon and H-Y-Zeolite (Si/Al 20) breakthrough capacities.

Ads.	breakthrough capacity mg DBT/g ads	break through capacity mg S/g ads
H-Y-Zeolite (Si/Al 20)	0.24	0.04
AC	9.25	1.61

4.3 Optimizing the fuel model

4.3.1. Effect of model fuel composition

In the literature, several papers reported high desulfurization efficiency for their adsorbents using model fuels with high sulfur and without using aromatics in their model fuel content. (Katie et al, 2013) reported a breakthrough capacity of MOF-505 83 g S/kg of the adsorbent for DBT. However, the model diesel used did not contain any aromatics nor any compound that mimics aromatics in liquid fuels. The model diesel contained 2000 ppm Benziothiophene, 2000 ppm Dibenzothiophene, and 700 ppm 4,6 DMDBT. In addition, the aromatic content and the sulfur content of the liquid fuel play an important role in the breakthrough capacity on the desulfurization efficiency. Another example is Kim Et al (2006) reported a breakthrough capacity of 6.3 mg S/g of activated carbon (1800 m^2/g). The model diesel fuel used for this study contain 687 ppmw sulfur without any aromatics. Zhou et al 2009 reported a breakthrough capacity of 6.4 mg S/g of calgon carbon (900 m2/g). They used a model diesel fuel containing 400 ppmw S in a 50:50 mixture of decane and dodecane without any aromatics and the feedstock is not complementary to HDS process.

Therefore, the model diesel should be representative of the real diesel which is not the case in several papers. It is important to note that the breakthrough capacity increases as the total sulfur increases and as the aromatic contents in model fuel decreases. In this work, aromatic content in the model fuel was considered and tested in order to measure the effect of desulfurization performance. Table 17 shows the variation of the aromatic and sulfur

content of six model diesel fuel (MD-1 to MD-6). These six model fuels are used to determine the important factors for desulfurization effect of diesel as such:

- Indexing the adsorbents on the order of desulfurization efficiency
- Studying the effect of the aromatic content on the adsorbent desulfurization efficiency. Therefore, several model fuels were prepared with varying toluene concentrations to mimic various aromatic content as illustrated in Table 28.
- Studying the effect of the total sulfur on the adsorbent desulfurization efficiency. Therefore, several model fuels were prepared with varying DBT concentration to mimic various sulfur content as illustrated in Table 28.

Table 28. Summary of model diesel composition used for this study.

Model fuel	[DBT] ppm	[Toluene] %	[Isooctane] %	Total sulfur ppm
MD-1	96	16	84	16.7
MD-2	96	100	0	16.7
MD-3	96	57	43	16.7
MD-4	287	16	84	50
MD-5	707	16	84	123
MD-6	1977	16	84	344

By using a model fuel, the capacity of the adsorbents and can be used to index them based on their breakthrough capacity. For this, MD-1 was used for testing the adsorbents

performance. All the model fuels (MD-1 to MD-6) were used to study the effect of aromatic and sulfur content. In addition, MD-4 was used also to study the performance of the adsorbent at a different level of sulfur in fuels.

4.3.2. Effect of total aromatic content on sulfur breakthrough

The aromatics content of diesel feedstocks can vary widely. The aromatic content of straight run diesels is within the range of 20-40 vol% (Assim and Yoes 1983). To study the effect of the aromatic content on the adsorbent desulfurization efficiency, several model fuels were prepared with varying toluene concentrations to mimic various aromatic content as illustrated in Table 29. Three model fuels (MD-1, MD-2 and MD-3) were tested using the fixed bed absorber process with activated carbon as the adsorbent as shown in Figure 44 in order to obtain the breakthrough capacity at different concentration of toluene. These three model fuels have the same [DBT] of 96 ppm with varied [toluene] ranging from 16 % to 100%.

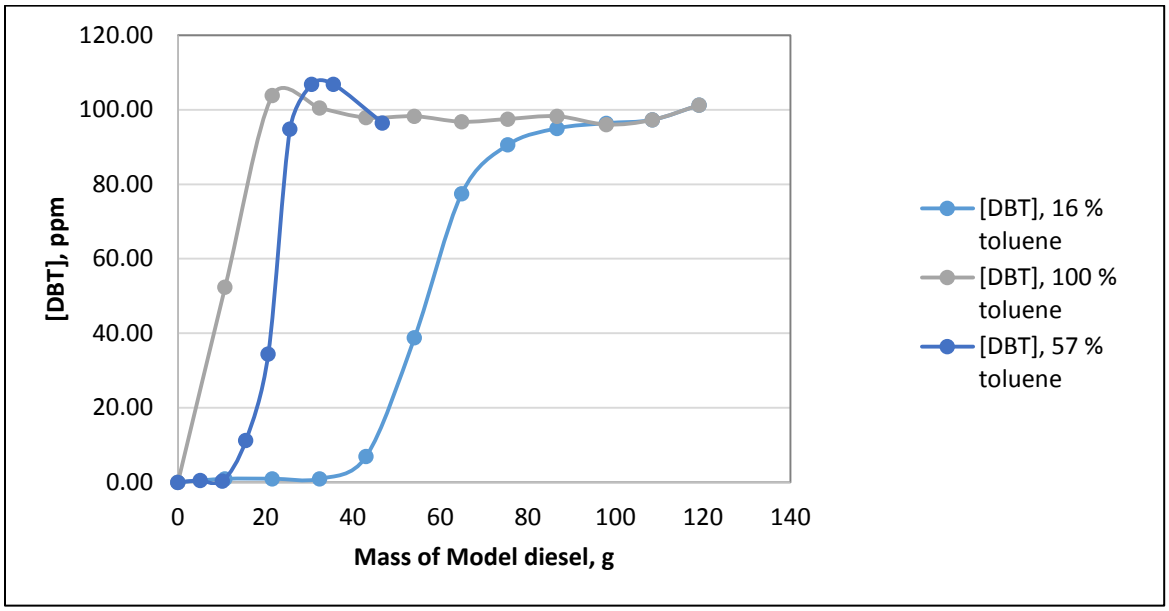

Figure 44. The activated carbon breakthrough curves using model fuels with different aromatic content.

From the breakthrough curve shown in Figure 28, the breakthrough capacity of activated carbon at different [toluene] is obtained and illustrated in Table 21. The breakthrough capacity decreases as the [toluene] increases. The relationship is graphed in Figure 45 and it shows breakthrough capacity mg S/g ads as a function of [toluene %]. The relationship is linear with a correlation factor (r^2=0.947). This indicates the importance of considering the aromatic content when designing the model fuel. Furthermore, it explains the difference in breakthrough capacities of activated carbon when compared with other studies.

Table 29. The activated carbon breakthrough capacity at different [toluene].

Model Fuel	[Toluene] %	Breakthrough capacity mg S/ g ads
MD-2	100%	0.05
MD-3	57%	0.53
MD-1	16%	1.61

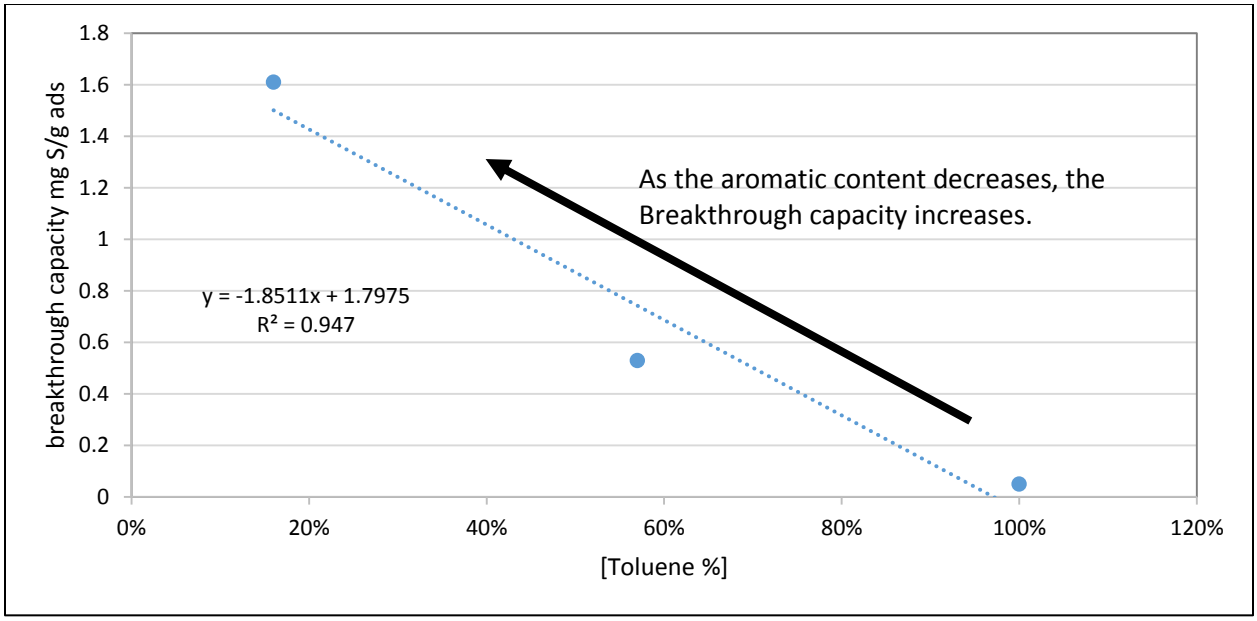

Figure 45. The breakthrough capacity mg S/g of activated carbon ads as a function of [toluene].

4.3.3. Effect of Total sulfur content on sulfur breakthrough

Another important factor is the effect of total sulfur on the adsorbent desulfurization efficiency. The total sulfur effect was studied by preparing several model fuels with

varying DBT concentrations to mimic various sulfur content as illustrated in Table 22 with fixed aromatics concentration. Four model fuels (MD-1, MD-4, MD-5 and MD-6) were tested using the fixed bed absorber process with activated carbon as the adsorbent as shown in Figure 46 to obtain the breakthrough capacity at different concentration of DBT. These four model fuels have the same toluene concentration of 16% with varied [DBT] ranging from 96 to 1977 ppm.

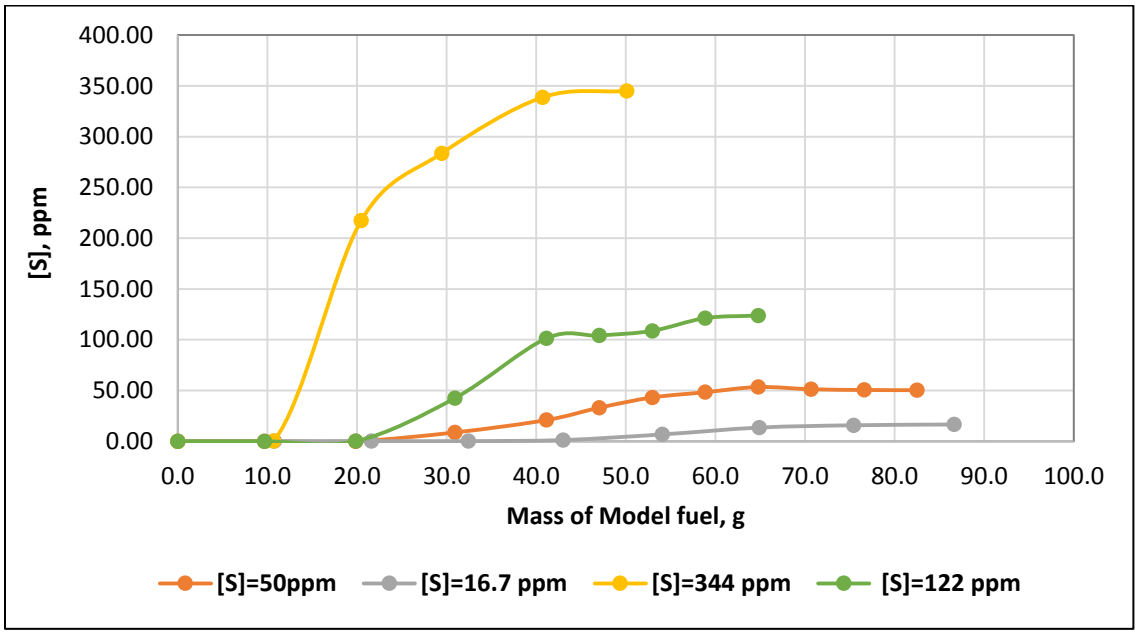

Figure 46. The breakthrough curves using model fuels with different sulfur content and activated carbon.

From the breakthrough curve shown in Figure 30, the breakthrough capacity of activated carbon at different [DBT, ppm] is obtained and tabulated in Table 30. The breakthrough capacity increases as the [DBT, ppm] increases. The relationship is graphed in Figure 47, the breakthrough capacity mg S/g ads as a function of [DBT, ppm]. The relationship is linear with a correlation factor (r^2=0.909).

Table 30. The activated carbon breakthrough capacity at different [sulfur, ppm].

Model fuel	[DBT],ppm	Total sulfur, ppm	breakthrough capacity mg S/ g ads
MD-1	96	16.7	1.61
MD-4	287	50	3.14
MD-5	707	123	6.14
MD-6	1977	344	8.98

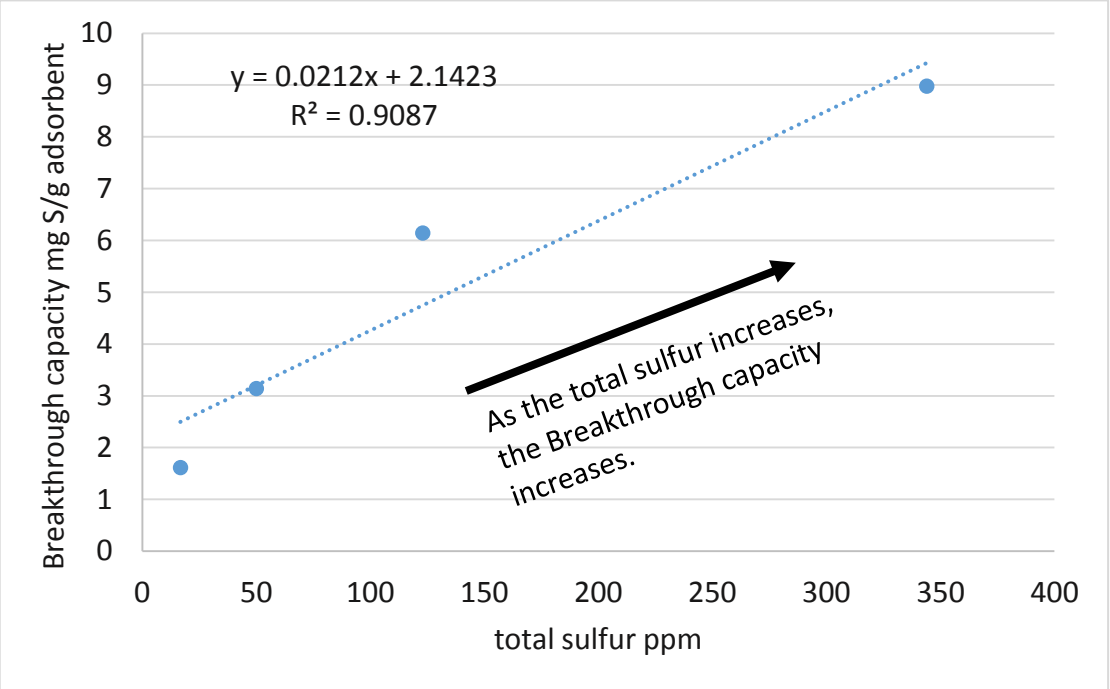

Figure 47. The breakthrough capacity mg S/g ads as a function of total sulfur content in ppm.

From this study, the model fuel total sulfur content is an important parameter that can affect the adsorbent desulfurization performance. Furthermore, it explains the variance in the breakthrough capacity of an adsorbent when tested using different model fuels. This indicates the importance of considering the aromatic content and the total sulfur when designing the model fuel. Furthermore, it explains the difference in breakthrough capacities of activated carbon when compared with other studies.

4.4 Optimizing the metal nanoparticles loading

4.4.1. The effect of metal loading type on activated carbon using MD-1.

Several metals were impregnated on activated carbon to study the effect of various metals on the desulfurization performance of activated carbon. For this study, Activated carbon has been impregnated with several metals oxide including Iron, (Fe), Nickel (Ni), Tungsten (W), and lanthanum (La). As discussed in the introduction section, loading metal enhance the adsorption desulfurization by increasing the interaction to include metal-sulfur interaction and interaction by π-π complexation. The metals were loaded using the ion exchange method and 2% of each metal is loaded to the activated carbon. Then, each adsorbent is tested using MD-1 feed and the fixed bed absorber experiment to obtain the breakthrough curves. The breakthrough curve for activated carbon is included for comparison. From the breakthrough curve (Figure 48), the breakthrough capacity is obtained for every adsorbent and tabulated in Table 31.

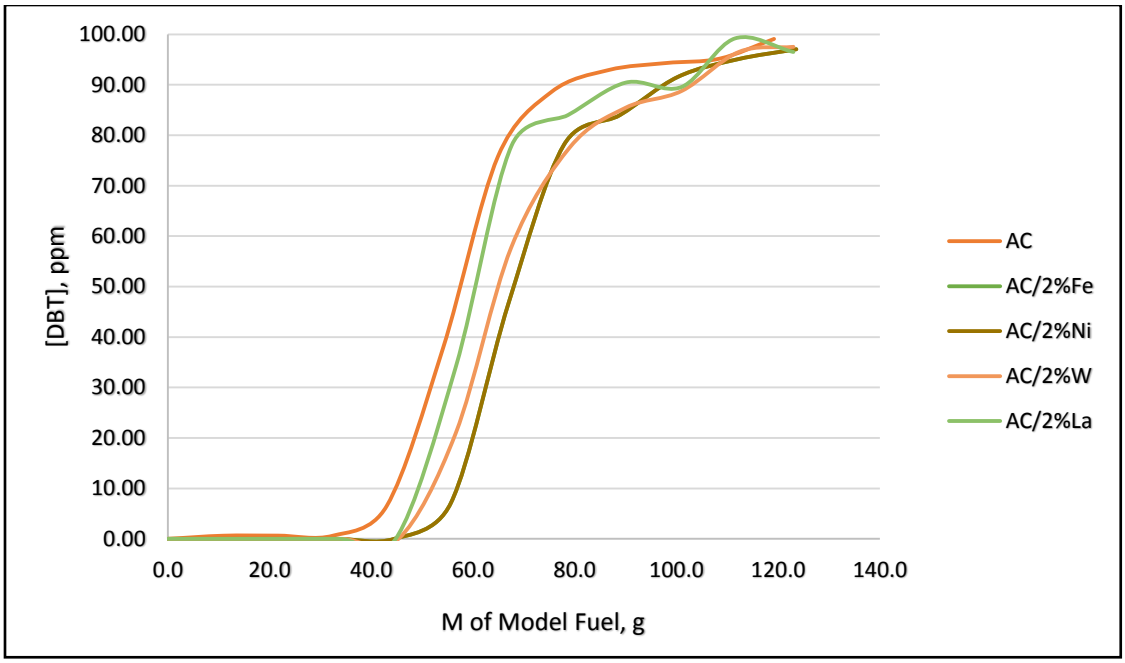

Figure 48. The breakthrough curve for various metals impregnated on activated carbon.

Table 31. The breakthrough capacity of activated carbon impregnated with different metals.

Ads	break through capacity mg DBT/g ads	break through capacity mg S/g ads
AC	9.25	1.61
AC/2%La	11.26	1.96
AC/2%Fe	11.67	2.03
AC/2%W	11.78	2.05
AC/2%Ni	12.64	2.20

As shown in Table 20 and Figure 49, the desulfurization performance follows the order: AC < 2% La/AC < 2% Fe/AC < 2% W/AC < 2% Ni/AC. The activated carbon of 2% NiO/AC showed the highest desulfurization performance using MD-1 as a model fuel. The

desulfurization performance of 2% Fe/AC and 2% W/AC is very similar yet the tungsten oxide seems to have higher adsorption capacity and thus higher desulfurization performance. Therefore, spiking metals at low concentration on activated carbon enhances the desulfurization performance by enhancing the adsorption capacity. Since these metals improved the desulfurization performance using MD-1, higher sulfur model fuel is used to test their performance at higher sulfur content fuels to observe any operational difference.

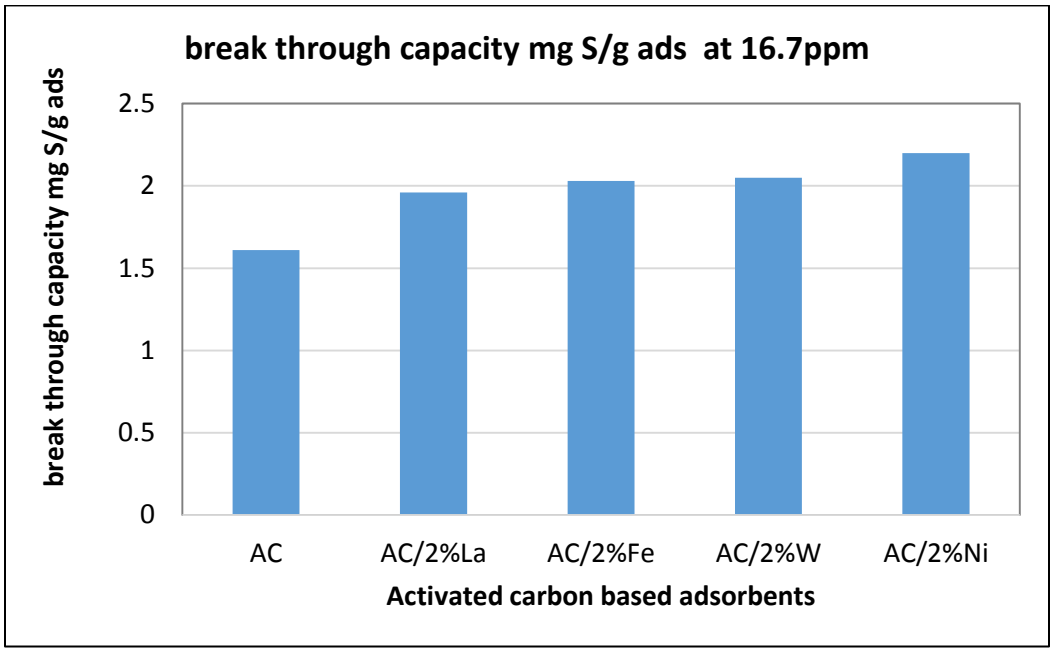

Figure 49. Comparison of the desulfurization performance of metal oxides on activated carbon using MD-1.

4.4.2. The effect of metal loading type on activated carbon using MD-4.

All the adsorbents (AC, 2% La/AC, 2% Fe/AC, 2% W/AC, and 2% NiO/AC) have been tested for the effect of metal loading using MD-1, are tested using a higher sulfur model fuel (MD-4). MD-1 has 16.7 ppm of sulfur while MD-4 has 50 ppm of sulfur. Both model fuels 1 and 4 have 16 % of toluene to mimic the aromatics. Then, each adsorbent is tested using the fixed bed absorber process to obtain the breakthrough curve. Then, the breakthrough capacity is obtained for each adsorbent and compared with the standalone AC at the different total sulfurs as tabulated in Table 32.

Table 32. The breakthrough capacity of various adsorbent using MD-4.

Ads	**Breakthrough capacity mg DBT/g ads at 50 ppm**	**Breakthrough capacity mg S/g ads at 50 ppm**
AC	18.05	3.14
2% La/AC	21.61	3.76
2% Fe/AC	22.18	3.86
2% W/AC	22.64	3.94
2% Ni/AC	24.71	4.30

As shown in Table 32 and Figure 50, the desulfurization performance follows the order: AC < 2% La/AC < 2% Fe/AC < 2% W/AC < 2% Ni/AC which is the same desulfurization performance order using MD-1. On the other hand, the material of 2% Ni/AC showed the highest desulfurization performance using MD-1 and MD- 4 as a model fuel. Moreover,

all the breakthrough capacities increased as the total sulfur of the model fuel increased which confirms the study of the effect of total sulfur on breakthrough capacity.

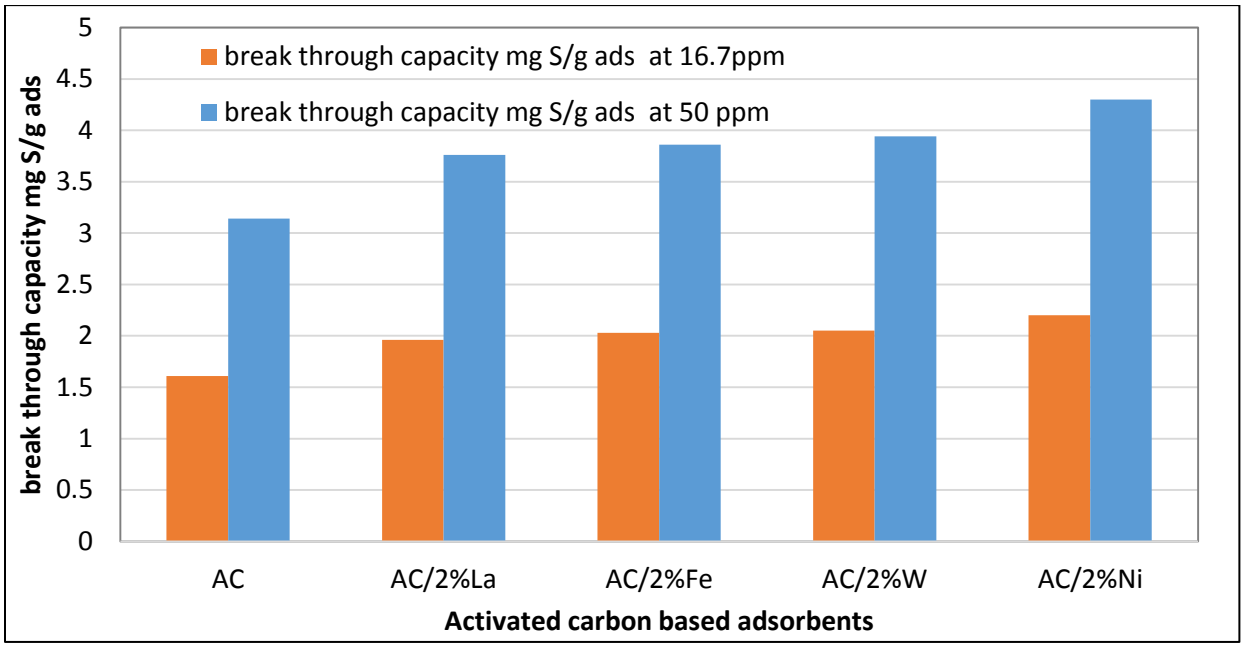

Figure 50. The breakthrough capacity of various adsorbent using MD-4 and MD-1.

4.4.3. Effect of metals loading amount on activated carbon.

The effect of loading iron oxide on activated carbon is studied. Iron oxide was impregnated with activated carbon at 2% and 15 % to study the effect of the metal loading on activated carbon. The 2% loading was conducted by using the ion exchange method where the 15 % loading was conducted by the wet impregnation method with precipitation because the ion exchange method cannot load high amount of metals on activated carbon. Figure 51 shows the breakthrough curves for the activated carbon impregnated with 2% and 15 % Fe in

comparison with activated carbon. Furthermore, Table 33 shows the comparison between the breakthrough capacities for each activated carbon, 2% Fe/AC and 15% Fe/AC.

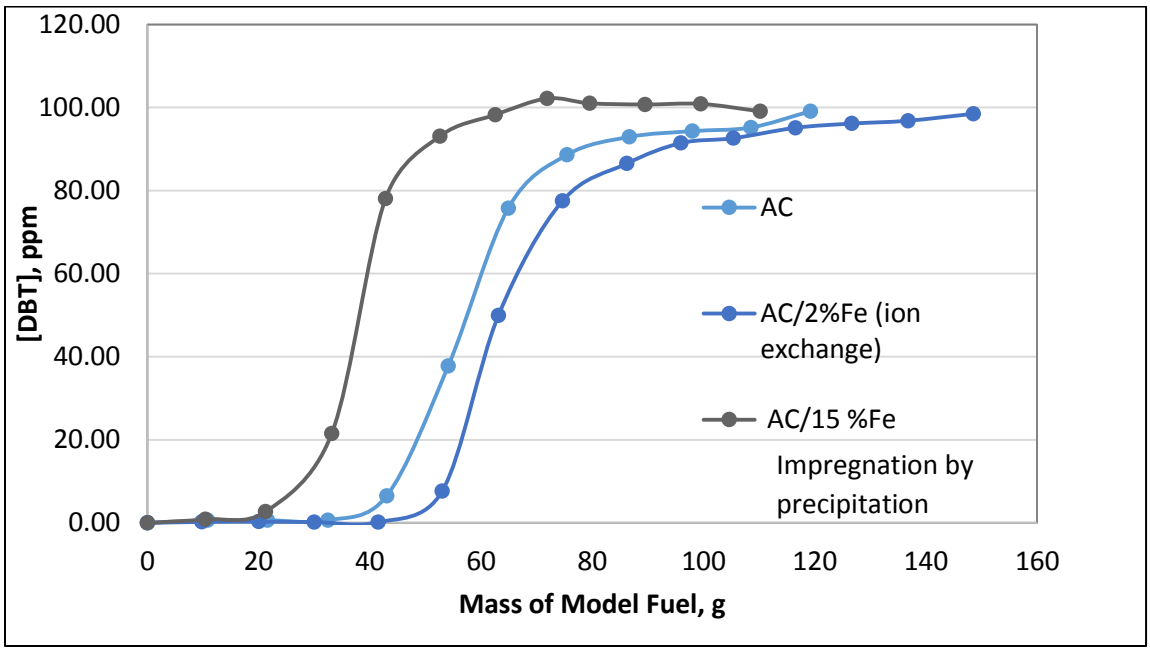

Figure 51. Comparison between AC, 2% Fe/AC and 15% Fe/AC breakthrough curve.

Table 33. Comparison between activated carbon, 2%Fe/AC and 15%Fe/AC breakthrough capacity.

Ads	breakthrough capacity mg DBT/g ads	breakthrough capacity mg S/g ads
15%Fe/AC	5.33	0.93
AC	9.25	1.61
2%Fe/AC	11.67	2.03

As shown in Figure 27 and Table 22, loading 15 % of Fe on activated carbon reduced its breakthrough capacity. This could be due to high loading plugging the activated carbon pores which reduce the adsorption capacity as shown in the BET data in the characterization section.. Loading 2% of Fe on activated enhanced the breakthrough capacity due to adding the sulfur-metal interaction in addition to the π-complexation interaction as illustrated in the introduction section. The results show that high metal loading plugs the pores of the activated carbon causing the breakthrough capacity to be lower because the π- complexation interaction is less. While low loading keeps the bores intact and adds another adsorption factor (metal-sulfur interaction) to the π- complexation interaction.

4.5 Effect of adsorbent preparation method:

There are two different methods to impregnate metals on activated carbon. The precipitation (P) method and the ion exchange (IE) method. The material based on 2% of iron is impregnated on activated carbon using both methods to compare the breakthrough capacity performance against standalone activated carbon. Figure 52 shows the breakthrough curves for the activated carbon impregnated with 2% Fe using ion exchange and precipitation methods in comparison with activated carbon. Furthermore, Table 34 shows the comparison between the breakthrough capacity for activated carbon, 2% Fe/AC (IE) and 2% Fe/AC (P).

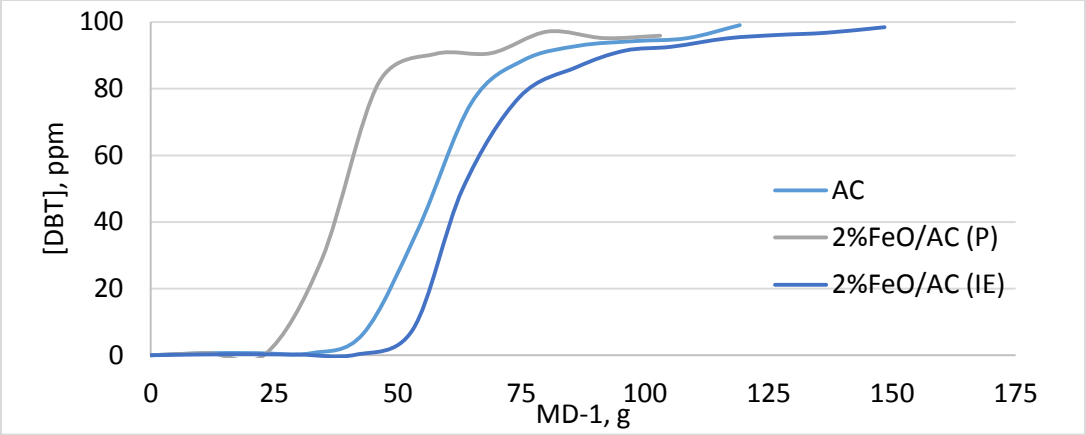

Figure 52. The breakthrough curves for the activated carbon impregnated with 2% Fe using ion exchange and precipitation methods in comparison with activated carbon.

Table 34. Comparison between the breakthrough capacities of activated carbon and 2%Fe/prepared using ion exchange and precipitation methods.

Ads	**breakthrough capacity mg DBT/g ads**	**breakthrough capacity mg S/g ads**
2%FeO/AC (P)	6.17	1.07
AC	9.25	1.61
2%FeO/AC (IE)	11.67	2.03

As shown in Figure 36 and Table 34, metal impregnation on activated carbon using the precipitation method reduced its breakthrough capacity. This could be due to high loading plugging the activated carbon pores which reduce the adsorption capacity. The SEM and BET data are shown in the characterization section. Loading 2% of Fe on activated using the ion exchange method enhanced the breakthrough capacity due to adding the sulfur-

metal interaction in addition to the π-complexation interaction. Furthermore, the adsorbent surface could be altered by the increasing the surface functional groups.

4.6 Effect of bimetallic oxide loading on the adsorbent sulfur capacity:

Based on the result in the previous sections, the metal oxides impregnation on activated carbon found to boost the sulfur adsorption capacity as shown with several metal impregnations. For example, the iron and nickel oxides improved the activated carbon breakthrough capacity by 14 and 36%, respectively. Also, tungsten oxide improved the breakthrough capacity of activated carbon by 18%. This motivated the attempt to impregnate two metals mixture on the same activated carbon and study the effect on breakthrough capacity.

The bimetallic oxide mixtures have been prepared using the ion exchange method as shown in Figure 53. These bimetallic oxide material supported by AC were all tested using the fixed bed absorption process using MD-1 as a feed. Table 35 shows that all bimetallic impregnation had an improvement over the standalone activated carbon except for the 1% Fe-1% La/AC had the less breakthrough capacity. However, excluding 1% Ni-1% W/AC, all adsorbents have less breakthrough capacity than single metal impregnation. On the other hand, the bimetallic oxide of 1% Ni-1% W/AC shows the highest breakthrough capacity tested in this study using MD-1.

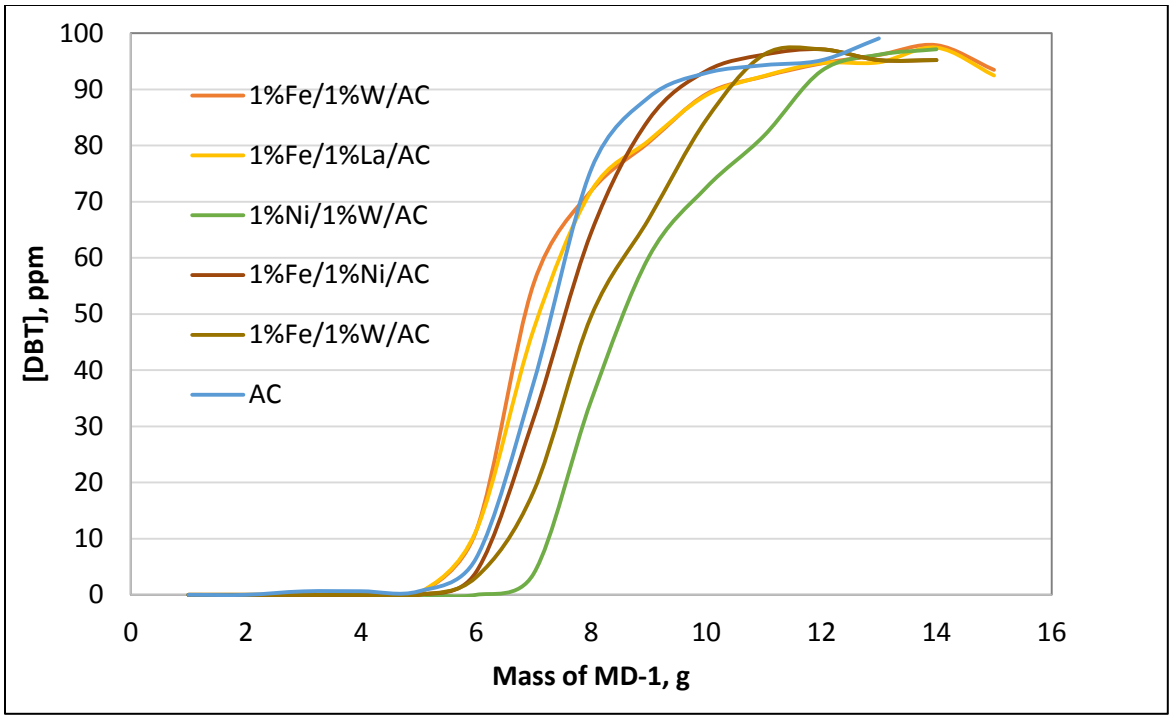

Figure 53. Comparison of the breakthrough curve for activated carbon and bimetallic impregnation on activated carbon.

Table 35. Comparison of the breakthrough capacities for activated carbon and bimetallic impregnation on activated carbon.

Ads	breakthrough capacity mg DBT/g ads	breakthrough capacity mg S/g ads
1% Fe-1% La/AC	9.19	1.60
AC	9.27	1.61
1% Fe-W/AC (LL)	9.51	1.65
1% Fe-1% Ni/AC (ULL	10.61	1.85
1% Fe-1% W/AC (ULL)	11.29	1.97
1% Ni-1% W/AC	13.71	2.30

As shown in Figure 54, the order of breakthrough capacity is: AC-Fe-La< AC < AC-Fe-W-LL < AC-Fe-Ni-ULL < AC/2%La < AC-Fe-W-ULL < AC/2%Fe < AC/2%W < AC/2%Ni < 1%NiO/1%WO3/AC. The nickel and tungsten oxides have significant interaction with the sulfur compounds where they showed the best performance compared with the other metals tested.

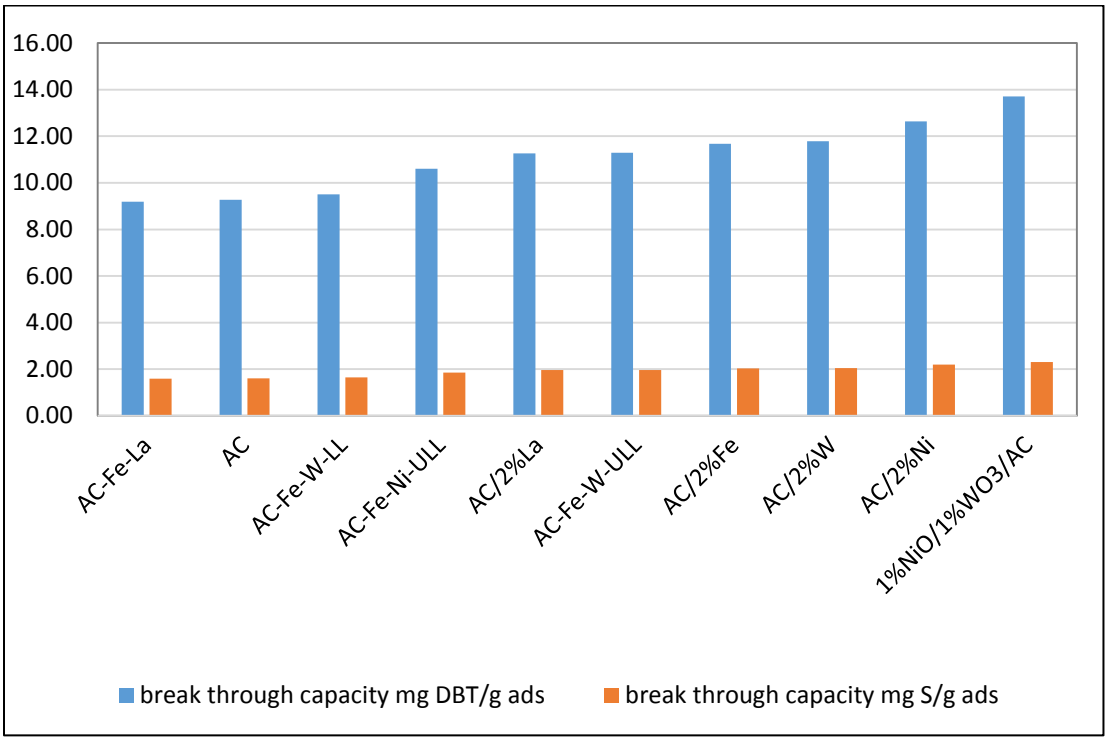

Figure 54. Comparison bimetallic oxide impregnation on AC with single metals loading.

4.7 HDS Diesel studies:

A real HDS diesel sample was used to test the activated carbon and 1%NiO-1%WO3/AC. The HDS diesel sample has a total sulfur 65 ppm and 27 % aromatics. Figure 55 shows the breakthrough curves for the activated carbon impregnated with 1%NiO/1%WO3 in

comparison with activated carbon for HDS diesel. Furthermore, Table 36 shows the comparison between the breakthrough capacities for %NiO/1%WO3 in comparison with activated carbon.

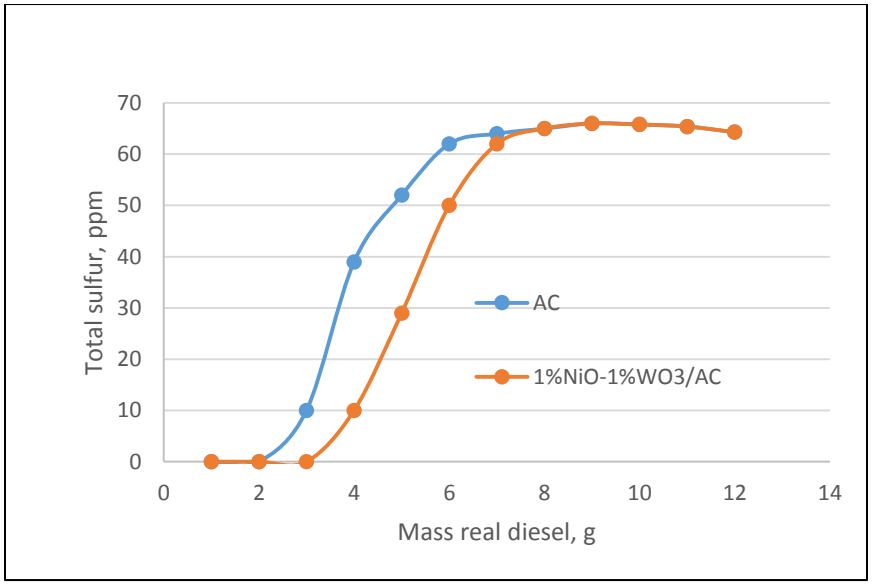

Figure 55. Comparison of the breakthrough curve for activated carbon and 1%NiO-1%WO3/AC for HDS sample.

Table 36. Comparison of the breakthrough capacities for activated carbon and 1%NiO-1%WO3/AC.

Ads	Breakthrough capacity mg S/g ads
AC	0.1
1% Ni-1% W/AC	1.0

As shown in Figure 55 and Table 25, the real HDS sample is more difficult to desulfurize than model fuel due to lower capacities when compared with model fuels. This could be due to fuel additives and additional compounds such as olefins, aromatic compounds,

nitrogen compounds which are present in a significant concentration in the real fuels but not included in the model fuels. These compounds can compete with the sulfur compounds for the activated carbon active sites especially that after HDS, usually the most sterically hindered compounds with low reactivity toward the HDS catalyst remain in the sample. This could explain the low capacity of activated carbon based adsorbents when desulfurizing actual HDS samples.

1 % loading impregnation of nickel and tungsten on activated carbon increases the desulfurization performance for actual HDS sample when compared with activated carbon. This could be due to the high selectivity for nickel and tungsten toward sulfur compounds by direct sulfur-metal and π-π interactions. As shown in the previous section, for metal oxides including nickel and tungsten oxides that have been loaded on the activated carbon, the direct sulfur-to-metal (S-M) interaction could occur via two coordination geometries η_1S and S-μ3. In addition, as per the molecular orbital π-calculations, it is suggested the highest occupied molecular orbital (HOMO) on the sulfur atom can interact with the lowest unoccupied molecular orbital (LUMO) of the metal species. The HOMO for thiophene (T), benzothiophene (BT), and dibenzothiophene (DBT) is on the sulfur atom, but the HOMO for aromatics benzenes and naphthalene is on the six-member ring. This explains the selectivity of activated carbon impregnated with metal oxides toward organosulfur compounds since the direct metal to sulfur interaction is added as another adsorption parameter. Furthermore, as shown for the model fuels, the selectivity of nickel and tungsten toward sulfur compounds is higher comparing to other metal tested.

CONCLUSION

Activated carbon shows a great potential to be applied as an adsorbent for ultra-low sulfur desulfurization for liquid fuels and fuel cell applications especially in being applied as a complementary step to Hydrodesulfurization. The breakthrough capacity results of Activated carbon showed that is superior to H-Y-zeolites using the fixed bed absorber process and model fuel. The model fuel composition affects the adsorbent desulfurization performance where aromatic content reduces the adsorbent breakthrough capacity and total sulfur increase it. Metal oxides loading can boost the desulfurization performance as long as they don plug the adsorbent pores. Metal oxides increase the interaction between sulfur and the adsorbent by direct S-M interactions. The surface area and pore volume were affected by high metal oxide loading over AC that showed lower sulfur breakthrough. The low metal loading and maintained the AC texture property of support showed higher desulfurization breakthrough. The study shows that the adsorbent preparation method affects the desulfurization performance. The adsorbents prepared by ion exchange method are superior to the ones prepared by precipitation. The real HDS sample showed the same trend in terms of indexing the adsorbents based on their desulfurization performance yet the breakthrough capacity is lower when compared with model fuels.

REFERENCES

1. Y. Shiraishi, T. Hirai, I. Komasaw. A Deep Desulfurization Process for Light Oil by Photochemical Reaction in an Organic Two-Phase Liquid−Liquid Extraction System. Ind Eng Chem Res. 37, 203, (1998)
2. Song, Chunshan. "An overview of new approaches to deep desulfurization for ultra-clean gasoline, diesel fuel and jet fuel." Catalysis today 86, no. 1 (2003): 211-263.
3. J. J. McKetta, Petroleum Processing Handbook, Marcel Dekker Inc. New York, (1992)
4. Mohammad FA, Abdullah AM, Bassam EA. Deep desulphurization of gasoline and diesel fuels using non-hydrogen consuming techniques. Fuel 2006;85:1354–63.
5. Mohebali G and Andrew BS, Biocatalytic desulfurization (BDS) of petrodiesel fuels. *Microbiology* **154**:2169–2183 (2008).
6. Soleimani M, Bassi A and Margaritis A, Biodesulfurization of refractory organic sulfur compounds in fossil fuels. *Biotechnology Advances* **25**:570–596 (2007).
7. M. Shakirullah, I. Ahmad, I. M. Ishaq, W. Ahmad. Study on the Role of Metal Oxides in Desulphurization of Some Petroleum Fractions. J. Chin. Chem. Soc. 56, 107, (2009)
8. Y. Shiraishi, Y. Taki, T. Hirai, I. Komasawa. A Novel Desulfurization Process for Fuel Oils Based on the Formation and Subsequent Precipitation of S-Alkylsulfonium Salts. 1. Light Oil Feedstocks. Ind. Eng. Chem. Res. 40, 1213, (2001)
9. Dehkordi AM, Sobati MA and Nazem MA, Oxidative desulfurization of non-hydrotreated kerosene using hydrogen peroxide and acetic acid. Chin J Chem Eng 17:869-874 (2009).
10. K. Yazu, M. Makino, K. Ukegawa, Chem Lett. 33, 1306, (2004) [1]C. Hempstead , W. E. Worthington , Encyclopedia of 20th-century technology, Vol2, 2005.
11. Ali, S. H., Hamad, D. M., Albusairi, B. H., and Fahim, M. A., 2009, *Removal of Benzothiophenes From Fuels by Oxy-Desulfurization*, Energy and Fuels, Vol. 23, PP. 5986-5994.
12. K. Tang, L. Song, L. Duan, X. Li, J. Gui, Z. Sun. Deep desulfurization by selective adsorption on a heteroatoms zeolite prepared by secondary synthesis. Fuel Proc. Technol. 89, 1, (2008)

13. J. C. Zhang, L. F. Song, J. Y. Hu, S. L. Ong, Y. H. Wang, J. G. Zhao, R. Y. Ma. Investigation on gasoline deep desulfurization for fuel cell applications. Energy Convers. Manage. 46, 1, (2005)
14. SHAKIRULLAH, W. AHMAD, I. AHMAD, M. ISHAQ AND M. I. KHAN. DESULPHURIZATION OF LIQUID FUELS BY SELECTIVE ADSORPTION THROUGH MINERAL CLAYS AS ADSORBENTS. J. Chil. Chem. Soc. vol.57 no.4 Concepción 2012
15. J.P. Ruparelia, S.P. Duttaguptab, A.K. Chatterjeec, S. Mukherjia. Potential of carbon nanomaterials for removal of heavy metals from water. De salination 232 (2008) 145–156.
16. Chang Yu Æ Jie Shan Qiu Æ Yu Feng Sun Æ Xian Hui Li Æ Gang Chen Æ Zong Bin Zhao. Adsorption removal of thiophene and dibenzothiophene from oils with activated carbon as adsorbent: effect of surface chemistry. J Porous Mater (2008) 15: 151. doi:10.1007/s10934-007-9116-4.
17. Shaker Haji and Can Erkey . Removal of Dibenzothiophene from Model Diesel by Adsorption on Carbon Aerogels for Fuel Cell Applications. Ind. Eng. Chem. Res., 2003, 42 (26), pp 6933–6937.
18. Xiaoliang Ma, Michael Sprague, and Chunshan Song. Deep Desulfurization of Gasoline by Selective Adsorption over Nickel-Based Adsorbent for Fuel Cell Applications. Ind. Eng. Chem. Res. 2005, 44, 5768-5775.
19. Guo-hui Yuan *, Zhao-hua Jiang, Akiko Aramata, Yun-zhi Gao. Electrochemical behavior of activated-carbon capacitor material loaded with nickel oxide. Carbon 43 (2005) 2913–2917.
20. Dias J. M. , Alvim-Ferraz M. C. M. , Almeida M. F. , Riverra-Urtella J., Sanchez-Polo M. , 2007. Waste materials for activated carbon prepration and its use in aqueous-phase treatment: a review. J. Environ. Manage. 85,833-846.
21. Derbyshire F. , Jagtoyen M., Andrews R., Rao A., Martin-gullon I., Grulke E., 2001. Carbon Materials in Enviromental Applications. Marcel Decker, New York.
22. Kim JH, Ma XL, Zhou AN, Song CS. Ultra-deepdesulfurization and denitrogenation of diesel fuel byselective adsorption over three different adsorbents:a study on adsorptive selectivity and mechanism.Catal Today 2006;111(1e2):74e83.

23. Kim JH, Ma XL, Zhou AN, Song CS. Ultra-deepdesulfurization and denitrogenation of diesel fuel byselective adsorption over three different adsorbents:a study on adsorptive selectivity and mechanism.Catal Today 2006;111(1e2):74e83.
24. Zhou AN, Ma XL, Song CS. Liquid-phase adsorptionof multi-ring thiophenic sulfur compounds oncarbon materials with different surface properties.J Phys Chem B 2006;110(10):4699e707.
25. Zhou A, Ma X, Song C. Effects of oxidative modif-cation of carbon surface on the adsorption of sulfur compounds in diesel fuel. Appl Catal B: Env 2009;87(3e4):190e9.
26. Song, C., Fuel processing for low-temperature and high-temperature fuel cells: Challenges, and opportunities for sustainable development in the 21st century. Catalysis Today 2002, 77, (1-2), 17-49.
27. Novochinskii, I. I.; Song, C.; Ma, X.; Liu, X.; Shore, L.; Lampert, J.; Farrauto, R. J., Low-Temperature H2S Removal from Steam-Containing Gas Mixtures with ZnO for Fuel Cell Application. 1. ZnO Particles and Extrudates. Energy Fuels 2004, 18, (2), 576-583.
28. EPA, Control of Air Pollution from New Motor Vehicles: Heavy-Duty Engine and Vehicle Standards and Highway Diesel Fuel Sulfur Control Requirements. In EPA Federal Register Online, 2011; pp 9.
29. Song, C., Fuel processing for low-temperature and high-temperature fuel cells: Challenges, and opportunities for sustainable development in the 21st century. Catalysis Today 2002, 77, (1-2), 17-49.
30. Hernandez-Maldonado, A. J.; Yang, R. T.; Cannella, W., Desulfurization of commercial jet fuels by adsorption via pi-complexation with vapor phase ion exchange Cu(I)-Y zeolites. Industrial & Engineering Chemistry Research 2004, 43, (19), 6142-6149.
31. Kim, J. H.; Ma, X.; Zhou, A.; Song, C., Ultra-deep desulfurization and denitrogenation of diesel fuel by selective adsorption over three different adsorbents: A study on adsorptive selectivity and mechanism. Catalysis Today 2006, 111, (1-2), 74-83.
32. M. Parsi, A. Knowles, and N. Ladommatos, "The Effect of Fuel Cetane Improver on Diesel Pollutant Emissions," Fuel , vol. 75, pp. 8-14, 1996

33. S. Dasgupta, A. N. Goswami, B. R. Nautiyal, T. V. Rao, B. Sain, Y. K. Sharma, S. M. Nanoti, M. O. Garg, P. Gupta, and A. Nanoti, "Mesoporous silica as selective sorbents for removal of sulfones from oxidized diesel fuel," Microporous and Mesoporous Materials, vol. 124, pp. 94-99, 2009
34. Levy, R.E., et al. Unipure's Oxidative Desulfurization Process Creates New Market Opportunities For Supply Of Ultra-low Sulfur Fuels. in AIChE Spring Meeting. 2002. New Orleans.
35. Babich, I.V. and J.A. Moulijn, Science and technology of novel processes for deep desulfurization of oil refinery streams: a review. Fuel, 2003. 82: p. 607-631.
36. Shiraishi, Y. and T. Hirai, Desulfurization of vacuum gas oil based on chemical oxidation followed by liquid-liquid extraction. Energy & Fuels, 2004. 18(1): p. 37-40.
37. Collins, F.M., A.R. Lucy, and C. Sharp, Oxidative desulphurisation of oils via hydrogen peroxide and heteropolyanion catalysis. Journal of Molecular Catalysis A-Chemical, 1997. 117(1-3): p. 397-403.
38. Yazu, K., et al., Oxidation of dibenzothiophenes in an organic biphasic system and its application to oxidative desulfurization of light oil. Energy & Fuels, 2001. 15(6): p. 1535-1536.
39. M.J. Grossman, M.K. Lee, R.C. Prince, K.K. Garrett, G.N. George, I.J. Pickering, Applied and Environmental Microbiology 65 (1999) 3264-3264.
40. B.L. McFarland, D.J. Boron, W. Deever, J.A. Meyer, A.R. Johnson, R.M. Atlas, Critical Reviews in Microbiology 24 (1998) 99-147.
41. R.B. Qi, Y.J. Wang, J. Chen, J.D. Li, S.L. Zhu, Separation and Purification Technology 57 (2007) 170-175.
42. Babich IV, Moulijn JA. Science and technology of novel processes for deep desulfurization of oil refinery streams and the adsorption mechanism of several adsorbents of activated carbon, zeolite 5A, zeolite 13X, silica-alumina, and alumina. (a review. Fuel 2003;82(6):607e31.
43. Yuesong Shen, Peiwen Li, b Xinhai Xub and Hong Liu. Selective adsorption for removing sulfur: a potential ultra-deep desulfurization approach of jet fuels. RSC Advances, 2012, 2, 1700–1711.

44. Anslyn, E.V.; Dougherty, D.A. Modern Physical Organic Chemistry; University Science Books; Sausalito, CA, 2005 ISBN 1-891389-31-9.
45. M. Seredych and T. J. Bandosz, Langmuir, 2007, 23, 6033–6041.
46. X.L. Ma, L. Sun and C. S. Song, Catal. Today, 2002, 77, 107–116.
47. Huntley, D. R.; Mullins, D. R.; Wingeier, M. P. J. Phys. Chem. 1996, 100, 19620.
48. J.A. Zazo a, A.F. Fraile a, A. Rey b, A. Bahamonde b,*, J.A. Casas a, J.J. Rodriguez.Optimizing calcination temperature of Fe/activated carbon catalysts for CWPO. Catalysis Today 143 (2009) 341–346.
49. Assim, M.Y. and Yoes, J.R., "Confronting New Challenges in Distillate Hydrotreating", AM-87-59, NPRA AM March 1987.
50. Johnson, A.D., "Study Shows Marginal Cetane Gains From Hydrotreating", Oil and Gas J., May 30, 1983, p. 79.
51. McCulloch, D.C., Edgar, M.D. and Pistorious, J.T., "High Severity Diesel Hydrotreating", AM-87-58, NPRA AM, March 1987.
52. A. J. Hernandez-Maldonado, F. H. Yang, G. Qi and R. T. Yang, Appl. Catal., B, 2005, 56, 111–126.
53. A. Takahashi, H. Yang and R. T. Yang, Ind. Eng. Chem. Res., 2002, 41, 2487–2496.
54. A. J. Hernandez-Maldonado, G. S. Qi and R.T. Yang, Appl. Catal., B, 2005, 61, 212–218.
55. Y. J. Jin, H. L. Song and L. J. Chou, Chem. Ind. Eng. Process, 2009, 28, 1540–1545.
56. K. Liu, C.S. Song, S. Velu, Hydrogen and Syngas Production and Purification Technologies. John Wiley & Sons, Inc.: Hoboken, New Jersey, 2009.
57. P. J. Bailes, "Solvent extraction in an electrostatic field," *Industrial & Engineering Chemistry Process Design and Development* , vol. 20, pp. 564–570, July, 1981.
58. Bond, G. C., *Heterogeneous Catalysis: Principles and Applications*. 2 ed.; Oxford University Press: New York, 1987.
59. Y. A. Alhamed, and H. S. Bamufleh, "Sulfur removal from model diesel fuel using granular activated carbon from dates' stones activated by ZnCl2," Fuel, vol. 88, pp. 87–94, 2009.

60. J. K. Thomas, "A Flow Calorimetric Study of Adsorption of Dibenzothiophene, Naphthalene and Quinoline on Zeolites," M.S. thesis, Department of Chemical Engineering, University of Waterloo, Ontario, Canada, 2008.
61. S. A. Dastgheib, R. K. Elham, and S. Moosavi, "Adsorption of Thiophenic Compounds from Model Diesel Fuel Using Copper and Nickel Impregnated Activated Carbons," *Energies* , vol. 5, pp. 4233-4250, 2012.
62. S. A. Nair, "Desulfurization of Hydrocarbon Fuels at Ambient Conditions Using Supported Silver Oxide-Titania Sorbents," PhD thesis, Department of Chemical Engineerig, Auburn University, Alabama, 2010.
63. A. Bassi, A. Margaritis, and M. Soleimani, "Biodesulfurization of refractory organic sulfur compounds in fossil fuels," Biotechnology Advances, vol. 25, pp. 570–596, 2007.
64. M. J. Lee, M. K. Prince, R. C. Garrett, K. K. George, G. N. Pickering, and I. J. Grossman, "Microbial desulfurization of a crude oil middle-distillate fraction: Analysis of the extent of sulfur removal and the effect of removal on remaining sulfur," Applied and Environmental Microbiology, vol. 65, pp. 181-188, 1999.
65. J. Klein, "Biological processing of fossil fuels," Applied Microbiology and Biotechnology, vol. 52, pp. 2-15, 1999.
66. A. S. Ball, and G. Mohebali, "Biocatalytic desulfurization (BDS) of petrodiesel fuels," Microbiology, vol. 154, pp. 2169–2183, 2008.
67. D. J. Monticello, "Biodesulfurization and the upgrading of petroleum distillates," Current Opinion in Biotechnology, vol. 11, pp. 540–546, 2000.
68. M. A. Kertesz, "Riding the sulfur cycle-metabolism of sulfonates and sulfate esters in Gram-negative bacteria," *FEMS Microbiology Review*, vol. 24, pp. 135–75, 1999.
69. T. Aida, and I. Funakoshi, "Process for recovering organic sulfur compounds from fuel oil," U.S. Patent 5753102 A, May 19, 1998.
70. P. Forte, "Process for the removal of sulfur from petroleum fractions," US5582714 A, 1996.
71. P. Topalova, and L. Toteva, "extractive dearomatization and desulphurdesulphurization of a distillate gasoil cut with dimethylformamide," Univ. Chem. Technol. Metall., vol. 42, pp. 17–20, 2007.

72. J. Edward, F.Maginn, and F. J. Brennecke, "Ionic liquids: innovative fluids for chemical processing," AIChE Journal , vol. 47, pp. 2384 - 2389, 2004.
73. L. Datsevich, A. Jess, A. Lauter, C. Schmitza, P. Wasserscheida, and A. Bösmann, "Deep desulfurization of diesel fuel by extraction with ionic liquids," Chemical Communications, 2001.
74. I. Lopez-Martin, G. Rothenberg, K. R. Seddon, G. Silvero, X. Zheng, and J.D. Holbrey, "Desulfurization of oils using ionic liquids: selection of cationic and anionic components to enhance extraction efficiency," Green Chemistry, vol. 10, pp. 87–92, 2008.
75. W. Zhu, H. Li, W. Jiang, Y. Jiang, W. Huang, and Y. Yan Zhang, "Deep oxidative desulfurization of fuels by Fenton-like reagent in ionic liquids," Green Chemistry, vol. 11, pp. 1801–1807, 2009.
76. G. Loh, C. G. Gwie, S. Dewiyanti, M. Tasrif, A. Borgna, and J. Bu, "Desulfurization of diesel fuels by selective adsorption on activated carbons: Competitive adsorption of polycyclic aromatic sulfur heterocycles and polycyclic aromatic hydrocarbons," Chemical Engineering Journal, vol. 166, pp. 207–217, 2011.
77. V. Chandra, and S. R. Kumar, "Studies on Adsorptive Desulfurization by Activated Carbon," Clean-Soil Air Water, vol. 40, pp.545–550, 2012.
78. I. Al Zubaidy, F. Bin Tarsh, N. N. Darwish, B. Sweidan, S. Abdul Majeed, A. Al Sharafi, and L. Abu Chacra "Adsorption Process of Sulfur Removal from Diesel Oil Usi ng Sorbent Materials," Journal of Clean Energy Technologies, vol. 1, pp. 66 - 68, 2013.
79. Song, C., An overview of new approaches to deep desulfurization for ultra-clean gasoline, diesel fuel and jet fuel. Catalysis Today 2003, 86, (1-4), 211-263.
80. Babich, I. V.; Moulijn, J. A., Science and technology of novel processes for deep desulfurization of oil refinery strams: a review. Fuel 2003, 82, 607-631.
81. Kim, J. H.; Ma, X.; Zhou, A.; Song, C., Ultra-deep desulfurization and denitrogenation of diesel fuel by selective adsorption over three different adsorbents: A study on adsorptive selectivity and mechanism. Catalysis Today 2006, 111, (1-2), 74-83.

82. Etemadi, O.; Yen, T. F., Selective Adsorption in Ultrasound-Assisted Oxidative Desulfurization Process for Fuel Cell Reformer Applications. Energy Fuels 2007, 21, (4), 2250-2257.
83. EPA, Control of Air Pollution from New Motor Vehicles: Heavy-Duty Engine and Vehicle Standards and Highway Diesel Fuel Sulfur Control Requirements. In EPA Federal Register Online, 2001; pp 5001-5050, 5135-5193.
84. Song, C., Fuel processing for low-temperature and high-temperature fuel cells: Challenges, and opportunities for sustainable development in the 21st century. Catalysis Today 2002, 77, (1-2), 17-49.
85. Ma, X.; Sun, L.; Song, C., A new approach to deep desulfurization of gasoline, diesel fuel and jet fuel by selective adsorption for ultra-clean fuels and for fuel cell applications. *Catalysis Today* **2002,** 77, (1-2), 107-116.
86. Velu, S.; Ma, X.; Song, C.; Namazian, M.; Sethuraman, S.; Venkataraman, G., Desulfurization of JP-8 Jet Fuel by Selective Adsorption over a Ni-based Adsorbent for Micro Solid Oxide Fuel Cells. *Energy Fuels* **2005,** 19, (3), 1116-1125.
87. Zhou, A.; Ma, X.; Song, C., Liquid-phase adsorption of multi-ring thiophenic sulfur compounds on carbon materials with different surface properties. Journal of Physical Chemistry B 2006, 110, (10), 4699.
88. Xue, M.; Chitrakar, R.; Sakane, K.; Hirotsu, T.; Ooi, K.; Yoshimura, Y.; Feng, Q.; Sumida, N., Selective adsorption of thiophene and 1-benzothiophene on metal-ion-exchange zeolites in organic medium. Journal of Colloid and Interface Science 2005, 285, (2), 487-492.
89. Hernandez-Maldonado, A. J.; Yang, R. T., Desulfurization of Liquid Fuels by Adsorption via Pi-Complexation with Cu(I)-Y and Ag-Y Zeolite. Ind. Eng. Chem. Res. 2003, 42, 123-129.
90. Bhandari, V. M.; Hyun Ko, C.; Geun Park, J.; Han, S.-S.; Cho, S.-H.; Kim, J.-N., Desulfurization of diesel using ion-exchange zeolites. Chemical Engineering Science 2006, 61, (8), 2599-2608.
91. Yang, R. T., Desulfurization of Transportation Fuels with Zeolites Under Ambient Conditions. Science 2003, 301, (5629).

92. Hernandez-Maldonado, A. J.; Yang, R. T., New sorbents for desulfurization of diesel fuels via pi-complexation. AIChE Journal 2004, 50, (4), 791-801.
93. ConocoPhillips Technologies Position ConocoPhillips for the Future. http://www.conocophillips.com/NR/rdonlyres/DDBD0D76-1DFF-49BC-A4A3-242BDD28B259/0/cp02op07.pdf (June 14, 2008),
94. Ma, X.; Velu, S.; Kim, J. H.; Song, C., Deep desulfurization of gasoline by selective adsorption over solid adsorbents and impact of analytical methods on ppm-level sulfur quantification for fuel cell applications. Applied Catalysis B: Environmental 2005, 56, (1-2), 137-147.
95. Haji, S.; Erkey, C., Removal of Dibenzothiophene from Model Diesel by Adsorption on Carbon Aerogenls for Fuel Cell Application. Ind. Eng. Chem. Res. 2003, 42, 6933-6937.
96. Ania, C. O.; Bandosz, T. J., Importance of Structural and Chemical Heterogeneity of Activated Carbon Surfaces for Adsorption of Dibenzothiophene. Langmuir 2005, 21, (17), 7752-7759.
97. 43-Katie A. Cychosz, Antek G. Wong-Foy, and Adam J. Matzger*. Liquid Phase Adsorption by Microporous Coordination Polymers: Removal of Organosulfur Compounds. 10.1021/ja802121u CCC: JACS.
98. S. Nair, B.J. Tatarchuk, Adsorption-Journal of the International Adsorption Society 17 (2011) 663-673.
99. Ramirez, G. Macias, L. Cedeno, A. Gutierrez-Alejandre, R. Cuevas, P. Castillo, Catalysis Today 98 (2004) 19-30.
100. G.S. Walker, E. Williams, A.K. Bhattacharya, Journal of Materials Science 32 (1997) 5583 5592.
101. M.S. Rana, S.K. Maity, J. Ancheyta, G.M. Dhar, T. Rao, Applied Catalysis a-General 253 (2003) 165-176.
102. Li, F.L., et al., Deep desulfurization of hydrodesulfurization-treated diesel oil by a facultative thermophilic bacterium Mycobacterium sp. X7B. FEMS Microbiology Letters, 2003. 223(2): p. 301-307.

103. Borole, A.P., et al., Comparison of the emulsion characteristics of Rhodococcus erythropolis and Ecsherichia coli SOXC-5 cells expressing biodesulfurization genes. Biotechnology Progress, 2002. 18(1): p. 88-93.
104. Gray, K.A., G.T. Mrachko, and C.H. Squires, Biodesulfurization of fossil fuels. Current Opinion in Microbiology, 2003. 6(3): p. 229-235.
105. Zainudin, N.F., et al., Study of adsorbent prepared from oil palm ash (OPA) for flue gas desulfurization. Separation and Purification Technology, 2005. In Press, Corrected Proof.
106. Levy, R.E., et al. Unipure's Oxidative Desulfurization Process Creates New Market Opportunities For Supply Of Ultra-low Sulfur Fuels. in AIChE Spring Meeting. 2002. New Orleans.
107. Kroschwitz, J. and M. Howe-Grant, eds. Kirk-Othmer Encyclopedia of Chemical Technology. 4th ed. ed. Vol. Vols. 1, 2, 9, 10. 1991, John Wiley and Son: New York.
108. Babich, I.V. and J.A. Moulijn, Science and technology of novel processes for deep desulfurization of oil refinery streams: a review. Fuel, 2003. 82: p. 607-631.
109. Shiraishi, Y. and T. Hirai, Desulfurization of vacuum gas oil based on chemical oxidation followed by liquid-liquid extraction. Energy & Fuels, 2004. 18(1): p. 37-40.
110. Yazu, K., et al., Oxidation of dibenzothiophenes in an organic biphasic system and its application to oxidative desulfurization of light oil. Energy & Fuels, 2001. 15(6): p. 1535-1536.
111. F. M. Al-Malki, A. El-Ali, B. Martinie, G. Siddiqui, and N. M. Ali, "Deep desulphurization of gasoline and diesel fuels using non-hydrogen consuming techniques," Fuel , vol. 85, pp. 54-63, 2006.
112. S. Wang, B. Cui, B. Sun, and L. Liu, "Deep desulfurization of diesel oil oxidized by Fe (VI) systems," Fuel, vol. 87, pp. 422-428, 2008.
113. Song, C., Fuel processing for low-temperature and high-temperature fuel cells: Challenges, and opportunities for sustainable development in the 21st century. Catalysis Today 2002, 77, (1-2), 17-49.
114. Ito, E.; van Veen, J. A. R., On novel processes for removing sulphur from refinery streams. Catalysis Today 2006, 116, (4), 446-460.

115. Hernandez-Maldonado, A. J.; Yang, R. T.; Cannella, W., Desulfurization of commercial jet fuels by adsorption via pi-complexation with vapor phase ion exchange Cu(I)-Y zeolites. Industrial & Engineering Chemistry Research 2004, 43, (19), 6142-6149.i

116. T.A. Saleh, G.I. Danmaliki, Influence of acidic and basic treatments of activated carbon derived from waste rubber tires on adsorptive desulfurization of thiophenes, J. Taiwan Inst. Chem. Eng. 60 (2016) 460–468.

117. T.A. Saleh, The influence of treatment temperature on the acidity of MWCNT oxidized by HNO3 or a mixture of HNO3/H2SO4, Appl. Surf. Sci. 257 (2011) 7746–7751.

118. T.A. Saleh, Mercury sorption by silica/carbon nanotubes and silica/activated carbon: a comparison study, J. Water Supply Res. T. 64 (8) (2015) 892–903.

119. N. Takahashi, A. Suda, I. Hachisuka, M. Sugiura, H. Sobukawa and H. Shinjoh, Appl. Catal. A, 72, 1–2 (2007) 187-195.

120. E.P. Barrett, L.G. Joyner and P.P. Halenda, J. Am. Chem. Soc. 73 (1951) 373–380.

121. T. Horikawa, D.D. Do and D. Nicholson, Adv. Colloid Interface Sci., 169 (2011) 40–58.

VITAE

Name	**:** Faisal A. Alrasheed
Nationality	**:** Saudi
Date of Birth	**:**6/15/1986
Email	**:** faisal.alrasheed@aramco.com
Address	**:** 62 Dhahran, 31311Saudi Arabia
Academic Background	: Faisal has received his B.Sc. in Chemistry from Michigan State University in December, 2009. Faisal has worked as a research scientist with Saudi Aramco in the Research and Development Center applying research in oil and gas fields and providing technical support for various Saudi Aramco research and operations until 2016. In 2013, Faisal has a one year field deployment assignment in Abqaiq plants as process engineer providing engineering and chemical treatment support to oil and utility operations. Currently, Faisal is working as an analytical support scientist in Southern Area Lab Department supporting Saudi Aramco southern area and environmental operations.